Benjamin C. Waldrep
Vice President
Harris Nuclear Plant
5413 Shearon Harris Road
New Hill, NC 27562-9300

919.362.2502

10 CFR 50.55a

October 21, 2016
Serial: HNP-16-095

ATTN: Document Control Desk
U.S. Nuclear Regulatory Commission
Washington, DC 20555-0001

Shearon Harris Nuclear Power Plant, Unit 1
Docket No. 50-400/Renewed License No. NPF-63

Subject: Relief Request I3R-16, Reactor Vessel Closure Head Nozzle Repair Technique, Inservice Inspection Program, Third Ten-Year Interval, Non-Proprietary Version of Calculation

Ladies and Gentlemen:

Duke Energy Progress, LLC (Duke Energy), requested NRC approval of relief request I3R-16 for the Shearon Harris Nuclear Power Plant, Unit 1 (HNP) inservice inspection program in a letter dated October 19, 2016 (Agencywide Documents Access and Management System (ADAMS) Accession Nos. ML16294A218 and ML16294A219). The October 19, 2016, letter contained the relief request and the proprietary version of the AREVA Inc. calculation to support this request. The purpose of this letter is to provide the non-proprietary version of the calculation provided in the October 19, 2016, letter.

This letter does not contain any regulatory commitments.

Please refer any questions regarding this submittal to John Caves, HNP Regulatory Affairs Manager, at (919) 362-2406.

Sincerely,

Benjamin C. Waldrep

Enclosure: Calculation 32-9215680-002, Shearon Harris Unit 1 CRDM/CET Nozzle As-Left J-groove Weld Analysis (Non-Proprietary)

cc: Mr. M. Riches, NRC Resident Inspector, HNP
Ms. M. Barillas, NRC Project Manager, HNP
NRC Regional Administrator, Region II

Benjamin C. Waldrep
Vice President
Harris Nuclear Plant
5413 Shearon Harris Road
New Hill, NC 27562-9300

919.362.2502

10 CFR 50.55a

October 21, 2016
Serial: HNP-16-095

ATTN: Document Control Desk
U.S. Nuclear Regulatory Commission
Washington, DC 20555-0001

Shearon Harris Nuclear Power Plant, Unit 1
Docket No. 50-400/Renewed License No. NPF-63

Subject: Relief Request I3R-16, Reactor Vessel Closure Head Nozzle Repair Technique, Inservice Inspection Program, Third Ten-Year Interval, Non-Proprietary Version of Calculation

Ladies and Gentlemen:

Duke Energy Progress, LLC (Duke Energy), requested NRC approval of relief request I3R-16 for the Shearon Harris Nuclear Power Plant, Unit 1 (HNP) inservice inspection program in a letter dated October 19, 2016 (Agencywide Documents Access and Management System (ADAMS) Accession Nos. ML16294A218 and ML16294A219). The October 19, 2016, letter contained the relief request and the proprietary version of the AREVA Inc. calculation to support this request. The purpose of this letter is to provide the non-proprietary version of the calculation provided in the October 19, 2016, letter.

This letter does not contain any regulatory commitments.

Please refer any questions regarding this submittal to John Caves, HNP Regulatory Affairs Manager, at (919) 362-2406.

Sincerely,

Benjamin C. Waldrep

Enclosure: Calculation 32-9215680-002, Shearon Harris Unit 1 CRDM/CET Nozzle As-Left J-groove Weld Analysis (Non-Proprietary)

cc: Mr. M. Riches, NRC Resident Inspector, HNP
Ms. M. Barillas, NRC Project Manager, HNP
NRC Regional Administrator, Region II

HNP-16-095

Shearon Harris Nuclear Power Plant, Unit 1
Docket No. 50-400/Renewed License No. NPF-63

Relief Request I3R-16,
Reactor Vessel Closure Head Nozzle Repair Technique,
Inservice Inspection Program, Third Ten-Year Interval, Non-Proprietary Version of Calculation

Enclosure

Calculation 32-9215680-002 Shearon Harris Unit 1 CRDM/CET Nozzle As-Left J-groove Weld Analysis
(Non-Proprietary)

AREVA

CALCULATION SUMMARY SHEET (CSS)

Document No. 32 - 9215680 - 002

Safety Related: ☒Yes ☐ No

Title Shearon Harris Unit 1 CRDM/CET Nozzle As-Left J-groove Weld Analysis (Non Proprietary)

PURPOSE AND SUMMARY OF RESULTS:

AREVA NP Proprietary information in the document are indicated by pairs of brackets “ [ ] ”. The proprietary version of this document is in AREVA document 32- 9176350-003.

Purpose

The purpose of the present fracture mechanics analysis is to determine the suitability of leaving degraded J-groove weld and butter material in the Shearon Harris Unit 1 reactor vessel head following the repair of either a Control Rod Drive Mechanism (CRDM) nozzle or Core Exit Thermocouple (CET) nozzle by the ID temper bead (IDTB) weld procedure. It is postulated that a small flaw in the head would combine with a large stress corrosion crack in the weld and butter to form a radial corner flaw that would propagate into the low alloy steel head by fatigue crack growth under cyclic loading conditions.

The purpose of Rev 001 is to revise the primary stress limit analysis performed in Section 6.5 (updated analysis in Appendix C) by performing a detailed primary stress limit analysis considering each of the CRDM repairs performed on Shearon Harris Unit 1’s RVCH. Also, the objective is to determine the RVCH service life considering all the repaired CRDM configurations that have been performed to date as of the Spring (April) 2015 Outage.

The purpose of Rev 002 is to add a brief evaluation for nozzle repair at penetrations 30, 40 and 51 in the absence of original J-groove weld sizes and head thickness at these locations for additional 5 years operation.

Summary of Results

Based on a combination of linear elastic and elastic-plastic fracture mechanics analysis of a postulated remaining flaw in the original Alloy 182 J-groove weld and butter material, a Shearon Harris Unit 1 CRDM or CET nozzle is considered to be acceptable for 30 years of operation following an IDTB weld repair based on EPFM analysis consideration only. The controlling loading condition is a large loss of coolant accident, for which it was shown that with safety factors of 3 on primary loads and 1.5 on secondary loads that the applied J-integral (2.359 kips/in) was still less than the J-integral of the low alloy steel head material (2.474 kips/in) at a crack extension of 0.1 inch.

Rev 001: Based on the evaluation presented in Appendix C, the RVCH repairs are acceptable for an additional 12 years beyond the Spring (April) 2015 outage (or 15 years from the time of installation).

Rev 002: Rev 001 conclusion for the nine repaired nozzles remains valid. Nozzle repairs at penetrations 30, 40 and 51 are acceptable for additional 5 years beyond the repair (Fall 2016 outage) based on the assumptions listed in Sub-Sections 3.1 and 3.2, and the analysis presented in Section C.7 of Appendix C. The limiting service life of all nozzle repairs is 5 years from the Fall 2016 outage.

If the computer software used herein is not the latest version per the EASI list, AP 0402-01 requires that justification be provided.

THE FOLLOWING COMPUTER CODES HAVE BEEN USED IN THIS DOCUMENT:

CODE/VERSION/REV	CODE/VERSION/REV
ANSYS 12.1 (Rev 000)	

THE DOCUMENT CONTAINS ASSUMPTIONS THAT SHALL BE VERIFIED PRIOR TO USE

☒ YES
☐ NO

Shearon Harris Unit 1 CRDM/CET Nozzle As-Left J-groove Weld Analysis (Non Proprietary)

Review Method: ☒ Design Review (Detailed Check)
☐ Alternate Calculation

Signature Block

Name and Title (printed or typed)	Signature	P/R/A and LP/LR	Date	Pages/Sections Prepared/Reviewed/Approved
Kaihong Wang Principal Engineer	[signature]	P	10/20/16	All
Tom Riordan Engineer IV	[signature]	R	20OCT2016	All
Tim M. Wiger Unit Manager	[signature]	A	10/20/16	All

Notes: P/R/A designates Preparer (P), Reviewer (R), Approver (A);
LP/LR designates Lead Preparer (LP), Lead Reviewer (LR)

In reviewing and approving the initial release (Rev. 000), the lead reviewer/approver shall designate 'All' in pages/sections reviewed/approved.

In reviewing and approving revisions, the lead preparer and lead reviewer shall use 'All' in the pages/sections reviewed/approved. 'All' means that the changes and the effect of the changes on the entire document have been reviewed/approved. It does not mean that the lead reviewer/approver has reviewed/approved all the pages of the document.

Project Manager Approval of Customer References (N/A if not applicable)

Name (printed or typed)	Title (printed or typed)	Signature	Date
Dave Skulina	Project Manager	[signature]	10/20/2016

Mentoring Information (not required per 0402-01)

Name (printed or typed)	Title (printed or typed)	Mentor to: (P/R)	Signature	Date
N/A	N/A	N/A	N/A	N/A

Record of Revision

Revision No.	Pages/Sections/Paragraphs Changed	Brief Description / Change Authorization
000	All	Original release. The corresponding proprietary version is in AREVA document 32- 9176350-001.
001	All	Updated with the latest form (0402-01-F01 Rev. 018).
	CSS page	Added purpose and summary of Rev 001.
	Section 6.5	Text deleted and replaced with statement referencing Appendix C for Limit Load Analysis.
	Section 7.0	Added statements to address the service life of the RVCH considering all the CRDM repaired configurations to-date as of April 2015.
	Appendix C	Added the updated Limit Load Analysis to address each of the repaired CRDM configurations to-date as of April 2015.
002	All	Updated with the latest form (0402-01-F01 Rev. 019).
	CSS page	Added purpose and summary of Rev 002.
	Throughout	Changed terminology from “limit load analysis” to “primary stress limit analysis” since limit load analysis is only one of the possible methods for satisfying primary stress limits.
	Pages 2-3	Updated for Rev 002.
	Section 3.1	Revised to include two unverified assumptions.
	Section 3.2	Added clarification to second paragraph. Added a justified assumption (last paragraph).
	Section 6.5	Updated service life discussion based on Appendix C revision.
	Section 7.1	Deleted discussion of service life due to primary stress limit, which was redundant with discussion in Section 7.2
	Section 7.2	Updated service life discussion based on Appendix C revision.
	Section 8.0	Updated Reference 1 to latest revision.
	Section C.2	Revised second paragraph and inserted a table.
	Sections C.4, C.6	Corrected table titles for Tables C9 and C10.
	Section C.7	Added to address the three nozzle repairs (#30, #40 and #51).
	Section C.8	Updated from C.7; added References C14 to C16; updated revision for References C2 and C12.

Table of Contents

Page

Table of Contents
(continued)

List of Tables

List of Figures

1.0 INTRODUCTION

Due to the susceptibility of Alloy 600 partial penetration nozzles to primary water stress corrosion cracking (PWSCC), the Progress Energy plans to inspect the Control Rod Drive Mechanism (CRDM) and Core Exit Thermocouple (CET) nozzles in the Shearon Harris Unit 1 reactor vessel head. In the event that a repair is necessary, an ID temper bead weld repair procedure has been developed wherein the lower portion of the nozzle is removed by a boring procedure and the remaining portion is welded to the low alloy steel reactor vessel head above the original Alloy 82/182 J-groove attachment weld. The repair concept is illustrated in Figure 1-1, both with and without an overlap between the original J-groove weld and the new IDTB weld. The IDTB repair is more fully described by the design drawing [1] and the technical requirements document [2]. Since a potential flaw in the J-groove weld cannot be sized by currently available non-destructive examination techniques, it is assumed that the "as-left" condition of the remaining J-groove weld includes degraded or cracked weld material extending through the entire J-groove weld and Alloy 82/182 butter material.

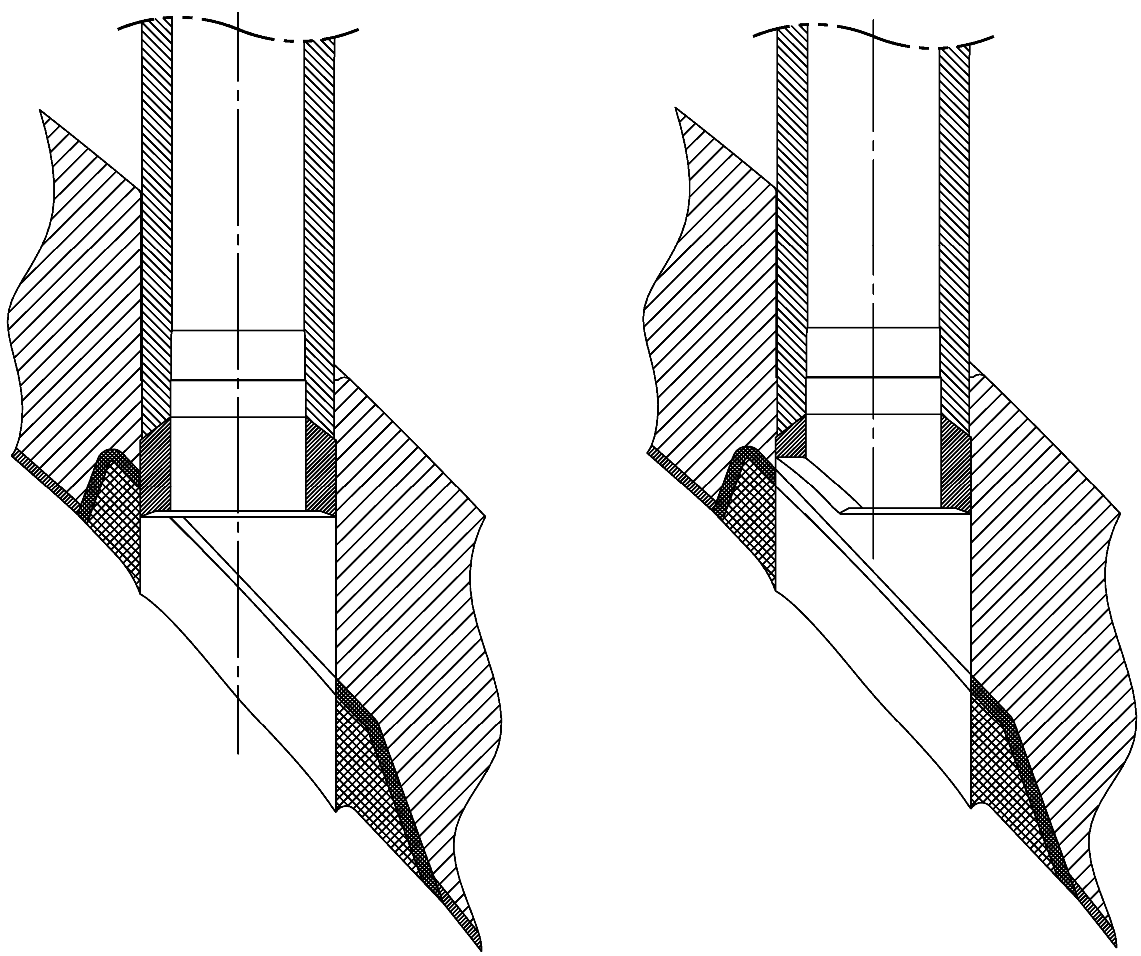

(a) With Weld Overlap (b) With Overlap Removed

Figure 1-1: ID Temper Bead Weld Repair

Since it is known from the residual stress analysis of the Shearon Harris reactor vessel head outermost nozzle penetration [3] that the hoop stress in the J-groove weld is greater than the axial stress at the same location, the preferential direction for cracking would be axial, or radial relative to the nozzle. It is postulated that a radial crack in the Alloy 82/182 weld metal would propagate by PWSCC, through the weld and butter, to the interface with the low alloy steel head material, where it is fully expected that such a crack would then blunt, or arrest, as discussed in Reference [4]. Since the vertical distance along the bored surface between the inside corner of the remnant J-groove weld and the point where the butter meets the head is more than two inches, a crack extending from the corner of the weld to the low alloy steel head would be very deep. Although primary water stress corrosion cracking would not extend into the head, it is further postulated that a small fatigue initiated flaw forms in the low alloy steel head and combines with the stress corrosion crack in the weld to form a large radial corner flaw that would propagate into the head by fatigue crack growth under cyclic loading conditions. Linear-elastic (LEFM) and elastic-plastic (EPFM) fracture mechanics procedures are utilized to evaluate this worst case flaw in the original J-groove weld and butter.

Key features of the fracture mechanics analysis are:

- This analysis applies specifically to the CRDM nozzle penetrations in the Shearon Harris Unit 1 reactor vessel closure head. A J-integral resistance curve is developed based on the Charpy V-notch upper-shelf energy for the Shearon Harris Unit 1 head plate material.
- Flaw growth is calculated for a 30 year period of operation, corresponding to 20 18-month fuel cycles.
- Final flaw acceptance is based on the available fracture toughness and ductile tearing resistance of the RVCH material considering the safety factors listed in Table 1-1.
- Since the same design is used at Shearon Harris Unit 1 for both the CRDM and CET nozzles and the CET nozzles are located within the same outermost penetration "circle" as the CRDM nozzles, the analysis performed herein for the CRDM nozzles is also applicable to the CET nozzles.

Table 1-1: Safety Factors for Flaw Acceptance

Linear-Elastic Fracture Mechanics			
Operating Condition	Evaluation Method	Fracture Toughness / K_I	
Normal/Upset	K_{Ia} fracture toughness	$\sqrt{10} = 3.16$	
Emergency/Faulted	K_{Ic} fracture toughness	$\sqrt{2} = 1.41$	
Elastic-Plastic Fracture Mechanics			
Operating Condition	Evaluation Method	Primary	Secondary
Normal/Upset	J/T based flaw stability	3.0	1.5
Normal/Upset	$J_{0.1}$ limited flaw extension	1.5	1.0
Emergency/Faulted	J/T based flaw stability	1.5	1.0
Emergency/Faulted	$J_{0.1}$ limited flaw extension	1.5	1.0

2.0 ANALYTICAL METHODOLOGY

A radial flaw at the inside corner of non-radial head penetration is evaluated based on a combination of linear elastic fracture mechanics (LEFM) and elastic-plastic fracture mechanics (EPFM), as outlined below.

1. Postulate radial flaws in the J-groove weld, extending from the inside corner of the penetration to the interface between the butter and head, as shown in Figure 2-1 and Figure 2-2 for the uphill and downhill sides of the penetration, respectively. Initial flaw size, a_o, is arbitrarily characterized by the vertical distance along the uphill side penetration bore, from the inside surface of the cladding to the weld-to-butter/head interface, as shown Figure 2-1. For the "constant depth" J-groove design used for the Shearon Harris head, this same flaw depth is also used for the downhill side flaw evaluations.
2. Develop finite element models of the reactor vessel head in the vicinity of the outermost nozzle penetration, with crack tip elements along the interface between the Alloy 82/182 butter and the low alloy steel base metal. These models will be used to obtain stress intensity factors at various positions along the crack front for linearly superimposed residual and operating stresses.
3. Develop a mapping procedure to transfer stresses from an uncracked finite element stress model to the crack face of each crack model. This will enable stress intensity factors to be calculated for arbitrary stress distributions over the crack face utilizing the principle of superposition.
4. Calculate fatigue crack growth, in one year increments, for cyclic loading conditions using operational stresses from pressure and thermal loads. Since the stresses used in the fatigue crack growth analysis are the combined residual plus operating stresses, the effect of the residual stresses on fatigue crack growth is captured by the R ratio, or K_{min}/K_{max}. Starting from the stress intensity factor calculated by the finite element crack model for the initial flaw size, stress intensity factors are updated for each increment of crack growth by the square root of the flaw size.
5. Utilize the screening criteria of ASME Code Section XI, Appendix C to determine the failure mode and appropriate method of analysis (LEFM, EPFM, or limit load) for flaws in ferritic materials, considering the applied stress, temperature, and material toughness. For LEFM flaw evaluations, compare the stress intensity factor at the final flaw size to the available fracture toughness, with appropriate safety factors, as discussed in Section 2.2. When the material is more ductile and EPFM is the appropriate analysis method, evaluate flaw stability and crack driving force as described in Section 2.3. A primary stress limit analysis would be performed to satisfy the primary stress limits of the ASME Code, as described in Section 2.3.2.

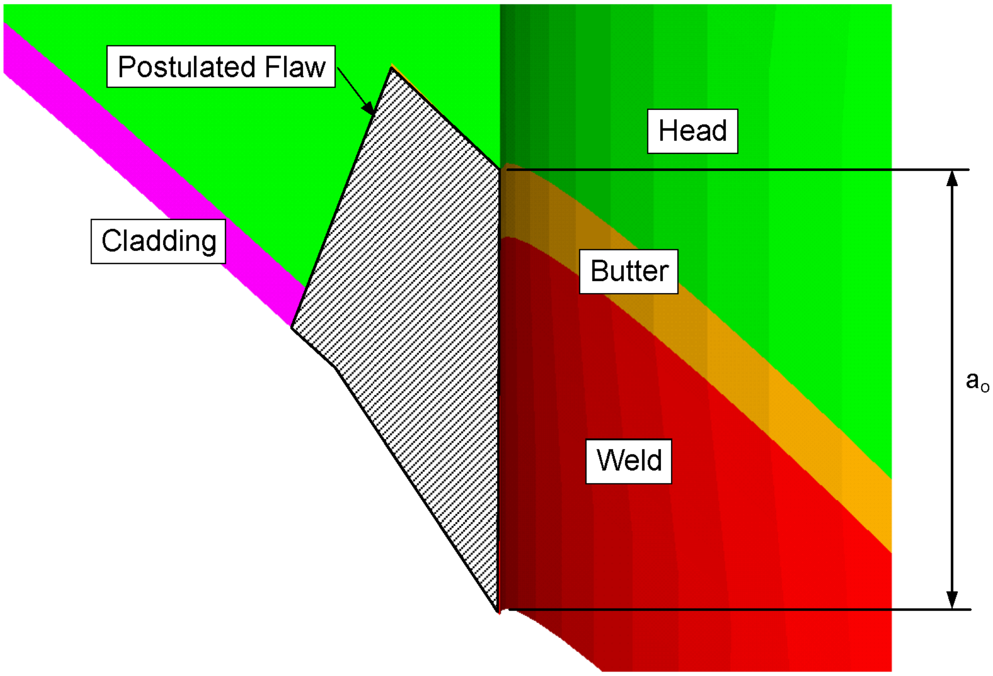

Figure 2-1: Postulated Radial Flaw on Uphill Side

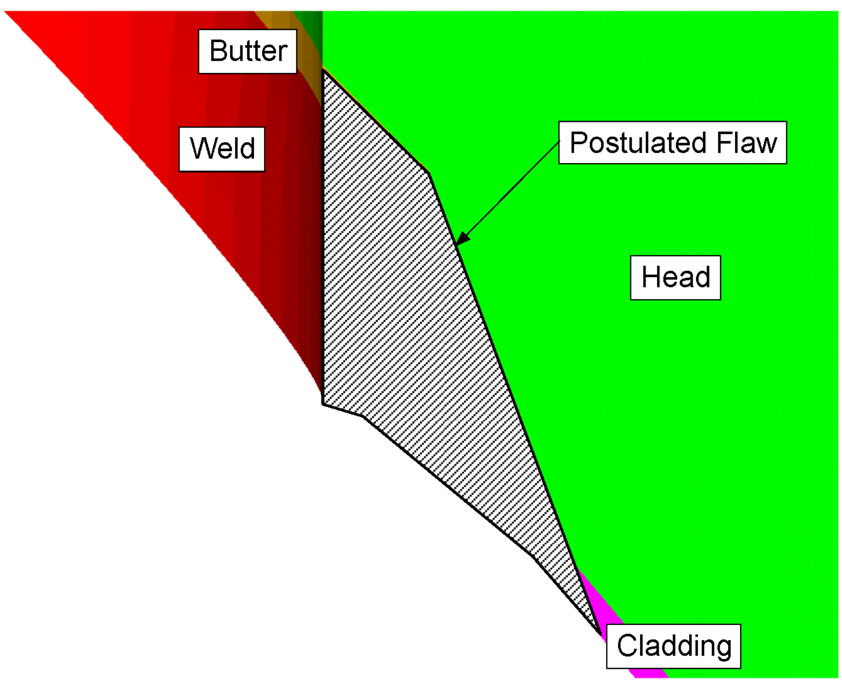

Figure 2-2: Postulated Radial Flaw on Downhill Side

2.1 Stress Intensity Factor Solution

Stress intensity factors for corner flaws at a non-radial nozzle penetration are best determined by finite element analysis using three-dimensional models with crack tip elements along the crack front. Although loads can be applied to finite element crack models like any other structural model, the crack models were developed to serve as a flaw evaluation tool that could accept stresses from separate stress analyses. This strategy makes it possible, for example, to obtain pressure and thermal stresses from an independent thermal/structural analysis and then transfer these stresses to a crack model for flaw evaluations. Using the principle of superposition common to fracture mechanics analysis, the only stresses that need be considered for these flaw evaluations are the stresses on the crack face. A mapping procedure is developed to transfer stresses from a separate stress analysis to the crack face of the crack model.

2.1.1 Finite Element Crack Models

Three-dimensional finite element models are developed for the reactor vessel head in the vicinity of the outermost nozzle penetration, by modeling a portion of the head, cladding, and butter with the ANSYS finite element computer program [5]. Since stresses increase with penetration angle, it is conservative to base the finite element models on the outermost nozzle penetration.

A three-dimensional finite element model is first constructed to represent an unflawed non-radial nozzle penetration in the reactor vessel head using the ANSYS SOLID186 20-node structural element. Elements along the crack front are then replaced by a sub-model of crack tip elements along the interface between the Alloy 82/182 butter and the low alloy steel base metal. These elements consist of 20-node isoparametric elements that are collapsed to form a wedge with the appropriate mid-side nodes shifted to quarter-point locations to simulate the singularity at the crack tip. The final crack models are shown in Figure 2-3 and Figure 2-4 for the uphill and downhill sides of the nozzle, respectively.

Stress intensity factors will be obtained using the ANSYS CINT contour integral procedure at 17 positions along each crack front, as indicated in Figure 2-3 and Figure 2-4 for the two crack models. Position 1 is located on the cladding surface, Position 3 at the cladding/base metal interface, Position 11 at the “kink” in the crack profile, and Position 17 is at the bored surface in the head.

2.1.2 Stress Mapping

Stresses from the finite element stress model are mapped onto the crack faces of the uphill and downhill finite element crack models (Figure 2-3 and Figure 2-4). An ANSYS scripting language instruction (macro) has been developed to query the residual and operating stress models for nodal locations associated with each crack face node of the crack model. The nodal stress from the stress model is then transferred to the corresponding node on the crack model.

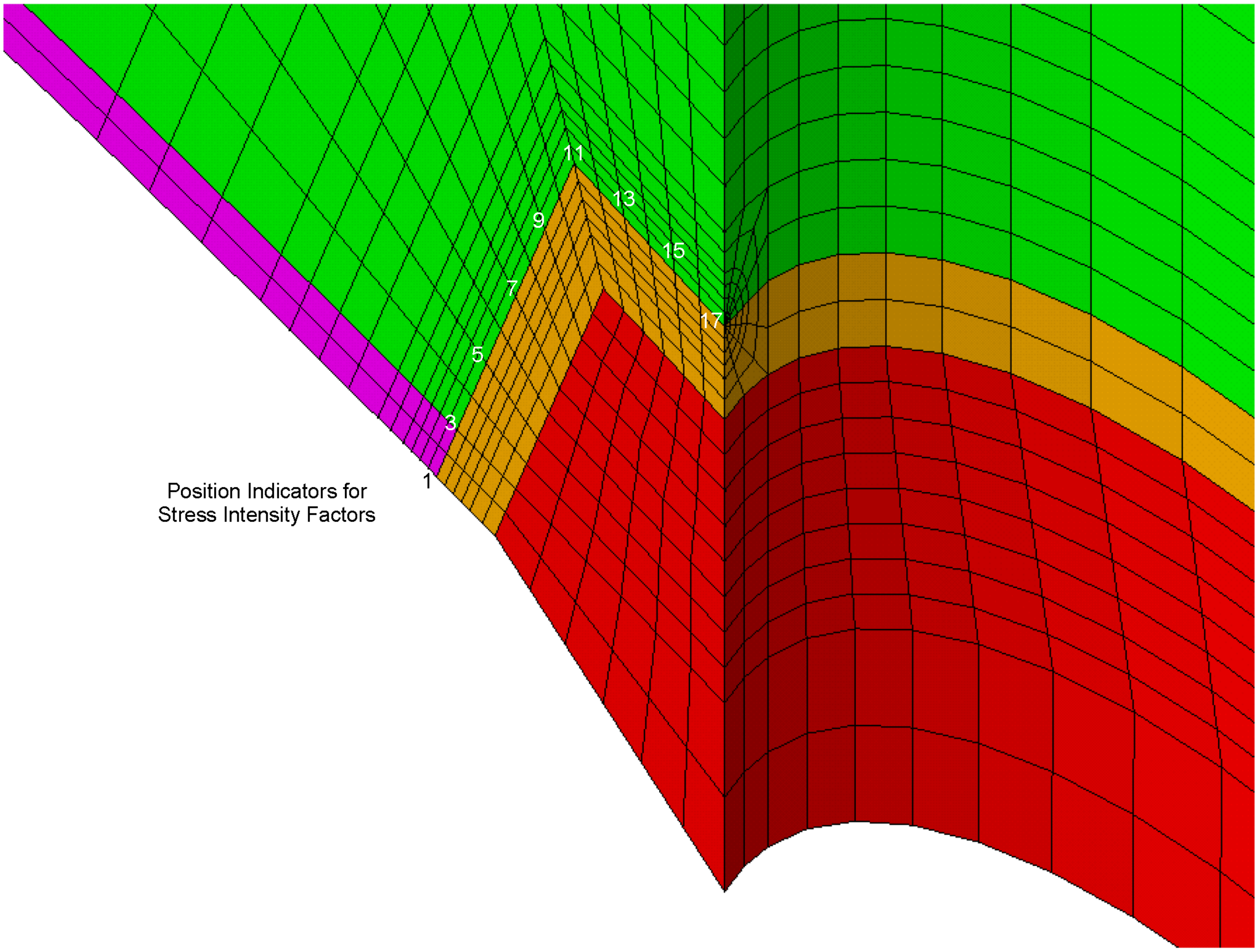

Figure 2-3: Finite Element Crack Model – Uphill Side

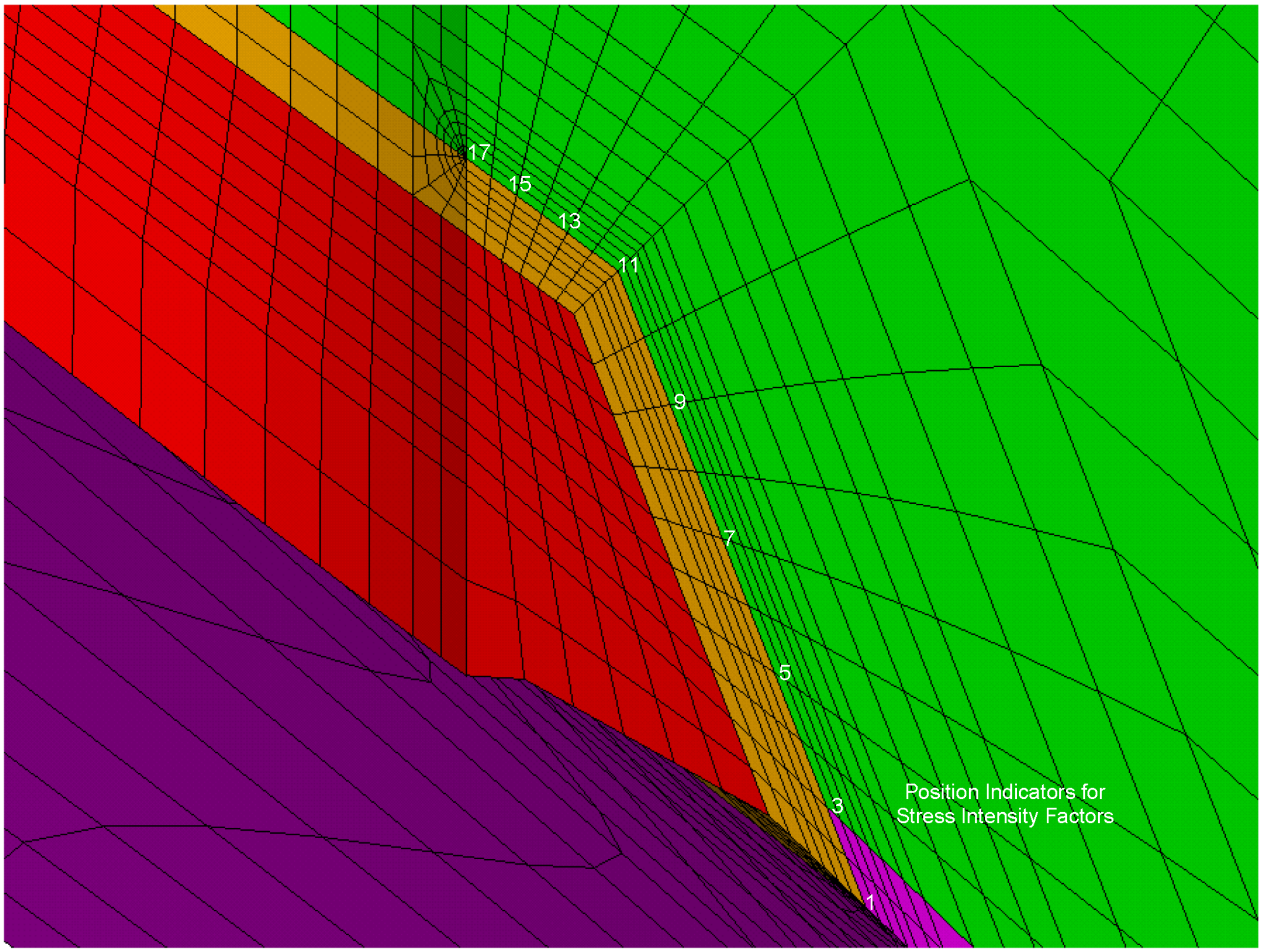

Figure 2-4: Finite Element Crack Model – Downhill Side

2.1.3 Crack Growth Considerations

The fundamental expression for the crack tip stress intensity factor is

$$K_I = \sigma\sqrt{\pi a}$$

Since each crack model is developed for a single flaw size, stress intensity factors are updated at each increment of crack growth by the square root of the flaw size; i.e.,

$$K_I(a_{i+1}) = K_I(a_i)\sqrt{\frac{a_{i+1}}{a_i}},$$

where a = flaw size

i = increment of crack growth.

Since the stress intensity factor is directly proportional to the magnitude of the stress and both residual and operating stresses decrease in the direction of crack growth, this procedure produces conservative estimates of stress intensity factor as the crack extends into the head and stresses diminish over the expanding crack face.

2.1.4 Plastic Zone Correction

The Irwin plasticity correction is used to account for a moderate amount of yielding at the crack tip. For plane strain conditions, this correction is

$$r_y = \frac{1}{6\pi}\left(\frac{K_I(a)}{\sigma_y}\right)^2, \qquad \text{[Ref. 6, Eqn. (2.63)]}$$

where $K_I(a)$ = stress intensity factor based on the actual crack size, a

σ_y = material yield strength.

A stress intensity factor, $K_I(a_e)$, is then calculated for an effective crack size,

$$a_e = a + r_y,$$

based on the same scaling technique utilized for crack growth; i.e,

$$K_I(a_e) = K_I(a)\sqrt{\frac{a_e}{a}}.$$

2.2 Linear Elastic Fracture Mechanics

Section XI, Article IWB-3612 [11] requires that the applied stress intensity factor, K_I, at the final flaw size be less than the available fracture toughness at the crack tip temperature, with appropriate safety factors, as outlined below.

Normal Conditions: $K_I < K_{Ia} / \sqrt{10}$

where K_{Ia} is the fracture toughness based on crack arrest.

Faulted Conditions: $K_I < K_{Ic} / \sqrt{2}$

where K_{Ic} is the fracture toughness based on crack initiation.

Section XI, Article IWB-3613 [11] provides alternate fracture toughness requirements for shell regions near structural discontinuities, such as nozzle penetrations, when the pressure does not exceed 20% of the design pressure and the temperature is not less than RT_{NDT} + 60 °F. Within these operational limits a lower safety factor may be used to evaluate fracture toughness margin. For the Shearon Harris Unit 1 reactor vessel head, the design pressure is [ ] psig [13] and the fracture toughness reference temperature is [ ] [9]. Thus for pressures at or below [ ] psig and crack tip temperatures at or above [ ] the acceptance criterion for applied stress intensity factor is as follows:

At pressures ≤ [ ] psig and temperatures ≥ [ ]

$$K_I < K_{Ia} / \sqrt{2}$$

2.3 Elastic-Plastic Fracture Mechanics

Elastic-plastic fracture mechanics (EPFM) will be used as alterative acceptance criteria when the flaw related failure mechanism is unstable ductile tearing. This type of failure falls between rapid, non-ductile crack extension and plastic collapse. Linear elastic fracture mechanics (LEFM) would be used to assess the potential for non-ductile failure, whereas primary stress limit analysis would be used to check for plastic collapse.

2.3.1 Screening Criteria

Screening criteria for determining failure modes in ferritic materials may be found in Appendix C of Section XI. Although Appendix C, Article C-4221 [11] contains specific rules for evaluating flaws in Class 1 ferritic piping, its screening criteria may be adapted to other ferritic components, such as the reactor vessel head, as follows:

Let,

$$K_r' = K_{Iapp} / K_{Ic}$$

$$S_r' = \sigma_{max} / \sigma_f$$

Then the appropriate method of analysis is determined by the following limits:

LEFM Regime:	$K_r' / S_r' \geq 1.8$
EPFM Regime:	$1.8 > K_r' / S_r' \geq 0.2$
Limit Load Regime:	$0.2 > K_r' / S_r'$

2.3.2 Primary Stress Limit Analysis

While in most instances the screening criteria identify EPFM as the appropriate method of analysis, there are cases where low stress intensity factors (K_r') relative to the applied stress (S_r') places the analysis in the limit load regime. Such cases are analyzed through consideration of the primary stress limits of ASME Code Section III as embodied in the equation in Article NB-3324 [7] for the minimum required thickness (t_{min}) of the spherical closure head,

$$t_{min} = \frac{PR_o}{2S_m},$$

where

P = design pressure, [ ] psig [13]

R_o = outside radius, [ ] [1]

S_m = design stress intensity, 26.7 ksi [12]

A conservative primary stress limit analysis would be to limit the remaining net-section of the head after “removal” of the final volume of weld material (after fatigue crack growth) to the minimum required design thickness, t_{min}. This is equivalent to removing a uniform depth of material along the inner surface of the vessel to encompass the final flaw and comparing the remaining thickness to

$$t_{min} = 3.74 \text{ in.}$$

2.3.3 Flaw Stability and Crack Driving Force

Elastic-plastic fracture mechanics analysis will be performed using a J-integral/tearing modulus (J-T) diagram to evaluate flaw stability under ductile tearing, where J is either the applied (J_{app}) or the material (J_{mat}) J-integral, and T is the tearing modulus, defined as $(E/\sigma_f^2)(dJ/da)$. The crack driving force, as measured by J_{app}, is also checked against the J-R curve at a crack extension of 0.1 inch ($J_{0.1}$). Consistent with industry practice for the evaluation of flaws in partial penetration welds used to attach nozzles to vessels, different safety factors will be utilized for primary and secondary loads. Flaw stability assessments for normal and upset conditions will consider a safety factor of 3 on the stress intensity factor due to primary (pressure) stresses and a safety factor of 1.5 for secondary (residual plus thermal) stresses. The crack driving force will be calculated using safety factors of 1.5 and 1 for primary and secondary stresses, respectively. For EPFM analysis of faulted conditions, safety factors of 1.5 and 1 will be used for flaw stability assessments and 1.5 and 1 for evaluations of crack driving force.

The general methodology for performing an EPFM analyses is outlined below.

Let $E' = E/(1-\nu^2)$

Final flaw depth = a

Total applied K_I = K_{Iapp}

K_I due to pressure (primary) = K_{Ip}

K_I due to residual plus thermal (secondary) = $K_{Is} = K_{Iapp} - K_{Ip}$

Safety factor on primary loads = SF_p

Safety factor on secondary loads = SF_s

For small scale yielding at the crack tip, a plastic zone correction is used to calculate an effective flaw depth based on

$$a_e = a + [1/(6\pi)]\ [\ (K_{Ip} + K_{Is})\ /\ \sigma_y\ ]^2,$$

which is used to update the stress intensity factors based on

$$K'_{Ip} = K_{Ip}\sqrt{\frac{a_e}{a}}$$

and

$$K'_{Is} = K_{Is}\sqrt{\frac{a_e}{a}}\ .$$

The applied J-integral is then calculated using the relationship

$$J_{app} = (SF_p{*}K'_{Ip} + SF_s{*}K'_{Is})^2/E'.$$

The final parameter needed to construct the J-T diagram is the tearing modulus. The applied tearing modulus, T_{app}, is calculated by numerical differentiation for small increments of crack size (da) about the final crack size (a), according to

$$T_{app} = \frac{E}{\sigma_f^2}\left[\frac{J_{app}(a+da) - J_{app}(a-da)}{2(da)}\right].$$

Using the power law expression for the J-R curve,

$$J_R = C(\Delta a)^m,$$

the material tearing modulus, T_{mat}, can be expressed as

$$T_{mat} = (E/\sigma_f^2)Cm(\Delta a)^{m-1}.$$

Constructing the J-T diagram,

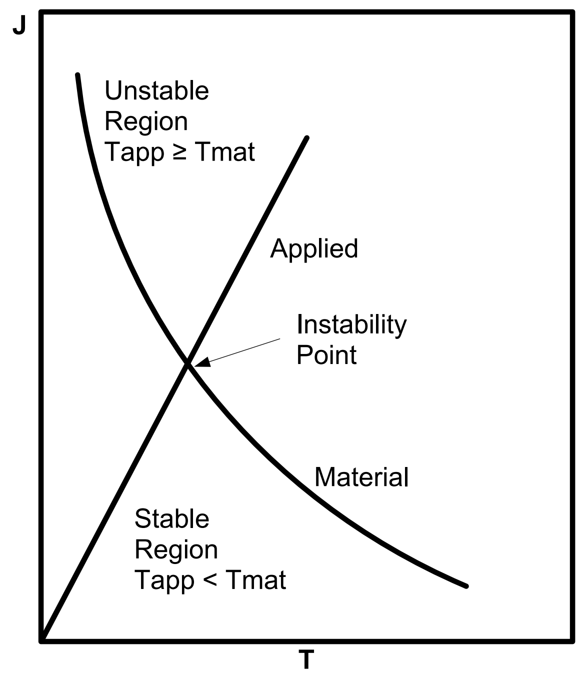

flaw stability is demonstrated at an applied J-integral when the applied tearing modulus is less than the material tearing modulus. Alternately, the applied J-integral is less than the J-integral at the point of instability.

To complete the EPFM analysis, it must be shown that the applied J-integral is less than $J_{0.1}$, demonstrating that the crack driving force falls below the J-R curve at a crack extension of 0.1 inch.

3.0 ASSUMPTIONS

This section discusses assumptions and modeling simplifications applicable to the present analysis.

3.1 Unverified Assumptions

This analysis contains the following two assumptions used in Appendix C for Nozzles 30, 40 and 51 that must be verified before structural integrity of the ASME Code Class 1 Reactor Vessel is assured.

1) The RV head wall thickness at any of the three penetrations (30, 40 and 51) is assumed to be no less than [ ] inches.

2) The J-groove weld size (in terms of cross-sectional area) of penetration 37 is assumed for penetrations 30 and 40; the J-groove weld size of penetration 49 is assumed for penetration 51.

3.2 Justified Assumptions

The austenitic cladding is assumed to be adequately represented by 18Cr-8Ni (Type 304) stainless steel material.

In the body of the document, the size of the J-groove weld prep and the thickness of the buttering are based on nominal dimensions. This is considered to be standard practice in stress analysis and fracture mechanics analysis. It is conservatively assumed that the postulated flaw extends through the entire J-groove weld and butter.

In Appendix C, the crack growth areas at the three penetrations 30, 40 and 51 are estimated by the crack growth areas at Nozzles 14 and 37 (Figures C8 to C10). A review of Figures C8 to C10 indicates that closer the nozzle to the head center higher the crack growth area results. Therefore the crack growth area of Nozzle 14 for 15 years operation is taken as the bounding case for the three nozzles. A linear crack grown is assumed in the 15 years which is conservative, as the crack grown area in earlier years is less than that in later years.

3.3 Modeling Simplifications

The finite element computer models used to generate residual stresses do not include the ID temper bead repair weld. This is deemed to be an appropriate modeling simplification since compressive stresses induced in the material adjacent to the repair weld would lower stresses on the uphill side of the J-groove weld (in close proximity to the repair weld) and have negligible effect on the downhill side of the J-groove weld (far removed from the repair weld).

4.0 DESIGN INPUTS

This section provides basic input data needed to perform a fatigue crack growth analysis and a flaw evaluation of the final flaw size.

4.1 Materials

4.1.1 Mechanical and Thermal Properties

Table 4-1, Table 4-2, and Table 4-3 list the temperature dependent values of modulus of elasticity (E), Poisson's ratio (ν), and coefficient of thermal expansion (α) properties used in the finite element crack models. These properties are obtained from the ASME Code, Section II [8], except for Poisson's ratio, where 0.3 is a typical value used in structural analysis. The flow stress in Table 4-1 is the average of the yield and ultimate strengths.

Component	Material
Head	SA-533, Grade B Class 1 [Ref. 2, Par. 6.1.1]
Cladding	use Type 304 stainless steel (SA-240)
J-groove weld filler	Equivalent to Alloy 600, SB-167 [Ref. 2, Par. 6.1.5]
J-groove weld butter	use Alloy 600, SB-167

Table 4-1: Material Properties for Head

Component	Head					
Material	SA-533 Grade B Class 1 (Mn-$^1/_2$Mo-$^1/_2$Ni)					
Temperature	E (10^6 psi)	ν	α (10^{-6} in./in./^{o}F)	σ_y (ksi)	σ_u (ksi)	σ_f (ksi)
70	29.20	0.3	7.0	50.0	80.0	65.0
100	29.04	0.3	7.1	50.0	80.0	65.0
150	28.77	0.3	7.2	48.1	80.0	64.1
200	28.50	0.3	7.3	47.0	80.0	63.5
250	28.25	0.3	7.3	46.2	80.0	63.1
300	28.00	0.3	7.4	45.5	80.0	62.8
350	27.70	0.3	7.5	44.9	80.0	62.4
400	27.40	0.3	7.6	44.2	80.0	62.1
450	27.20	0.3	7.6	43.7	80.0	61.9
500	27.00	0.3	7.7	43.2	80.0	61.6
550	26.70	0.3	7.8	42.7	80.0	61.3
600	26.40	0.3	7.8	42.1	80.0	61.1
650	25.85	0.3	7.9	41.5	80.0	60.8
700	25.30	0.3	7.9	40.7	80.0	60.4

Table 4-2: Material Properties for Weld Metal

Component	Weld Butter and Weld Filler		
Material	Use Alloy 600, SB-167 (72Ni-15Cr-8Fe) – UNS N06600		
Temperature	E (10^6 psi)	ν	α (10^{-6} in./in./°F)
70	31.00	0.3	6.8
100	30.82	0.3	6.9
150	30.51	0.3	7.0
200	30.20	0.3	7.1
250	30.00	0.3	7.2
300	29.80	0.3	7.3
350	29.65	0.3	7.4
400	29.50	0.3	7.5
450	29.25	0.3	7.6
500	29.00	0.3	7.6
550	28.85	0.3	7.7
600	28.70	0.3	7.8
650	28.45	0.3	7.8
700	28.20	0.3	7.9

Table 4-3: Material Properties for Cladding

Component	Cladding		
Material	Use Type 304 Stainless Steel (18Cr-8Ni)		
Temperature	E (10^6 psi)	ν	α (10^{-6} in./in./°F)
70	28.30	0.3	8.5
100	28.14	0.3	8.6
150	27.87	0.3	8.8
200	27.60	0.3	8.9
250	27.30	0.3	9.1
300	27.00	0.3	9.2
350	26.75	0.3	9.3
400	26.50	0.3	9.5
450	26.15	0.3	9.6
500	25.80	0.3	9.7
550	25.55	0.3	9.8
600	25.30	0.3	9.8
650	25.05	0.3	9.9
700	24.80	0.3	10.0

4.1.2 Toughness Properties

The reference temperature for nil-ductility transition for the SA-533 Grade B Class 1 plate material in the dome portion of the Shearon Harris reactor vessel closure head is reported as RT_{NDT} = [ ] [9] and the Charpy upper-shelf energy is [ ] [9] in the transverse (weak) direction. Based on the welding procedure qualification record [10] for the ID temperature bead weld, a temperature of +5 °F should be added to the RT_{NDT} of the base material to account for embrittlement in the heat affected zone, so that the effective RT_{NDT} is [ ] for flaw evaluations in the head.

4.1.3 Fracture Toughness

From Article A-4200 of Section XI [11], the lower bound K_{Ia} fracture toughness for crack arrest can be expressed as

$$K_{Ia} = 26.8 + 12.445 \exp [0.0145 (T - RT_{NDT})],$$

where T is the crack tip temperature, RT_{NDT} is the reference nil-ductility temperature of the material, K_{Ia} is in units of ksi√in, and T and RT_{NDT} are in units of °F. In the present flaw evaluations, K_{Ia} is limited to a maximum value of 200 ksi√in (upper-shelf fracture toughness). Using the above equation with an RT_{NDT} of [ ] K_{Ia} equals 200 ksi√in at a crack tip temperature of [ ] .

A higher measure of fracture toughness is provided by the K_{Ic} fracture toughness for crack initiation, approximated in Article A-4200 of Section XI [11] by

$$K_{Ic} = 33.2 + 20.734 \exp [0.02 (T - RT_{NDT})].$$

4.1.4 J-integral Resistance Curve

The J-integral resistance (J-R) curve, needed for the EPFM method of analysis, is obtained from the following power law expression for nuclear reactor pressure vessel steels,

$$J_R = C(\Delta a)^m,$$

where the coefficient, C, and exponent, m, depend on the Charpy V-notch upper-shelf energy, CVN, and the flow stress, σ_o or σ_f, as shown in Figure 4-1 and Figure 4-2.

Using the above referenced Charpy V-notch upper-shelf energy correlation for the J-integral resistance curve with a Charpy V-notch upper-shelf energy of [ ] the coefficients of the power law equation over a wide range of temperatures are:

C = [ ]

m = [ ]

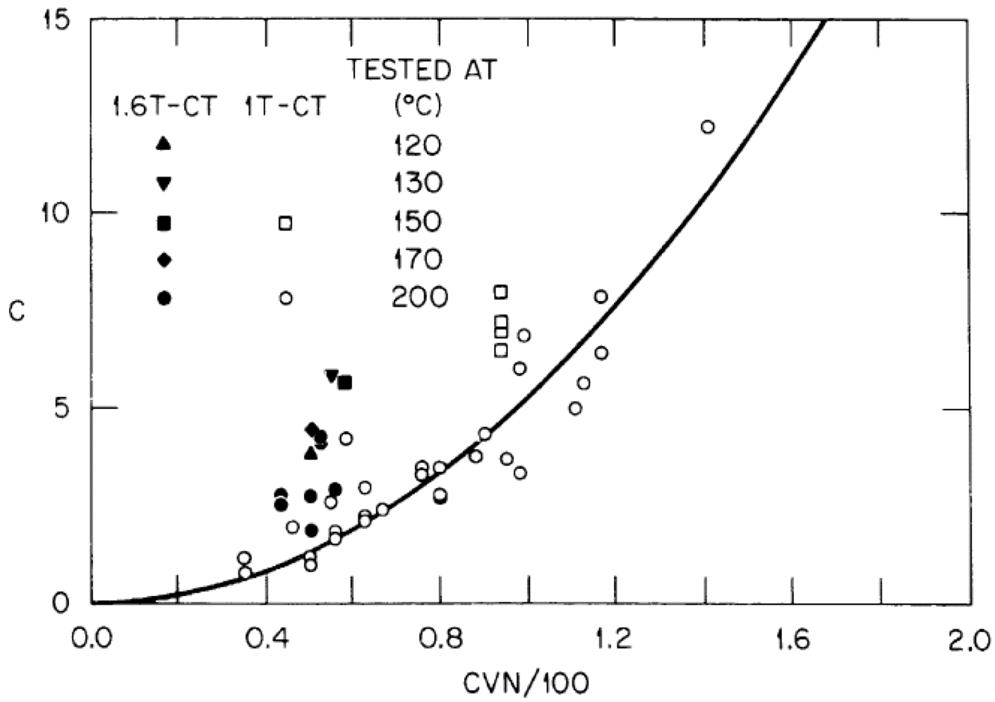

Figure 4-1: Correlation of Coefficient, C, of Power Law with Charpy V-Notch Upper Shelf Energy

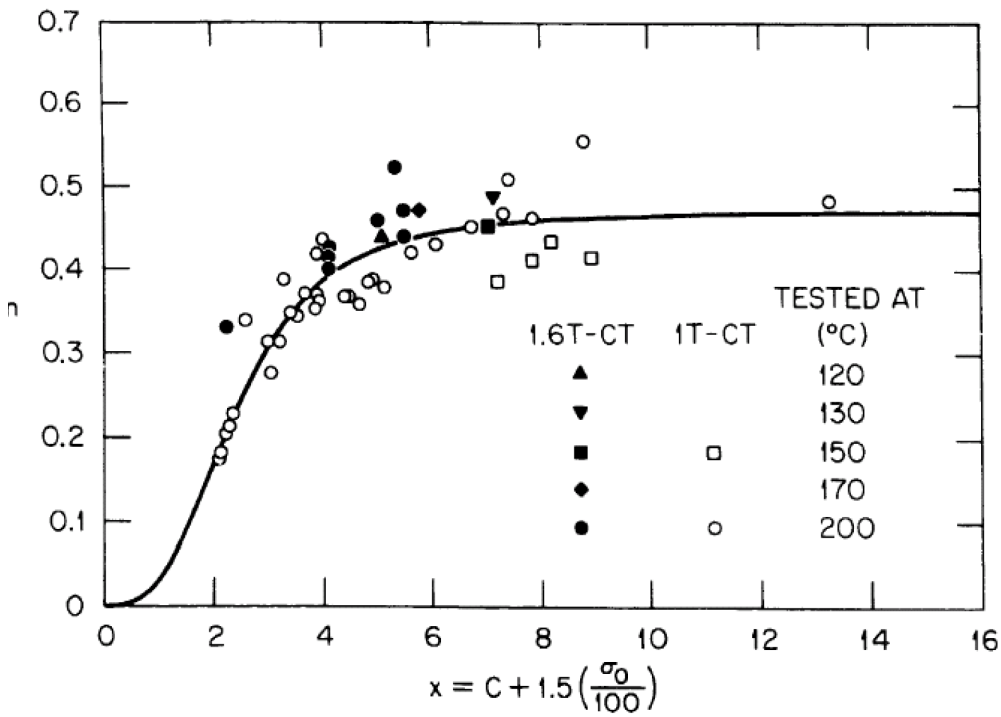

Figure 4-2: Correlation of Exponent, m, of Power Law with Coefficient, C, and Flow Stress, σ_o

4.1.5 Fatigue Crack Growth Rate

Flaw growth due to cyclic loading is calculated using the fatigue crack growth rate model from Article A-4300 of Section XI [11],

$$\frac{da}{dN} = C_o (\Delta K_I)^n ,$$

where ΔK_I is the stress intensity factor range in ksi√in and da/dN is in inches/cycle. The crack growth rates for a surface flaw will be used for the evaluation of the corner crack since it is assumed that the degraded condition of the J-groove weld and butter exposes the low alloy steel head material to the primary water environment.

The following equations from Section XI [11] are used to model fatigue crack growth.

$$\Delta KI = KI_{max} - KI_{min}$$
$$R = KI_{min} / KI_{max}$$

$0 \leq R \leq 0.25$: $\Delta K_I < 17.74$,

$$n = 5.95$$
$$C_o = 1.02 \times 10^{-12} \times S$$
$$S = 1.0$$

$\Delta K_I \geq 17.74$,

$$n = 1.95$$
$$C_o = 1.01 \times 10^{-7} \times S$$
$$S = 1.0$$

$0.25 \leq R \leq 0.65$: $\Delta K_I < 17.74 \, [\, (3.75R + 0.06) / (26.9R - 5.725) \,]^{0.25}$,

$$n = 5.95$$
$$C_o = 1.02 \times 10^{-12} \times S$$
$$S = 26.9R - 5.725$$

$\Delta K_I \geq 17.74 \, [\, (3.75R + 0.06) / (26.9R - 5.725) \,]^{0.25}$,

$$n = 1.95$$
$$C_o = 1.01 \times 10^{-7} \times S$$
$$S = 3.75R + 0.06$$

$0.65 \leq R < 1.0$: $\Delta K_I < 12.04$,

$$n = 5.95$$
$$C_o = 1.02 \times 10^{-12} \times S$$
$$S = 11.76$$

$\Delta K_I \geq 12.04$,

$$n = 1.95$$
$$C_o = 1.01 \times 10^{-7} \times S$$
$$S = 2.5$$

4.2 Basic Geometry

The reactor vessel head and CRDM nozzle penetration are described by the following key dimensions:

Spherical radius to base metal	= [ ]	in. [9]
Head thickness	= [ ]	in. [9]
Cladding thickness	= [ ]	in. [9]
Butter thickness	= [ ]	in. [9]
Penetration bore	= [ ]	in. [9]
Horizontal radius to outermost penetration	= [ ]	in. [9]
Penetration angle at outermost nozzle	= [ ]	deg. (derived*)

* ($\sin^{-1}$(horizontal radius/spherical radius))

4.3 Operating Transients

Based on bounding transients developed for the companion ASME Code Section III fatigue stress analysis [12], fatigue crack growth will be calculated for the normal and upset condition transients listed in Table 4-4. Since crack growth will be calculated in one-year increments, the number of cycles is obtained by dividing the forty-year design life cycles by 40. While not physically meaningful, a fractional yearly cycle count is computationally acceptable since it is merely used to determine an increment of crack growth from a calculated value of da/dN.

Table 4-5 lists the emergency and faulted condition transients applicable to Shearon Harris reactor vessel components [13]. From a review of the pressure and temperature time-history definitions for these transients, it is clear that the large LOCA and large steam line break transients would bound the remaining transients for emergency and faulted condition flaw evaluations.

Table 4-4: Bounding Transients for Normal and Upset Conditions

[ ]

Table 4-5: Emergency and Faulted Condition Transients

[ ]

* Bounding transients to be considered in emergency and faulted condition flaw evaluations

4.4 Applied Stresses

Two sources of applied stress are considered for the present flaw evaluations, residual stresses from welding and stresses that occur during plant operation.

4.4.1 Residual Stresses

Residual stresses are obtained from a three-dimensional elastic-plastic finite element stress analysis [3] that simulates fabrication of the outermost nozzle to head partial penetration weld and the effect of subsequent hydrostatic tests and operating cycles on stresses in the welded joint. It is widely accepted that stresses at the outermost CRDM nozzle location conservatively bound stresses at all other nozzle locations exhibiting a smaller penetration angle (the angle between the nozzle and inside surface of the head on the downhill side of the penetration). Stresses are transferred from the finite element residual stress model in the form of nodal arrays contained in ANSYS parameter save files.

4.4.2 Operating Stresses

Operating stresses are obtained from the three-dimensional finite element stress analysis [12] used to qualify the nozzle repair to ASME Code Section III requirements. Hoop stresses from the Section III analysis are conservatively superimposed on the residual stresses to represent the crack face opening stresses during operation. Stresses are transferred from the finite element operating stress model in the form of nodal arrays contained in ANSYS parameter save files. Pressure is added to the operating stresses to account for the additional loading on the crack face due to pressure.

5.0 COMPUTER USAGE

This section describes computer resources, software testing, and stored computer files.

5.1 Hardware/Software

[ ]

5.2 Installation/Validation Test

[ ]

Table 5-1: Test Case Results

Verification Problem VM256

Fracture Mechanics Analysis of a Crack in a Plate

File: vm256.vrt

```
---------------------------------------- VM256 RESULTS COMPARISON ----------------------------------------

                  |  TARGET  |  ANSYS  |  RATIO

*******************************************************************************
              USING PLANE 183 ELEMENT (2-D ANALYSIS)
*******************************************************************************
        KI          1.0249      1.0038      0.979

*******************************************************************************
              USING SOLID 185 ELEMENT (3-D ANALYSIS)
*******************************************************************************
        KI          1.0249      1.0383      1.013

*******************************************************************************
      USING SOLID 186 ELEMENT - SURFACE CRACK (3-D ANALYSIS)
*******************************************************************************
        KI          1.4000      1.4132      1.009

-----------------------------------------------------------------------------------------------------------
```

5.3 Computer Files

The computer files listed below are stored in the AREVA ColdStor repository in the directory "\cold\41304\32-9176350-000\official".

ANSYS Models

File Name	Description	ColdStor Storage Date	ColdStor Storage Time	Checksum
[ ]	[ ]	04-15-12	09:01:06	22856
[ ]	[ ]	04-15-12	09:00:56	18509

ANSYS Macros

File Name	Description	ColdStor Storage Date	ColdStor Storage Time	Checksum
[ ]	[ ]	04-15-12	09:01:22	15845
[ ]	[ ]	04-15-12	09:01:21	11056

ANSYS Input Files

File Name	Description	ColdStor Storage Date	ColdStor Storage Time	Checksum
[ ]	[ ]	04-15-12	09:01:42	32454
[ ]	[ ]	04-15-12	09:01:41	08793

ANSYS Result Files for Uphill Stress Intensity Factors

File Name	Loading Condition	ColdStor Storage Date	ColdStor Storage Time	Checksum
		04-15-12	09:04:35	22371
		04-15-12	09:04:07	16344
		04-15-12	09:04:03	19578
		04-15-12	09:04:10	45340
		04-15-12	09:04:10	36382
		04-15-12	09:04:09	50736
		04-15-12	09:04:08	46959
		04-15-12	09:04:09	35163
		04-15-12	09:04:07	46631
		04-15-12	09:04:04	15882
		04-15-12	09:04:05	54622
		04-15-12	09:04:08	25345
		04-15-12	09:04:04	17221
		04-15-12	09:04:03	01071
		04-15-12	09:04:06	55706
		04-15-12	09:04:05	62230
		04-15-12	09:04:06	06099

ANSYS Result Files for Downhill Stress Intensity Factors

File Name	Loading Condition	ColdStor Storage Date	ColdStor Storage Time	Checksum
		04-15-12	09:04:34	59428
		04-15-12	09:03:13	59492
		04-15-12	09:03:10	49475
		04-15-12	09:03:16	50217
		04-15-12	09:03:17	37165
		04-15-12	09:03:16	34304
		04-15-12	09:03:15	19734
		04-15-12	09:03:16	29947
		04-15-12	09:03:14	23156
		04-15-12	09:03:11	35585
		04-15-12	09:03:12	60112
		04-15-12	09:03:15	42106
		04-15-12	09:03:11	65275
		04-15-12	09:03:10	04872
		04-15-12	09:03:13	36168
		04-15-12	09:03:12	09825
		04-15-12	09:03:13	31095

Excel Spreadsheets

File Name	Description	ColdStor Storage Date	ColdStor Storage Time	Checksum
[		04-15-12	09:06:58	58102
		04-15-12	09:06:57	00505
		04-15-12	09:06:57	38955
		04-15-12	09:06:57	63694
		04-15-12	09:06:56	21575
	]	04-15-12	09:06:56	25218

ANSYS Test Cases

File Name	Description	ColdStor Storage Date	ColdStor Storage Time	Checksum
[ ]	[ ]	04-15-12	09:07:25	49343

6.0 CALCULATIONS

Propagation of a postulated initial flaw in the J-groove weld and butter is calculated to determine the final flaw size after 30 years of service. Flaw evaluations are then performed to assess the acceptability of the final flaw size.

6.1 Initial Flaw Size

It is both difficult and unnecessary to prescribe initial flaw sizes for the "non-classical" flaw shapes comprising the postulated uphill and downhill flaws in the J-groove weld and butter. Since the explicit finite element crack models described in Section 2.1.1 were developed to realistically capture the basic geometry of the J-shaped flaws, any characteristic dimension of the flaws may be used to track flaw growth during cyclic fatigue. The "constant depth" J-groove design suggests that a common value can be utilized to describe the initial depth of the uphill and downhill flaws. Accordingly, the vertical distance along the uphill side penetration bore, from the inside surface of the cladding to the weld-to-butter/head interface, is used to define the initial flaw size, a_o (as shown Figure 2-1). From the uphill crack model, the initial flaw size value is determined to be 2.1482″.

As discussed in Section 2.1.3, crack tip stress intensity factors are calculated directly from the finite element crack models for the initial flaw size and then updated based on incremental crack growth according to

$$K_I(a_{i+1}) = K_I(a_i)\sqrt{\frac{a_{i+1}}{a_i}},$$

so that after the first increment of crack growth,

$$K_I(a_i) = K_I(a_0)\sqrt{\frac{a_1}{a_0}}.$$

6.2 Fatigue Crack Growth

Although it is believed that a PWSCC flaw would be confined to the J-groove weld and butter, it is postulated that a fatigue flaw would initiate in the low alloy steel head, combine with the PWSCC flaw, and propagate farther into the head under cyclic loads. Fatigue crack growth is calculated from finite element based stress intensity factors using residual and operational stresses from References [3] and [12], respectively. The actual flaw growth calculations are presented in Appendix A for the uphill flaw and Appendix B for the downhill flaw, along with a comparison of the final stress intensity factor for each transient with the fracture toughness requirements of Section XI. Table 6-1 and Table 6-2 summarize the flaw growth analyses for the uphill and downhill sides of the flaw, respectively. These tables serve several purposes; they present the final flaw size at the end the design life, they compare stress intensity factors at the final flaw size with LEFM acceptance criteria, and they serve as a means of screening for the worst case loading conditions and stress intensity factors for subsequent EPFM analysis.

Crack growth is calculated in one-year increments for each of the analyzed transients, while uniformly distributing the growth over the service life by linking the yearly crack growth between the crack growth tables in Appendix A for the uphill flaw and the tables in Appendix B for the downhill flaw.

Stress intensity factors are provided in the crack growth tables for all locations along the postulated crack fronts, including the cladding. It is apparent from the tables in Appendix A that on the uphill side of the penetration, the highest stress intensity factors in the low alloy steel head occur near the cladding surface (Position 3) for residual stresses and near the penetration bore (Position 16) for operating stresses. It is noted that due to residual tensile strain in the cladding material, cladding stresses and the associated stress intensity factors may be higher than those in the adjacent head material. However, stress intensity factors within the stainless steel cladding portion of the crack front need not be considered in the evaluation of the potential for non-ductile failure of the low alloy steel head. Fatigue crack growth analysis performed for both Position 3 and 16 showed that the operating stresses controlled, producing higher final stress intensity factors at Position 16. Thus Position 16 on the uphill side will be used to calculate fatigue crack growth and evaluate the final stress intensity factors for each transient considering flaw acceptance standards for the low alloy steel head material. The downhill side crack growth tables in Appendix B, use Position 7 to calculate crack growth and evaluate fracture toughness margins since the highest stress intensity factors occur either at or near this crack front position for both the residual and operating stresses.

Table 6-1: LEFM Fracture Toughness Margins for Uphill Side

Period of Operation: Time = 30 years

Flaw Size: a = [ ]

	Loading Conditions															
Temperature Pressure																
Fracture Toughness, KIc	200.0	200.0	98.0	200.0	200.0	200.0	63.5	200.0	200.0	200.0	200.0	200.0	200.0	63.5	200.0	ksi√in
Fracture Toughness, KIa	200.0	85.5	55.2	200.0	200.0	200.0	43.2	200.0	200.0	200.0	200.0	200.0	200.0	43.2	200.0	ksi√in
	Position 16															
KI(a)	73.546	50.736	31.531	78.325	79.225	94.843	64.199	82.085	72.962	109.077	73.540	96.413	89.569	233.116	190.113	ksi√in
a_e	3.1971	3.0955	3.0602	3.2163	3.2219	3.2883	3.1266	3.2381	3.1944	3.3708	3.1972	3.2988	3.2369	4.1923	3.9097	in.
$KI(a_e)$	75.434	51.204	31.640	80.576	81.573	98.653	65.117	84.729	74.802	114.874	75.428	100.448	92.437	273.795	215.630	ksi√in
Margin = KIc / $KI(a_e)$	n/a	n/a	n/a	n/a	n/a	n/a	n/a	n/a	n/a	n/a	n/a	n/a	n/a	0.23	0.93	
Margin = KIa / $KI(a_e)$	2.65	1.67	1.75	2.48	2.45	2.03	0.66	2.36	2.67	1.74	2.65	1.99	2.16	n/a	n/a	
Required Margin	3.16	1.41	1.41	3.16	3.16	3.16	1.41	3.16	3.16	3.16	3.16	3.16	3.16	1.41	1.41	
Acceptable by LEFM?	No	Yes	Yes	No	No	No	No	No	No	No	No	No	No	No	No	

where: $ae = a + 1/(6\pi)\,[KI(a)/Sy]^2$

$KI(a_e) = KI(a)*\sqrt{(a_e/a)}$

Table 6-2: LEFM Fracture Toughness Margins for Downhill Side

Period of Operation: Time = 30 years

Flaw Size: a = [ ]

	Loading Conditions															
	[														]	
Temperature																
Pressure																
Fracture Toughness, KIc	200.0	200.0	98.0	200.0	200.0	200.0	63.5	200.0	200.0	200.0	200.0	200.0	200.0	63.5	200.0	ksi√in
Fracture Toughness, KIa	200.0	85.5	55.2	200.0	200.0	200.0	43.2	200.0	200.0	200.0	200.0	200.0	200.0	43.2	200.0	ksi√in
	Position 7															
KI(a)	56.220	22.499	17.076	58.314	58.716	65.540	55.130	59.913	55.969	72.039	56.216	66.756	65.585	77.409	63.626	ksi√in
a_e	2.3201	2.2388	2.2339	2.3259	2.3279	2.3467	2.2923	2.3337	2.3191	2.3724	2.3201	2.3515	2.3338	2.3549	2.3255	in.
$KI(a_e)$	57.373	22.555	17.099	59.585	60.021	67.267	55.923	61.322	57.105	74.341	57.369	68.584	67.127	79.587	65.007	ksi√in
Margin = KIc / $KI(a_e)$	n/a	n/a	n/a	n/a	n/a	n/a	n/a	n/a	n/a	n/a	n/a	n/a	n/a	0.80	3.08	
Margin = KIa / $KI(a_e)$	3.49	3.79	3.23	3.36	3.33	2.97	0.77	3.26	3.50	2.69	3.49	2.92	2.98	n/a	n/a	
Required Margin	3.16	1.41	1.41	3.16	3.16	3.16	1.41	3.16	3.16	3.16	3.16	3.16	3.16	1.41	1.41	
Acceptable by LEFM?	Yes	Yes	Yes	Yes	Yes	No	No	Yes	Yes	No	Yes	No	No	No	Yes	

where: $ae = a + 1/(6\pi)\,[KI(a)/Sy]^2$

$KI(a_e) = KI(a)*\sqrt{(a_e/a)}$

6.3 LEFM Flaw Evaluations

Results of the linear-elastic fracture mechanics flaw evaluations are summarized below for the final flaw size after 30 years of crack growth.

6.3.1 Normal and Upset Conditions

Listed below are the controlling LEFM fracture toughness margins from the fatigue crack growth tables.

		Uphill Side	Downhill Side
Flaw Sizes			
Initial flaw size,	a_i =	2.148 in.	2.148 in.
Final flaw size,	a_f =	[ ] in.	[ ] in.
Flaw growth,	Δa =	[ ] in.	[ ] in.
Operating Conditions		Reactor Trip	Reactor Trip
Temperature,	T =	[ ] °F	[ ] °F
Fracture toughness,	K_{Ia} =	200.0 ksi√in	200.0 ksi√in
Final stress intensity factor,	$K_I(a_f)$ =	109.1 ksi√in	72.04 ksi√in
Effective flaw size,	a_e =	3.371 in.	2.372 in.
Effective stress intensity factor,	$K_I(a_e)$ =	114.9 ksi√in	74.34 ksi√in
Fracture toughness margin (> 3.16),	$K_{Ia}/K_I(a_e)$ =	1.74	2.69
Low Temperature Conditions		Refueling	Refueling
Temperature,	T =	[ ] °F	[ ] °F
Fracture toughness,	K_{Ia} =	43.2 ksi√in	43.2 ksi√in
Final stress intensity factor,	$K_I(a_f)$ =	64.20 ksi√in	55.13 ksi√in
Effective flaw size,	a_e =	3.127 in.	2.292 in.
Effective stress intensity factor,	$K_I(a_e)$ =	65.12 ksi√in	55.92 ksi√in
Fracture toughness margin (> 1.41),	$K_{Ia}/K_I(a_e)$ =	0.66	0.77

Since the above fracture toughness margins for the controlling normal and upset conditions are less than the Code required minimums, EPFM flaw evaluations will be performed in Section 6.4 to account for the ductile behavior of the low alloy steel under stable crack propagation.

6.3.2 Faulted Conditions

The bounding faulted condition stress intensity factors are evaluated below for the final flaw size after 30 years of crack growth.

		Uphill Side	Downhill Side
Flaw Sizes			
Final flaw size,	a_f =	[ ] in.	[ ] in.
Large Loss of Coolant Accident			
Temperature,	T =	[ ] °F	[ ] °F
Fracture toughness,	K_{Ic} =	63.5 ksi√in	63.5 ksi√in
Final stress intensity factor,	$K_I(a_f)$ =	233.1 ksi√in	77.41 ksi√in
Effective flaw size,	a_e =	4.192 in.	2.355 in.
Effective stress intensity factor,	$K_I(a_e)$ =	273.8 ksi√in	79.59 ksi√in
Fracture toughness margin (> 1.41),	$K_{Ic}/K_I(a_e)$ =	0.23	0.80
Large Steam Line Break			
Temperature,	T =	[ ] °F	[ ] °F
Fracture toughness,	K_{Ic} =	200.0 ksi√in	200.0 ksi√in
Final stress intensity factor,	$K_I(a_f)$ =	190.1 ksi√in	63.63 ksi√in
Effective flaw size,	a_e =	3.910 in.	2.326 in.
Effective stress intensity factor,	$K_I(a_e)$ =	215.6 ksi√in	65.01 ksi√in
Fracture toughness margin (> 1.41),	$K_{Ic}/K_I(a_e)$ =	0.93	3.08

Since some of the above fracture toughness margins for the controlling faulted conditions are less than the Code required minimums, EPFM flaw evaluations will be performed in Section 6.4 to account for the ductile behavior of the low alloy steel under stable crack propagation.

6.4 EPFM Flaw Evaluations

The EPFM analysis is used to evaluate the limiting loading conditions that fail the LEFM-based Code margins. In this context, EPFM is meant to include either classical elastic-plastic fracture mechanics or primary stress limit analysis, as applicable.

6.4.1 Operating Conditions

Controlling Conditions		Uphill Side Reactor Trip	Downhill Side Reactor Trip
Flaw size at 30 years of service,	$a =$	[ ] in.	[ ] in.
Effective flaw size,	$a_e =$	3.371 in.	2.373 in.

SCREENING PROCEDURE

		Uphill Side	Downhill Side
	$T =$	[ ] °F	[ ] °F
	$E =$	27200 ksi	27200 ksi
	$\nu =$	0.3	0.3
	$E' = E/(1-\nu^2) =$	29890 ksi	29890 ksi
	$\sigma_y =$	43.6 ksi	43.6 ksi
	$\sigma_u =$	80.0 ksi	80.0 ksi
	$\sigma_f =$	61.8 ksi	61.8 ksi
Crack initiation toughness,	$K_{Ic} =$	200.0 ksi√in	200.0 ksi√in
Total applied K_I,	$K_I(a_e) =$	114.9 ksi√in	74.34 ksi√in
	$K_r' = K_I(a_e) / K_{Ic} =$	0.574	0.372

From finite element analysis, the maximum crack face stresses due to residual stress, pressure, and thermal gradients are

		Uphill Side	Downhill Side
	$\sigma_{max} =$	68.3 ksi	70.9 ksi
	$S_r' = \sigma_{max} / \sigma_f =$	1.105	1.147
Screening ratio,	$K_r' / S_r' =$	0.520	0.324
		$(1.8 > K_r' / S_r' \geq 0.2)$	$(1.8 > K_r' / S_r' \geq 0.2)$
Analysis regime:		EPFM	EPFM

EPFM ANALYSIS

Controlling Conditions		Uphill Side Reactor Trip	Downhill Side Reactor Trip
K_I primary,	$K_{Ip}(a) =$	190.8 ksi√in	86.02 ksi√in
K_I secondary (residual plus thermal),	$K_{Is}(a) =$	68.19 ksi√in	65.05 ksi√in
Total K_I,	$K_I(a) =$	259.0 ksi√in	151.1 ksi√in
Effective flaw size,	$a_e =$	4.912 in.	2.865 in.
Total K_I,	$K_I'(a_e) =$	329.3 ksi√in	171.3 ksi√in

Table A-14 (uphill side) and Table B-14 (downhill side) develop all the data necessary to construct J-T diagrams for the controlling operating conditions. The J-T diagrams are presented in Figures A-1 and B-1 for the uphill and downhill sides, respectively.

Uphill Side:

It can be seen from Table A-14 that for an applied J-integral of 3.628 kips/in, corresponding to safety factors of 3 and 1.5, the applied tearing modulus, 8.502, is less than the material tearing modulus, 50.70, indicating flaw stability. Alternately, the applied J-integral is less than the J-integral, 8.181 kips/in, at the point of instability. For safety factors of 1.5 and 1, the applied J-integral of 0.785 kips/in is less than the $J_{0.1}$ value of 2.473 kips/in, demonstrating that the crack driving force falls below the J-R curve at a crack extension of 0.1 inch.

Downhill Side:

Table B-14 shows that for an applied J-integral of 0.982 kips/in, corresponding to safety factors of 3 and 1.5, the applied tearing modulus, 3.139, is less than the material tearing modulus, 242.0, indicating flaw stability. The applied J-integral is also less than the J-integral, 7.102 kips/in, at the point of instability. For safety factors of 1.5 and 1, the applied J-integral of 0.273 kips/in is less than the $J_{0.1}$ value of 2.473 kips/in, demonstrating that the crack driving force falls below the J-R curve at a crack extension of 0.1 inch.

6.4.2 Low Temperature Conditions

		Uphill Side	Downhill Side
Controlling Conditions		Refueling	Refueling
Flaw size at 30 years of service,	a =	[ ] in.	[ ] in.
Effective flaw size,	a_e =	3.127 in.	2.292 in.

SCREENING PROCEDURE

		Uphill Side	Downhill Side
	T =	[ ] °F	[ ] °F
	E =	29200 ksi	29200 ksi
	ν =	0.3	0.3
	$E' = E/(1-\nu^2)$ =	32080 ksi	32080 ksi
	σ_y =	50.0 ksi	50.0 ksi
	σ_u =	80.0 ksi	80.0 ksi
	σ_f =	65.0 ksi	65.0 ksi
Crack initiation toughness,	K_{Ic} =	63.5 ksi√in	63.5 ksi√in
Total applied K_I,	$K_I(a_e)$ =	65.12 ksi√in	55.92 ksi√in
	$K_r' = K_I(a_e) / K_{Ic}$ =	1.025	0.880

From finite element analysis, the maximum crack face stresses due to residual stress, pressure, and thermal gradients are

		Uphill Side	Downhill Side
	σ_{max} =	59.1 ksi	49.5 ksi
	$S_r' = \sigma_{max} / \sigma_f$ =	0.909	0.762
Screening ratio,	K_r' / S_r' =	1.127	1.156
		$(1.8 > K_r' / S_r' \geq 0.2)$	$(1.8 > K_r' / S_r' \geq 0.2)$
Analysis regime:		EPFM	EPFM

EPFM ANALYSIS

Controlling Conditions		Uphill Side Refueling	Downhill Side Refueling
K_I primary,	$K_{Ip}(a)$ =	0.0 ksi√in	0.0 ksi√in
K_I secondary (residual plus thermal),	$K_{Is}(a)$ =	96.30 ksi√in	82.70 ksi√in
Total K_I,	$K_I(a)$ =	96.30 ksi√in	82.70 ksi√in
Effective flaw size,	a_e =	3.236 in.	2.373 in.
Total K_I,	$K_I'(a_e)$ =	99.37 ksi√in	85.35 ksi√in

Table A-15 (uphill side) and Table B-15 (downhill side) develop all the data necessary to construct J-T diagrams for the controlling operating conditions. The J-T diagrams are presented in Figures A-2 and B-2 for the uphill and downhill sides, respectively.

Uphill Side:

It can be seen from Table A-15 that for an applied J-integral of 0.308 kips/in, corresponding to safety factors of 3 and 1.5, the applied tearing modulus, 0.700, is less than the material tearing modulus, 942.9, indicating flaw stability. Alternately, the applied J-integral is less than the J-integral, 8.179 kips/in, at the point of instability. For safety factors of 1.5 and 1, the applied J-integral of 0.132 kips/in is less than the $J_{0.1}$ value of 2.474 kips/in, demonstrating that the crack driving force falls below the J-R curve at a crack extension of 0.1 inch.

Downhill Side:

Table B-15 shows that for an applied J-integral of 0.227 kips/in, corresponding to safety factors of 3 and 1.5, the applied tearing modulus, 0.704, is less than the material tearing modulus, 1357, indicating flaw stability. The applied J-integral is also less than the J-integral, 7.101 kips/in, at the point of instability. For safety factors of 1.5 and 1, the applied J-integral of 0.097 kips/in is less than the $J_{0.1}$ value of 2.474 kips/in, demonstrating that the crack driving force falls below the J-R curve at a crack extension of 0.1 inch.

6.4.3 Faulted Conditions

		Uphill Side	Downhill Side
Controlling Conditions		LLOCA	LLOCA
Flaw size at 30 years of service,	a =	[ ] in.	[ ] in.
Effective flaw size,	a_e =	4.192 in.	2.355 in.

SCREENING PROCEDURE

		Uphill Side	Downhill Side
	T =	[ ] °F	[ ] °F
	E =	29200 ksi	29200 ksi
	ν =	0.3	0.3
	$E' = E/(1-\nu^2)$ =	32080 ksi	32080 ksi
	σ_y =	50.0 ksi	50.0 ksi
	σ_u =	80.0 ksi	80.0 ksi
	σ_f =	65.0 ksi	65.0 ksi
Crack initiation toughness,	K_{Ic} =	63.5 ksi√in	63.5 ksi√in
Total applied K_I,	$K_I(a_e)$ =	273.8 ksi√in	79.59 ksi√in
	$K_r' = K_I(a_e) / K_{Ic}$ =	4.310	1.253

From finite element analysis, the maximum crack face stresses due to residual stress, pressure, and thermal gradients are

		Uphill Side	Downhill Side
	σ_{max} =	198.3 ksi	163.2 ksi
	$S_r' = \sigma_{max} / \sigma_f$ =	3.051	2.511
Screening ratio,	K_r' / S_r' =	1.413	0.499
		$(1.8 > K_r' / S_r' \geq 0.2)$	$(1.8 > K_r' / S_r' \geq 0.2)$
Analysis regime:		EPFM	EPFM

EPFM ANALYSIS

Controlling Conditions		Uphill Side LLOCA	Downhill Side LLOCA
K_I primary,	$K_{Ip}(a)$ =	2.596 ksi√in	1.170 ksi√in
K_I secondary (residual plus thermal),	$K_{Is}(a)$ =	231.4 ksi√in	76.63 ksi√in
Total K_I,	$K_I(a)$ =	234.0 ksi√in	77.80 ksi√in
Effective flaw size,	a_e =	4.201 in.	2.356 in.
Total K_I,	$K_I'(a_e)$ =	275.1 ksi√in	80.01 ksi√in

Table A-16 (uphill side) and Table B-16 (downhill side) develop all the data necessary to construct J-T diagrams for the controlling operating conditions. The J-T diagrams are presented in Figures A-3 and B-3 for the uphill and downhill sides, respectively.

Uphill Side:

It can be seen from Table A-16 that for an applied J-integral of 2.359 kips/in, corresponding to safety factors of 1.5 and 1, the applied tearing modulus, 5.364, is less than the material tearing modulus, 82.38, indicating flaw stability. Alternately, the applied J-integral is less than the J-integral, 8.179 kips/in, at the point of instability. For safety factors of 1.5 and 1, the applied J-integral of 2.359 kips/in is less than the $J_{0.1}$ value of 2.474 kips/in, demonstrating that the crack driving force falls below the J-R curve at a crack extension of 0.1 inch.

Downhill Side:

Table B-16 shows that for an applied J-integral of 0.200 kips/in, corresponding to safety factors of 1.5 and 1, the applied tearing modulus, 0.619, is less than the material tearing modulus, 1584, indicating flaw stability. The applied J-integral is also less than the J-integral, 7.101 kips/in, at the point of instability. For safety factors of 1.5 and 1, the applied J-integral of 0.200 kips/in is less than the $J_{0.1}$ value of 2.474 kips/in, demonstrating that the crack driving force falls below the J-R curve at a crack extension of 0.1 inch.

6.5 Primary Stress Limit Analysis

The primary stress limit analysis (also referred to as primary stress limits of NB-3000) that addresses all the Shearon Harris repaired configurations as of the Fall 2016 outage are addressed in Appendix C. Based on this primary stress limit analysis, it is concluded that amongst the twelve repairs performed to-date as of October 2016, Nozzles 30, 40, and 51 yield the most limiting life of 5 years since the repairs were performed in October 2016.

7.0 SUMMARY OF RESULTS AND CONCLUSIONS

Linear-elastic and elastic-plastic fracture mechanics has been used to evaluate a postulated radial flaw in the J-groove weld and butter of an outermost CRDM nozzle reactor vessel head penetration. It was determined that an acceptable flaw size would be present after 30 years of fatigue crack growth, based on EPFM analysis consideration only, as summarized below.

7.1 Summary of Results

		Uphill Side	Downhill Side
Flaw Sizes			
Initial flaw size,	a_i =	2.148 in.	2.148 in.
Final flaw size after 30 years,	a_f =	[ ] in.	[ ] in.
Flaw growth,	Δa =	[ ] in.	[ ] in.
Operating Conditions		Reactor Trip	Reactor Trip
Temperature,	T =	[ ] °F	[ ] °F
Material tearing modulus,	T_{mat} =	50.70	242.0
Material J-integral at 0.1” crack extension,	$J_{0.1}$ =	2.473 kips/in.	2.473 kips/in.
Safety factors (primary/secondary),	SF =	3 / 1.5	3 / 1.5
Applied tearing modulus (< T_{mat})	T_{app} =	8.502	3.139
Safety factors (primary/secondary),	SF =	1.5 / 1	1.5 / 1
Applied J-integral (< $J_{0.1}$)	J_{app} =	0.785 kips/in	0.273 kips/in
Low Temperature Conditions		Refueling	Refueling
Temperature,	T =	[ ] °F	[ ] °F
Material tearing modulus,	T_{mat} =	942.9	1357
Material J-integral at 0.1” crack extension,	$J_{0.1}$ =	2.474 kips/in.	2.474 kips/in.
Safety factors (primary/secondary),	SF =	3 / 1.5	3 / 1.5
Applied tearing modulus (< T_{mat})	T_{app} =	0.700	0.704
Safety factors (primary/secondary),	SF =	1.5 / 1	1.5 / 1
Applied J-integral (< $J_{0.1}$)	J_{app} =	0.132 kips/in	0.097 kips/in

Summary of Results (Cont'd)

Faulted Conditions		LLOCA	LLOCA
Temperature,	T =	[ ] °F	[ ] °F
Material tearing modulus,	T_{mat} =	82.38	1584
Material J-integral at 0.1" crack extension,	$J_{0.1}$ =	2.474 kips/in.	2.474 kips/in.
Safety factors (primary/secondary),	SF =	1.5 / 1	1.5 / 1
Applied tearing modulus (< T_{mat})	T_{app} =	5.364	0.619
Safety factors (primary/secondary),	SF =	1.5 / 1	1.5 / 1
Applied J-integral (< $J_{0.1}$)	J_{app} =	2.359 kips/in	0.200 kips/in

7.2 Conclusion

Based on a combination of linear elastic and elastic-plastic fracture mechanics analysis of a postulated remaining flaw in the original Alloy 182 J-groove weld and butter material, the Shearon Harris Unit 1 CRDM and CET nozzles are considered to be acceptable for at least 30 years of operation following an IDTB weld repair. However, based on primary stress limit analysis, considering all the CRDM repaired configurations as of October 2016, the overall service life of the Shearon Harris Unit 1 RVCH is 5 years from the performance of the October 2016 repairs, as determined in Appendix C of the document.

8.0 REFERENCES

1. AREVA Drawing 02-9175500E-007, "Shearon Harris CRDM ID Temper Bead Weld Repair"
2. AREVA Document 08-9172870-003, "Shearon Harris RVCH CRDM and CET Nozzle Penetration Modification"
3. AREVA Document 32-9176344-000, "Shearon Harris Unit 1 IDTB CRDM/CET Nozzle Weld Residual Stress Analysis" - Proprietary Document
4. AREVA Document 51-5012047-00, "Stress Corrosion Cracking of Low Alloy Steel"
5. ANSYS Finite Element Computer Code, Version 12.1, ANSYS Inc., Canonsburg, PA.
6. T.L. Anderson, Fracture Mechanics: Fundamentals and Applications, CRC Press, 1991.
7. ASME Boiler and Pressure Vessel Code, Section III, Rules for Construction of Nuclear Facility Components, Division 1, Subsection NB, Class 1 Components, 2001 Edition with Addenda through 2003.

8. ASME Boiler and Pressure Vessel Code, Section II, Materials, 2001 Edition with Addenda through 2003.

9. AREVA Document 38-2200979-000, “Shearon Harris - Proprietary Document Transmittal 1”

10. AREVA Document 55-PQ7183-005, “Procedure Qualification Record PQ7183-005”

11. ASME Boiler and Pressure Vessel Code, Section XI, Rules for Inservice Inspection of Nuclear Power Plant Components, 2001 Edition with Addenda through 2003.

12. AREVA Document 32-9175220-003, “Shearon Harris Unit 1 Contingency CRDM IDTB Weld Repair Analysis”

13. AREVA Document 38-2201004-000, “Shearon Harris - Proprietary Document Transmittal 4”

APPENDIX A: DETAILED FLAW EVALUATIONS FOR UPHILL SIDE

This appendix presents the fatigue crack growth tables and the elastic-plastic fracture mechanics flaw evaluations for the uphill side of the CRDM penetration.

Table A-1: Stress Intensification Factors for Uphill Side – Welding Residual Stress

Condition	WRS	
Temperature	70.0	F
Pressure	n/a	psig
Sy	50.0	ksi
KIc	98.0	ksi√in
KIa	55.2	ksi√in
Crack Front Position	KI (ksi√in)	
1	45.118	
2	41.056	
3	38.435	
4	31.191	
5	27.747	
6	24.365	
7	20.513	
8	14.773	
9	18.055	
10	9.772	
11	-2.101	
12	7.352	
13	14.344	
14	18.763	
15	22.133	
16	26.509	
17	17.849	

Table A-2: Fatigue Crack Growth for Uphill Side – Heatup/Cooldown

STRESS INTENSITY FACTORS

Condition*	HU1	HU2	CD	SD	
Temperature	557.0	349.0	120.0	70.0	F
Pressure	2317	467	467	0	psig
Sy	42.6	44.9	49.2	50.0	ksi
KIc	200.0	200.0	200.0	98.0	ksi√in
KIa	200.0	200.0	85.5	55.2	ksi√in
Crack Front	Stress Intensity Factor, KI				
Position	(ksi√in)	(ksi√in)	(ksi√in)	(ksi√in)	
1	18.527	-18.920	13.250	0.000	
2	18.826	-17.438	12.738	0.000	
3	19.351	-15.934	12.257	0.000	
4	18.420	-13.078	10.820	0.000	
5	18.505	-11.272	10.097	0.000	
6	18.197	-9.462	9.289	0.000	
7	16.954	-7.589	8.195	0.000	
8	12.946	-5.678	6.169	0.000	
9	16.968	-5.646	7.508	0.000	
10	8.787	-3.529	4.085	0.000	
11	-3.688	-1.066	-0.898	0.000	
12	7.147	-2.712	3.264	0.000	
13	14.991	-4.996	6.623	0.000	
14	20.357	-7.186	9.121	0.000	
15	25.782	-9.743	11.777	0.000	
16	35.324	-13.262	16.147	0.000	
17	23.491	-9.495	10.995	0.000	

* Condition	Description
HU1	Time step 6 at 7.67 hr. (Heatup) - Maximum KI
HU2	Time step 3 at 2.29 hr. (Heatup) - Minimum KI
CD	Time step 15 at 14.37 hr. - Maximum KI at Low Temperature
SD	Shutdown at Ambient Conditions

FATIGUE CRACK GROWTH

Transient Description: 200 cycles over 40 years

ΔN = 5.0 cycles/year

Operating Time (end of yr.)	Cycle	a (in.)	Position 16 HU1 KI(a) (ksi√in)	HU2 KI(a) (ksi√in)	ΔKI (ksi√in)	Δa (in.)	CD KI(a) (ksi√in)	SD KI(a) (ksi√in)
0	0.0		61.833	13.247	48.586		42.656	26.509
1	5.0		61.857	13.252	48.604		42.672	26.519
2	10.0		62.217	13.329	48.888		42.921	26.674
3	15.0		62.579	13.407	49.172		43.171	26.829
4	20.0		62.943	13.485	49.458		43.422	26.985
5	25.0		63.309	13.563	49.746		43.674	27.142
6	30.0		63.678	13.642	50.035		43.929	27.300
7	35.0		64.048	13.722	50.326		44.184	27.459
8	40.0		64.420	13.801	50.619		44.441	27.618
9	45.0		64.795	13.881	50.913		44.699	27.779
10	50.0		65.171	13.962	51.209		44.959	27.940
11	55.0		65.550	14.043	51.506		45.220	28.102
12	60.0		65.930	14.125	51.805		45.483	28.266
13	65.0		66.313	14.207	52.106		45.747	28.430
14	70.0		66.698	14.289	52.409		46.012	28.595
15	75.0		67.085	14.372	52.713		46.279	28.761
16	80.0		67.474	14.455	53.018		46.547	28.927
17	85.0		67.865	14.539	53.326		46.817	29.095
18	90.0		68.258	14.624	53.635		47.089	29.264
19	95.0		68.654	14.708	53.946		47.362	29.433
20	100.0		69.052	14.794	54.258		47.636	29.604
21	105.0		69.452	14.879	54.572		47.912	29.775
22	110.0		69.854	14.965	54.888		48.189	29.948
23	115.0		70.258	15.052	55.206		48.468	30.121
24	120.0		70.665	15.139	55.526		48.749	30.295
25	125.0		71.073	15.227	55.847		49.031	30.471
26	130.0		71.484	15.315	56.170		49.314	30.647
27	135.0		71.898	15.403	56.494		49.599	30.824
28	140.0		72.313	15.492	56.821		49.886	31.002
29	145.0		72.731	15.582	57.149		50.174	31.181
30	150.0		73.151	15.672	57.479		50.464	31.361

Table A-3: Fatigue Crack Growth for Uphill Side – Unit Loading/Unloading

STRESS INTENSITY FACTORS

Condition*	UL	UU	
Temperature	533.8	574.3	F
Pressure	2265	2209	psig
Sy	42.9	42.4	ksi
KIc	200.0	200.0	ksi√in
KIa	200.0	200.0	ksi√in
Crack Front	KI		
Position	(ksi√in)	(ksi√in)	
1	23.007	10.659	
2	23.018	11.371	
3	23.249	12.295	
4	21.710	12.334	
5	21.430	12.954	
6	20.760	13.214	
7	19.115	12.658	
8	14.550	9.722	
9	18.795	13.197	
10	9.829	6.679	
11	-3.731	-3.452	
12	7.964	5.477	
13	16.596	11.668	
14	22.593	15.748	
15	28.716	19.782	
16	39.342	27.120	
17	26.287	17.846	

* Condition	Description
UL	Time step 12 at 0.29 hr. - Maximum KI
UU	Time step 11 at 0.29 hr. - Minimum KI

FATIGUE CRACK GROWTH

Transient Description: 18300 cycles over 40 years

ΔN = 457.5 cycles/year

Operating Time (end of yr.)	Cycle	a (in.)	Position 16 UL KI(a) (ksi√in)	UU KI(a) (ksi√in)	ΔKI (ksi√in)	Δa (in.)
0	0.0		65.851	53.629	12.222	
1	457.5		65.891	53.662	12.229	
2	915.0		66.275	53.974	12.301	
3	1372.5		66.661	54.288	12.372	
4	1830.0		67.049	54.604	12.444	
5	2287.5		67.439	54.922	12.517	
6	2745.0		67.831	55.241	12.589	
7	3202.5		68.225	55.563	12.663	
8	3660.0		68.622	55.886	12.736	
9	4117.5		69.021	56.210	12.810	
10	4575.0		69.422	56.537	12.885	
11	5032.5		69.825	56.865	12.960	
12	5490.0		70.230	57.196	13.035	
13	5947.5		70.638	57.528	13.110	
14	6405.0		71.048	57.861	13.187	
15	6862.5		71.460	58.197	13.263	
16	7320.0		71.875	58.535	13.340	
17	7777.5		72.291	58.874	13.417	
18	8235.0		72.710	59.215	13.495	
19	8692.5		73.132	59.559	13.573	
20	9150.0		73.555	59.904	13.652	
21	9607.5		73.981	60.250	13.731	
22	10065.0		74.410	60.599	13.811	
23	10522.5		74.841	60.950	13.890	
24	10980.0		75.274	61.303	13.971	
25	11437.5		75.709	61.657	14.052	
26	11895.0		76.147	62.014	14.133	
27	12352.5		76.587	62.372	14.215	
28	12810.0		77.030	62.733	14.297	
29	13267.5		77.475	63.095	14.379	
30	13725.0		77.922	63.460	14.462	

Table A-4: Fatigue Crack Growth for Uphill Side – Step Load Increase/Decrease

STRESS INTENSITY FACTORS

Condition*	SLI	SLD	
Temperature	551.4	570.8	F
Pressure	2367	2246	psig
Sy	42.7	42.5	ksi
KIc	200.0	200.0	ksi√in
KIa	200.0	200.0	ksi√in
Crack Front	KI		
Position	(ksi√in)	(ksi√in)	
1	22.974	11.043	
2	23.070	11.733	
3	23.434	12.620	
4	21.981	12.614	
5	21.803	13.209	
6	21.191	13.451	
7	19.546	12.878	
8	14.887	9.896	
9	19.268	13.414	
10	10.061	6.796	
11	-3.874	-3.486	
12	8.146	5.579	
13	16.990	11.874	
14	23.108	16.034	
15	29.318	20.161	
16	40.099	27.659	
17	26.771	18.203	

* Condition	Description
SLI	Time step 10 at 0.05 hr. - Maximum KI
SLD	Time step 10 at 0.042 hr. - Minimum KI

FATIGUE CRACK GROWTH

Transient Description: 4000 cycles over 40 years

ΔN = 100.0 cycles/year

Operating Time (end of yr.)	Cycle	a (in.)	Position 16 SLI KI(a) (ksi√in)	SLD KI(a) (ksi√in)	ΔKI (ksi√in)	Δa (in.)
0	0.0		66.608	54.168	12.440	
1	100.0		66.884	54.393	12.492	
2	200.0		67.274	54.709	12.564	
3	300.0		67.665	55.028	12.637	
4	400.0		68.059	55.348	12.711	
5	500.0		68.455	55.670	12.785	
6	600.0		68.853	55.994	12.859	
7	700.0		69.253	56.319	12.934	
8	800.0		69.656	56.647	13.009	
9	900.0		70.061	56.976	13.085	
10	1000.0		70.468	57.307	13.161	
11	1100.0		70.877	57.640	13.237	
12	1200.0		71.288	57.974	13.314	
13	1300.0		71.702	58.311	13.391	
14	1400.0		72.118	58.649	13.469	
15	1500.0		72.536	58.989	13.547	
16	1600.0		72.957	59.331	13.626	
17	1700.0		73.380	59.675	13.705	
18	1800.0		73.805	60.021	13.784	
19	1900.0		74.233	60.369	13.864	
20	2000.0		74.663	60.718	13.944	
21	2100.0		75.095	61.070	14.025	
22	2200.0		75.530	61.424	14.106	
23	2300.0		75.967	61.779	14.188	
24	2400.0		76.406	62.136	14.270	
25	2500.0		76.848	62.496	14.353	
26	2600.0		77.293	62.857	14.436	
27	2700.0		77.739	63.221	14.519	
28	2800.0		78.189	63.586	14.603	
29	2900.0		78.640	63.953	14.687	
30	3000.0		79.095	64.323	14.772	

Table A-5: Fatigue Crack Growth for Uphill Side – Turbine Roll Test

STRESS INTENSITY FACTORS

Condition*	TRT1	TRT2	
Temperature	443.4	557.4	F
Pressure	1692	2317	psig
Sy	43.8	42.6	ksi
KIc	200.0	200.0	ksi√in
KIa	200.0	200.0	ksi√in
Crack Front	KI		
Position	(ksi√in)	(ksi√in)	
1	40.587	7.354	
2	39.304	8.260	
3	38.158	9.378	
4	34.061	9.845	
5	32.161	10.713	
6	29.935	11.230	
7	26.687	10.973	
8	20.115	8.468	
9	24.921	11.756	
10	13.413	5.859	
11	-3.551	-3.409	
12	10.752	4.835	
13	21.987	10.400	
14	30.173	13.981	
15	38.799	17.463	
16	53.229	23.938	
17	36.060	15.642	

* Condition	Description
TRT1	Time step 5 at 0.278 hr. - Maximum KI
TRT2	Time step 8 at 1.418 hr. - Minimum KI

FATIGUE CRACK GROWTH

Transient Description: 80 cycles over 40 years

ΔN = 2.0 cycles/year

Operating Time (end of yr.)	Cycle	a (in.)	Position 16 TRT1 KI(a) (ksi√in)	TRT2 KI(a) (ksi√in)	ΔKI (ksi√in)	Δa (in.)
0	0.0		79.738	50.447	29.291	
1	2.0		80.133	50.697	29.436	
2	4.0		80.599	50.992	29.607	
3	6.0		81.069	51.289	29.780	
4	8.0		81.540	51.587	29.953	
5	10.0		82.015	51.887	30.127	
6	12.0		82.492	52.189	30.303	
7	14.0		82.971	52.493	30.479	
8	16.0		83.453	52.798	30.656	
9	18.0		83.938	53.104	30.834	
10	20.0		84.426	53.413	31.013	
11	22.0		84.916	53.723	31.193	
12	24.0		85.409	54.035	31.374	
13	26.0		85.905	54.348	31.556	
14	28.0		86.403	54.664	31.739	
15	30.0		86.904	54.981	31.923	
16	32.0		87.408	55.300	32.109	
17	34.0		87.915	55.620	32.295	
18	36.0		88.424	55.943	32.482	
19	38.0		88.937	56.267	32.670	
20	40.0		89.452	56.593	32.859	
21	42.0		89.970	56.920	33.050	
22	44.0		90.491	57.250	33.241	
23	46.0		91.014	57.581	33.433	
24	48.0		91.541	57.914	33.627	
25	50.0		92.070	58.249	33.821	
26	52.0		92.603	58.586	34.017	
27	54.0		93.138	58.924	34.213	
28	56.0		93.676	59.265	34.411	
29	58.0		94.217	59.607	34.610	
30	60.0		94.761	59.952	34.810	

Table A-6: Fatigue Crack Growth for Uphill Side – Refueling

STRESS INTENSITY FACTORS

Condition*	RF1	RF2	
Temperature	32.0	140.0	F
Pressure	0	0	psig
Sy	50.0	48.5	ksi
KIc	63.5	200.0	ksi√in
KIa	43.2	105.3	ksi√in
Crack Front	KI		
Position	(ksi√in)	(ksi√in)	
1	27.949	-4.885	
2	26.345	-4.536	
3	24.683	-4.194	
4	21.095	-3.491	
5	18.978	-3.063	
6	16.815	-2.617	
7	14.330	-2.135	
8	10.707	-1.614	
9	12.277	-1.643	
10	6.961	-1.007	
11	-0.430	-0.243	
12	5.491	-0.781	
13	10.857	-1.457	
14	15.170	-2.084	
15	19.962	-2.802	
16	27.466	-3.804	
17	19.022	-2.699	

* Condition	Description
RF1	Time step 7 at 0.171 hr. - Maximum KI
RF2	Time step 1 at 0.0001 hr. - Minimum KI

FATIGUE CRACK GROWTH

Transient Description: 80 cycles over 40 years

ΔN = 2.0 cycles/year

Operating Time (end of yr.)	Cycle	a (in.)	Position 16 RF1 KI(a) (ksi√in)	RF2 KI(a) (ksi√in)	ΔKI (ksi√in)	Δa (in.)
0	0.0		53.975	22.705	31.270	
1	2.0		54.247	22.819	31.427	
2	4.0		54.563	22.952	31.610	
3	6.0		54.880	23.086	31.794	
4	8.0		55.200	23.220	31.979	
5	10.0		55.521	23.355	32.165	
6	12.0		55.844	23.491	32.353	
7	14.0		56.168	23.628	32.541	
8	16.0		56.495	23.765	32.730	
9	18.0		56.823	23.903	32.920	
10	20.0		57.153	24.042	33.111	
11	22.0		57.485	24.181	33.303	
12	24.0		57.819	24.322	33.497	
13	26.0		58.154	24.463	33.691	
14	28.0		58.492	24.605	33.887	
15	30.0		58.831	24.748	34.083	
16	32.0		59.172	24.891	34.281	
17	34.0		59.515	25.035	34.480	
18	36.0		59.860	25.180	34.679	
19	38.0		60.207	25.326	34.880	
20	40.0		60.555	25.473	35.082	
21	42.0		60.906	25.621	35.285	
22	44.0		61.259	25.769	35.490	
23	46.0		61.613	25.918	35.695	
24	48.0		61.969	26.068	35.902	
25	50.0		62.328	26.219	36.109	
26	52.0		62.688	26.370	36.318	
27	54.0		63.051	26.523	36.528	
28	56.0		63.415	26.676	36.739	
29	58.0		63.781	26.830	36.951	
30	60.0		64.150	26.985	37.165	

Table A-7: Fatigue Crack Growth for Uphill Side – Loss of Load

STRESS INTENSITY FACTORS

Condition*	LL1	LL2	
Temperature	575.8	588.8	F
Pressure	2710	1844	psig
Sy	42.4	42.2	ksi
KIc	200.0	200.0	ksi√in
KIa	200.0	200.0	ksi√in
Crack Front	KI		
Position	(ksi√in)	(ksi√in)	
1	23.554	-4.474	
2	23.806	-3.022	
3	24.444	-1.387	
4	23.114	0.461	
5	23.111	2.069	
6	22.576	3.396	
7	20.873	4.163	
8	15.923	3.330	
9	20.646	5.710	
10	10.754	2.498	
11	-4.216	-2.966	
12	8.702	2.160	
13	18.163	5.054	
14	24.668	6.566	
15	31.190	7.815	
16	42.503	10.727	
17	28.370	6.584	

* Condition	Description
LL1	Time step 2 at 0.003 hr. - Maximum KI
LL2	Time step 12 at 0.033 hr. - Minimum KI

FATIGUE CRACK GROWTH

Transient Description: 210 cycles over 40 years

ΔN = 5.25 cycles/year

Operating Time (end of yr.)	Cycle	a (in.)	Position 16 LL1 KI(a) (ksi√in)	LL2 KI(a) (ksi√in)	ΔKI (ksi√in)	Δa (in.)
0	0.0		69.012	37.236	31.776	
1	5.3		69.364	37.426	31.938	
2	10.5		69.768	37.644	32.124	
3	15.8		70.174	37.863	32.311	
4	21.0		70.582	38.083	32.499	
5	26.3		70.993	38.305	32.688	
6	31.5		71.406	38.527	32.878	
7	36.8		71.821	38.751	33.069	
8	42.0		72.238	38.977	33.261	
9	47.3		72.658	39.203	33.455	
10	52.5		73.080	39.431	33.649	
11	57.8		73.504	39.660	33.844	
12	63.0		73.931	39.890	34.041	
13	68.3		74.360	40.122	34.238	
14	73.5		74.792	40.354	34.437	
15	78.8		75.225	40.588	34.637	
16	84.0		75.662	40.824	34.838	
17	89.3		76.100	41.060	35.040	
18	94.5		76.541	41.298	35.243	
19	99.8		76.985	41.538	35.447	
20	105.0		77.430	41.778	35.652	
21	110.3		77.879	42.020	35.859	
22	115.5		78.330	42.263	36.066	
23	120.8		78.783	42.508	36.275	
24	126.0		79.239	42.754	36.485	
25	131.3		79.697	43.001	36.696	
26	136.5		80.158	43.250	36.908	
27	141.8		80.621	43.500	37.121	
28	147.0		81.087	43.751	37.336	
29	152.3		81.555	44.004	37.551	
30	157.5		82.026	44.258	37.768	

Table A-8: Fatigue Crack Growth for Uphill Side – Loss of Power

STRESS INTENSITY FACTORS

Condition*	LP1	LP2	
Temperature	553.8	600.5	F
Pressure	2295	2464	psig
Sy	42.7	42.1	ksi
KIc	200.0	200.0	ksi√in
KIa	200.0	200.0	ksi√in
Crack Front	KI		
Position	(ksi√in)	(ksi√in)	
1	18.177	2.404	
2	18.484	3.685	
3	19.014	5.180	
4	18.116	6.387	
5	18.212	7.727	
6	17.922	8.703	
7	16.708	8.918	
8	12.759	6.975	
9	16.740	10.142	
10	8.663	4.906	
11	-3.661	-3.498	
12	7.047	4.105	
13	14.789	9.001	
14	20.078	12.011	
15	25.423	14.846	
16	34.833	20.362	
17	23.159	13.095	

* Condition	Description
LP1	Time step 2 at 0.003 hr. - Maximum KI
LP2	Time step 11 at 0.053 hr. - Minimum KI

FATIGUE CRACK GROWTH

Transient Description: 100 cycles over 40 years

ΔN = 2.5 cycles/year

Operating Time	Cycle	a	Position 16			
			LP1	LP2		
			KI(a)	KI(a)	ΔKI	Δa
(end of yr.)		(in.)	(ksi√in)	(ksi√in)	(ksi√in)	(in.)
0	0.0		61.342	46.871	14.471	
1	2.5		61.668	47.120	14.548	
2	5.0		62.027	47.395	14.633	
3	7.5		62.388	47.671	14.718	
4	10.0		62.751	47.948	14.803	
5	12.5		63.116	48.227	14.890	
6	15.0		63.483	48.507	14.976	
7	17.5		63.852	48.789	15.063	
8	20.0		64.224	49.073	15.151	
9	22.5		64.597	49.358	15.239	
10	25.0		64.972	49.645	15.327	
11	27.5		65.349	49.933	15.416	
12	30.0		65.729	50.223	15.506	
13	32.5		66.110	50.514	15.596	
14	35.0		66.494	50.807	15.686	
15	37.5		66.879	51.102	15.777	
16	40.0		67.267	51.398	15.869	
17	42.5		67.657	51.696	15.961	
18	45.0		68.049	51.996	16.053	
19	47.5		68.443	52.297	16.146	
20	50.0		68.840	52.600	16.240	
21	52.5		69.238	52.905	16.334	
22	55.0		69.639	53.211	16.428	
23	57.5		70.042	53.519	16.523	
24	60.0		70.447	53.828	16.619	
25	62.5		70.855	54.140	16.715	
26	65.0		71.264	54.453	16.812	
27	67.5		71.676	54.767	16.909	
28	70.0		72.090	55.084	17.007	
29	72.5		72.507	55.402	17.105	
30	75.0		72.926	55.722	17.204	

Table A-9: Fatigue Crack Growth for Uphill Side – Reactor Trip

STRESS INTENSITY FACTORS

Condition*	RT1	RT2	
Temperature	457.4	537.4	F
Pressure	2205	1803	psig
Sy	43.6	42.8	ksi
KIc	200.0	200.0	ksi√in
KIa	200.0	200.0	ksi√in
Crack Front	KI		
Position	(ksi√in)	(ksi√in)	
1	50.109	15.130	
2	48.502	15.368	
3	47.097	15.728	
4	42.010	14.966	
5	39.651	14.995	
6	36.864	14.741	
7	32.808	13.760	
8	24.760	10.481	
9	30.517	13.823	
10	16.474	7.136	
11	-4.144	-3.110	
12	13.197	5.817	
13	26.924	12.241	
14	36.980	16.629	
15	47.575	21.108	
16	65.196	29.058	
17	44.202	19.322	

* Condition	Description
RT1	Time step 13 at 0.171 hr. - Maximum KI
RT2	Time step 8 at 0.025 hr. - Minimum KI

FATIGUE CRACK GROWTH

Transient Description: 250 cycles over 40 years

ΔN = 6.25 cycles/year

Operating Time (end of yr.)	Cycle	a (in.)	Position 16 RT1 KI(a) (ksi√in)	RT2 KI(a) (ksi√in)	ΔKI (ksi√in)	Δa (in.)
0	0.0		91.705	55.567	36.138	
1	6.3		92.195	55.864	36.331	
2	12.5		92.732	56.189	36.543	
3	18.8		93.272	56.516	36.755	
4	25.0		93.814	56.845	36.969	
5	31.3		94.360	57.176	37.184	
6	37.5		94.909	57.508	37.401	
7	43.8		95.461	57.843	37.618	
8	50.0		96.016	58.179	37.837	
9	56.3		96.573	58.517	38.056	
10	62.5		97.134	58.857	38.278	
11	68.8		97.698	59.199	38.500	
12	75.0		98.266	59.542	38.723	
13	81.3		98.836	59.888	38.948	
14	87.5		99.409	60.235	39.174	
15	93.8		99.986	60.585	39.401	
16	100.0		100.566	60.936	39.630	
17	106.3		101.149	61.289	39.859	
18	112.5		101.735	61.644	40.090	
19	118.8		102.324	62.001	40.323	
20	125.0		102.917	62.361	40.556	
21	131.3		103.513	62.722	40.791	
22	137.5		104.112	63.085	41.027	
23	143.8		104.714	63.450	41.265	
24	150.0		105.320	63.817	41.503	
25	156.3		105.929	64.186	41.743	
26	162.5		106.542	64.557	41.985	
27	168.8		107.157	64.930	42.227	
28	175.0		107.777	65.305	42.471	
29	181.3		108.399	65.683	42.717	
30	187.5		109.025	66.062	42.963	

Table A-10: Fatigue Crack Growth for Uphill Side – Inadvertent Depressurization

STRESS INTENSITY FACTORS

Condition*	ID1	ID2	
Temperature	557.4	556.6	F
Pressure	2317	1161	psig
Sy	42.6	42.6	ksi
KIc	200.0	200.0	ksi√in
KIa	200.0	200.0	ksi√in
Crack Front	KI		
Position	(ksi√in)	(ksi√in)	
1	18.517	-4.170	
2	18.817	-3.034	
3	19.343	-1.801	
4	18.414	-0.310	
5	18.500	0.933	
6	18.193	1.996	
7	16.951	2.674	
8	12.944	2.112	
9	16.966	3.967	
10	8.786	1.655	
11	-3.689	-2.383	
12	7.146	1.450	
13	14.989	3.509	
14	20.354	4.514	
15	25.779	5.327	
16	35.319	7.414	
17	23.488	4.490	

* Condition	Description
ID1	Time step 1 at 0.0001 hr. - Maximum KI
ID2	Time step 9 at 0.022 hr. - Minimum KI

FATIGUE CRACK GROWTH

Transient Description: 100 cycles over 40 years

ΔN = 2.5 cycles/year

Operating Time (end of yr.)	Cycle	a (in.)	Position 16 ID1 KI(a) (ksi√in)	ID2 KI(a) (ksi√in)	ΔKI (ksi√in)	Δa (in.)
0	0.0		61.828	33.923	27.905	
1	2.5		62.182	34.117	28.065	
2	5.0		62.544	34.316	28.228	
3	7.5		62.908	34.515	28.392	
4	10.0		63.274	34.716	28.558	
5	12.5		63.642	34.918	28.724	
6	15.0		64.012	35.121	28.891	
7	17.5		64.384	35.325	29.059	
8	20.0		64.758	35.531	29.228	
9	22.5		65.135	35.737	29.397	
10	25.0		65.513	35.945	29.568	
11	27.5		65.893	36.154	29.740	
12	30.0		66.276	36.363	29.912	
13	32.5		66.660	36.574	30.086	
14	35.0		67.047	36.787	30.261	
15	37.5		67.436	37.000	30.436	
16	40.0		67.827	37.215	30.613	
17	42.5		68.220	37.430	30.790	
18	45.0		68.616	37.647	30.968	
19	47.5		69.013	37.865	31.148	
20	50.0		69.413	38.085	31.328	
21	52.5		69.815	38.305	31.510	
22	55.0		70.219	38.527	31.692	
23	57.5		70.625	38.750	31.875	
24	60.0		71.034	38.974	32.060	
25	62.5		71.445	39.199	32.245	
26	65.0		71.858	39.426	32.432	
27	67.5		72.273	39.654	32.619	
28	70.0		72.691	39.883	32.808	
29	72.5		73.110	40.113	32.997	
30	75.0		73.533	40.345	33.188	

Table A-11: Fatigue Crack Growth for Uphill Side – Excessive Feedwater Flow

STRESS INTENSITY FACTORS

Condition*	EFF1	EFF2	
Temperature	462.4	557.4	F
Pressure	1977	2317	psig
Sy	43.6	42.6	ksi
KIc	200.0	200.0	ksi√in
KIa	200.0	200.0	ksi√in
Crack Front	KI		
Position	(ksi√in)	(ksi√in)	
1	40.206	18.517	
2	39.093	18.817	
3	38.174	19.343	
4	34.281	18.414	
5	32.584	18.500	
6	30.503	18.193	
7	27.311	16.951	
8	20.626	12.944	
9	25.683	16.966	
10	13.771	8.786	
11	-3.839	-3.689	
12	11.051	7.146	
13	22.647	14.989	
14	31.036	20.354	
15	39.815	25.779	
16	54.549	35.319	
17	36.881	23.488	

* Condition	Description
EFF1	Time step 30 at 0.167 hr. - Maximum KI
EFF2	Time step 1 at 0.0001 hr. - Minimum KI

FATIGUE CRACK GROWTH

Transient Description: 40 cycles over 40 years

ΔN = 1.0 cycles/year

Operating Time (end of yr.)	Cycle	a (in.)	Position 16 EFF1 KI(a) (ksi√in)	EFF2 KI(a) (ksi√in)	ΔKI (ksi√in)	Δa (in.)
0	0.0		81.058	61.828	19.230	
1	1.0		81.529	62.187	19.342	
2	2.0		82.003	62.549	19.454	
3	3.0		82.480	62.913	19.567	
4	4.0		82.960	63.279	19.681	
5	5.0		83.443	63.647	19.796	
6	6.0		83.928	64.017	19.911	
7	7.0		84.416	64.389	20.027	
8	8.0		84.907	64.764	20.143	
9	9.0		85.400	65.140	20.260	
10	10.0		85.896	65.518	20.378	
11	11.0		86.395	65.899	20.496	
12	12.0		86.896	66.281	20.615	
13	13.0		87.401	66.666	20.735	
14	14.0		87.908	67.053	20.855	
15	15.0		88.418	67.442	20.976	
16	16.0		88.930	67.833	21.098	
17	17.0		89.446	68.226	21.220	
18	18.0		89.964	68.621	21.343	
19	19.0		90.485	69.019	21.466	
20	20.0		91.009	69.418	21.591	
21	21.0		91.536	69.820	21.716	
22	22.0		92.066	70.225	21.842	
23	23.0		92.599	70.631	21.968	
24	24.0		93.134	71.039	22.095	
25	25.0		93.673	71.450	22.223	
26	26.0		94.215	71.863	22.351	
27	27.0		94.759	72.279	22.480	
28	28.0		95.307	72.696	22.610	
29	29.0		95.857	73.116	22.741	
30	30.0		96.411	73.539	22.872	

Table A-12: Fatigue Crack Growth for Uphill Side – Leak Test

STRESS INTENSITY FACTORS

Condition*	LT1	LT2	
Temperature	238.0	82.0	F
Pressure	2351	602	psig
Sy	46.4	50.0	ksi
KIc	200.0	115.6	ksi√in
KIa	200.0	60.6	ksi√in

Crack Front Position	KI (ksi√in)	KI (ksi√in)
1	36.203	7.924
2	35.188	7.716
3	34.376	7.578
4	30.852	6.820
5	29.318	6.511
6	27.425	6.103
7	24.524	5.455
8	18.585	4.155
9	22.970	5.093
10	12.351	2.750
11	-3.258	-0.668
12	9.923	2.208
13	20.272	4.493
14	27.806	6.166
15	35.677	7.901
16	48.795	10.761
17	33.019	7.282

* Condition	Description
LT1	Time step 6 at 3.92 hr. - Maximum KI
LT2	Time step 2 at 0.12 hr. - Minimum KI

FATIGUE CRACK GROWTH

Transient Description: 280 cycles over 40 years

ΔN = 7.0 cycles/year

Operating Time (end of yr.)	Cycle	a (in.)	Position 16 LT1 KI(a) (ksi√in)	LT2 KI(a) (ksi√in)	ΔKI (ksi√in)	Δa (in.)
0	0.0		75.304	37.270	38.034	
1	7.0		75.743	37.487	38.255	
2	14.0		76.184	37.705	38.478	
3	21.0		76.627	37.925	38.702	
4	28.0		77.073	38.145	38.927	
5	35.0		77.521	38.367	39.154	
6	42.0		77.972	38.590	39.381	
7	49.0		78.425	38.815	39.610	
8	56.0		78.881	39.040	39.841	
9	63.0		79.339	39.267	40.072	
10	70.0		79.800	39.495	40.305	
11	77.0		80.263	39.725	40.539	
12	84.0		80.729	39.955	40.774	
13	91.0		81.198	40.187	41.011	
14	98.0		81.669	40.420	41.249	
15	105.0		82.143	40.655	41.488	
16	112.0		82.619	40.890	41.729	
17	119.0		83.098	41.127	41.970	
18	126.0		83.579	41.366	42.214	
19	133.0		84.064	41.605	42.458	
20	140.0		84.550	41.846	42.704	
21	147.0		85.040	42.089	42.951	
22	154.0		85.532	42.332	43.200	
23	161.0		86.027	42.577	43.450	
24	168.0		86.525	42.823	43.701	
25	175.0		87.025	43.071	43.954	
26	182.0		87.528	43.320	44.208	
27	189.0		88.034	43.571	44.464	
28	196.0		88.543	43.822	44.721	
29	203.0		89.054	44.075	44.979	
30	210.0		89.569	44.330	45.239	

Table A-13: Stress Intensification Factors for Uphill Side – Faulted Conditions

STRESS INTENSITY FACTORS FOR OPERATING CONDITIONS

Condition*	LLOCA	LSLB	
Temperature	32.0	204.3	F
Pressure	60	1331	psig
Sy	50.0	46.9	ksi
KIc	63.5	200.0	ksi√in
KIa	43.2	200.0	ksi√in
Crack Front	KI		
Position	(ksi√in)	(ksi√in)	
1	172.666	125.310	
2	162.695	118.971	
3	152.220	112.724	
4	129.976	97.510	
5	116.733	89.073	
6	103.336	80.161	
7	88.075	69.285	
8	65.634	51.855	
9	75.591	61.179	
10	42.758	34.017	
11	-3.101	-4.606	
12	33.734	26.937	
13	66.840	53.893	
14	93.354	74.686	
15	122.911	97.237	
16	169.481	133.327	
17	117.360	91.670	

TOTAL STRESS INTENSITY FACTORS WITH RESIDUAL STRESS

a_o = 2.1482 in.

Condition*	LLOCA	LSLB
Crack Front	KI	
Position	(ksi√in)	(ksi√in)
1	217.784	170.428
2	203.751	160.027
3	190.655	151.159
4	161.167	128.701
5	144.480	116.820
6	127.701	104.526
7	108.588	89.798
8	80.407	66.628
9	93.646	79.234
10	52.530	43.789
11	-5.202	-6.707
12	41.086	34.289
13	81.184	68.237
14	112.117	93.449
15	145.044	119.370
16	195.990	159.836
17	135.209	109.519

* Condition	Description
LLOCA	Time step 15 at 0.03889 hr. (140 sec.) - Maximum KI
LSLB	Time step 10 at 0.09889 hr. (356 sec.) - Maximum KI

Table A-14: EPFM Evaluations for Uphill Side – Reactor Trip

EPFM Equations:

$J_{mat} = C(\Delta a)^m$ C = [ ]

$T_{mat} = (E/\sigma_f^2)*Cm(\Delta a)^{m-1}$ m =

$J_{app} = [KI'(a_e)]^2/E'$

$T_{app} = (E/\sigma_f^2)*(dJ_{app}/da)$

Ductile Crack Growth Stability Criterion: $T_{app} < T_{mat}$

At instability: $T_{app} = T_{mat}$

Safety Factors		KI^*_p	KI^*_s	$KI^*(a)$	a_e	$KI'(a_e)$	J_{app}	T_{app}	Stable?
Primary	Secondary	(ksi√in)	(ksi√in)	(ksi√in)	(in.)	(ksi√in)	(kips/in)		
1.00	1.00	63.614	45.463	109.077	3.3712	114.881	0.442	1.035	Yes
2.00	1.00	127.227	45.463	172.690	3.8714	194.907	1.271	2.978	Yes
3.00	1.50	190.841	68.194	259.035	4.9117	329.307	3.628	8.502	Yes
4.00	1.00	254.455	45.463	299.918	5.5495	405.277	5.495	12.877	Yes
6.00	1.00	381.682	45.463	427.145	8.1310	698.669	16.331	38.270	No

Iterate on safety factor until $T_{app} = T_{mat}$ to determine $J_{instability}$:

							$J_{instability}$	T_{app}	T_{mat}
3.1437	3.1437	199.980	142.920	342.900	6.3206	494.503	8.181	19.171	19.171

at J_{mat} = 3.628 kips/in, T_{mat} = 50.698

Applied J-Integral Criterion: $J_{app} < J_{0.1}$

where, $J_{0.1} = J_{mat}$ at Δa = 0.1 in.

Safety Factors		KI^*_p	KI^*_s	$KI^*(a)$	a_e	$KI'(a_e)$	J_{app}	$J_{0.1}$	OK?
Primary	Secondary	(ksi√in)	(ksi√in)	(ksi√in)	(in.)	(ksi√in)	(kips/in)	(kips/in)	
1.50	1.00	95.421	45.463	140.883	3.5931	153.185	0.785	2.473	Yes

Figure A-1: J-T Diagram for Uphill Side – Reactor Trip

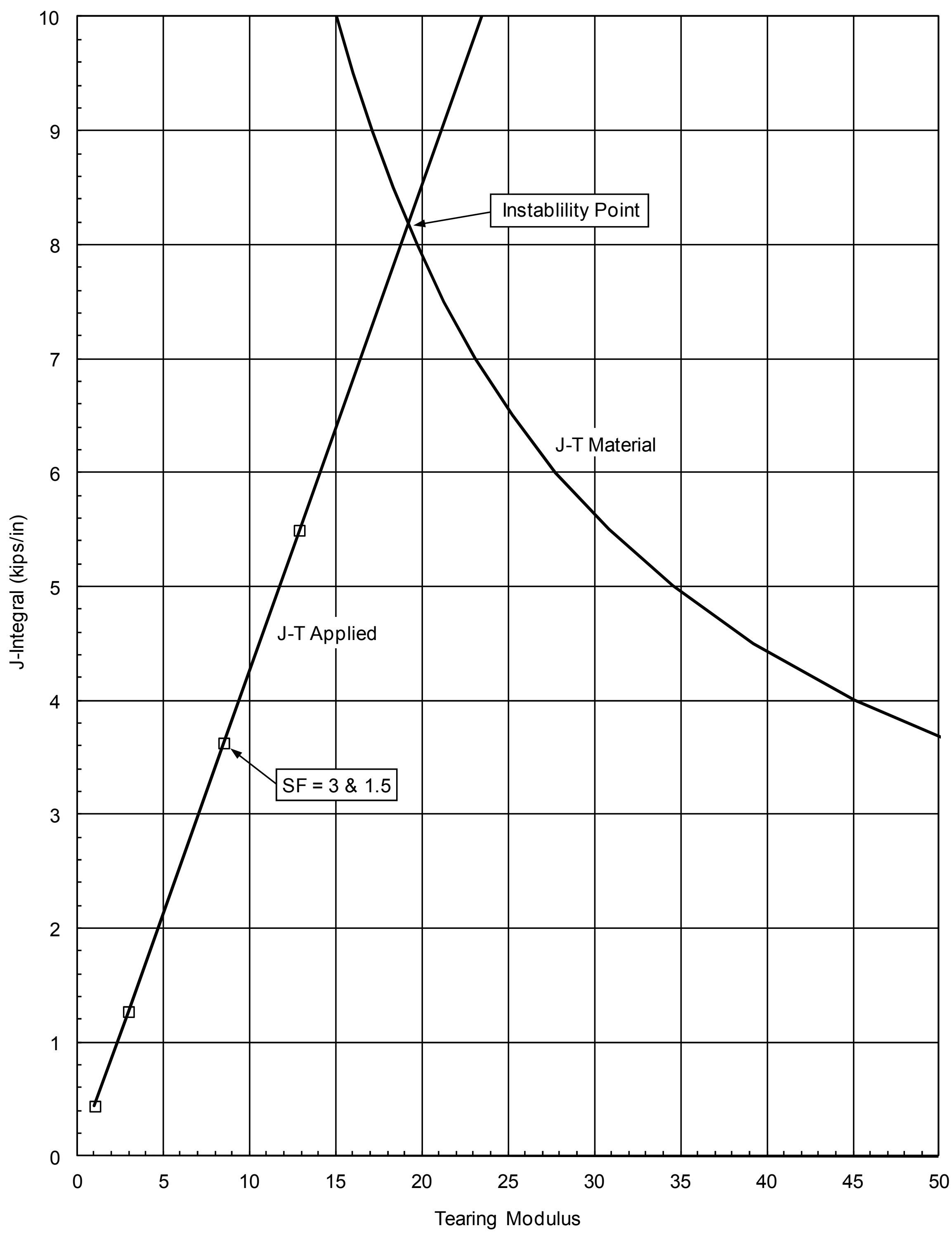

Table A-15: EPFM Evaluations for Uphill Side – Refueling

EPFM Equations:

$J_{mat} = C(\Delta a)^m$ C = [ ]

$T_{mat} = (E/\sigma_f^2)*Cm(\Delta a)^{m-1}$ m = [ ]

$J_{app} = [KI'(a_e)]^2/E'$

$T_{app} = (E/\sigma_f^2)*(dJ_{app}/da)$

Ductile Crack Growth Stability Criterion: $T_{app} < T_{mat}$

At instability: $T_{app} = T_{mat}$

Safety Factors		KI^*_p	KI^*_s	$KI^*(a)$	a_e	$KI'(a_e)$	J_{app}	T_{app}	Stable?
Primary	Secondary	(ksi√in)	(ksi√in)	(ksi√in)	(in.)	(ksi√in)	(kips/in)		
1.00	1.00	0.000	64.199	64.199	3.1266	65.117	0.132	0.301	Yes
3.00	1.50	0.000	96.299	96.299	3.2359	99.368	0.308	0.700	Yes
10.00	3.00	0.000	192.598	192.598	3.8263	216.106	1.456	3.311	Yes
10.00	4.00	0.000	256.798	256.798	4.4385	310.338	3.002	6.827	Yes
10.00	7.00	0.000	449.396	449.396	7.3248	697.672	15.173	34.504	No

Iterate on safety factor until $T_{app} = T_{mat}$ to determine $J_{instability}$:

							$J_{instability}$	T_{app}	T_{mat}
5.7241	5.7241	0.000	367.482	367.482	5.9048	512.230	8.179	18.599	18.599

at J_{mat} = 0.308 kips/in, T_{mat} = 942.947

Applied J-Integral Criterion: $J_{app} < J_{0.1}$

where, $J_{0.1} = J_{mat}$ at Δa = 0.1 in.

Safety Factors		KI^*_p	KI^*_s	$KI^*(a)$	a_e	$KI'(a_e)$	J_{app}	$J_{0.1}$	OK?
Primary	Secondary	(ksi√in)	(ksi√in)	(ksi√in)	(in.)	(ksi√in)	(kips/in)	(kips/in)	
1.50	1.00	0.000	64.199	64.199	3.1266	65.117	0.132	2.474	Yes

Figure A-2: J-T Diagram for Uphill Side – Refueling

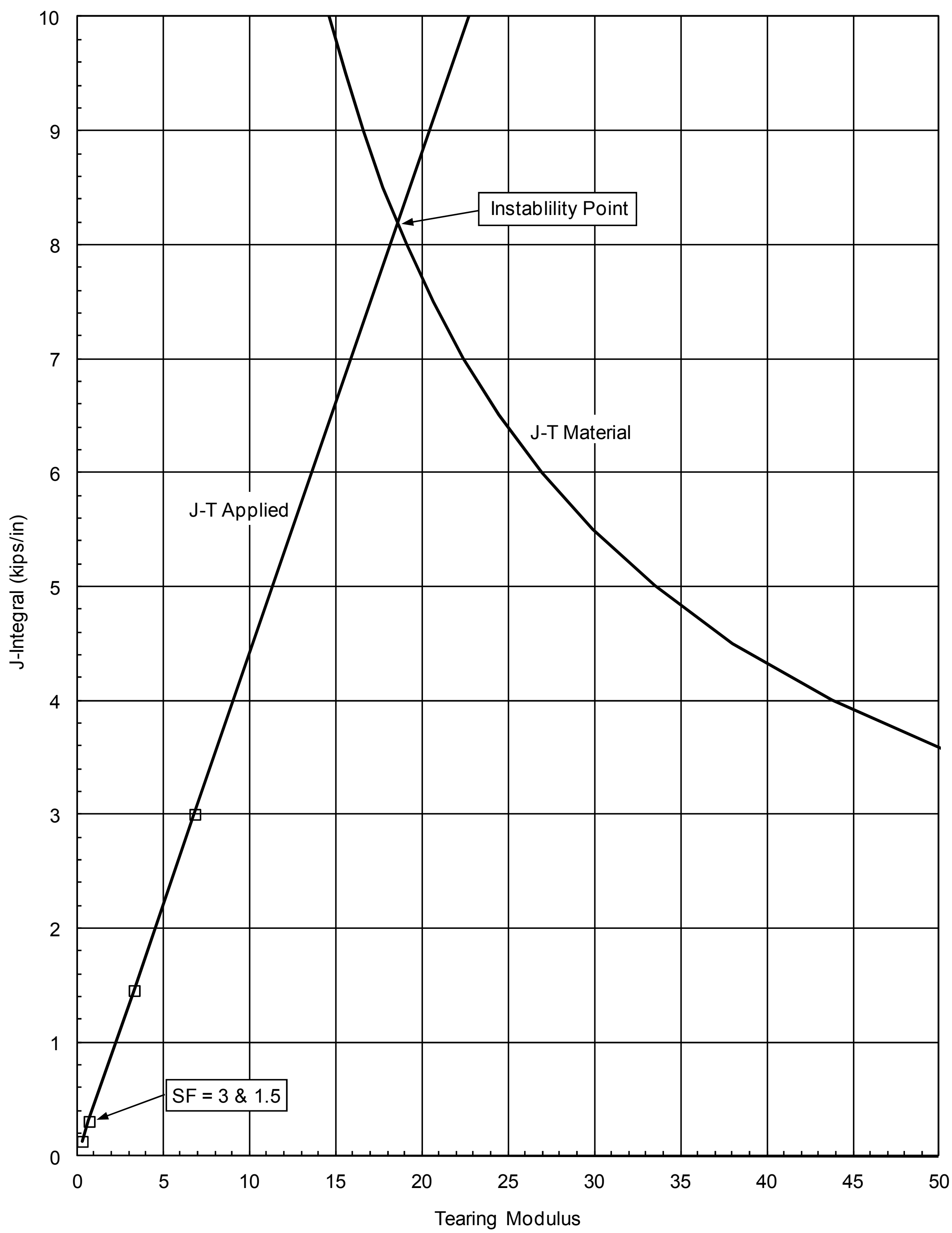

Table A-16: EPFM Evaluations for Uphill Side – LLOCA

EPFM Equations:

$J_{mat} = C(\Delta a)^m$ C = [ ]

$T_{mat} = (E/\sigma_f^2)*Cm(\Delta a)^{m-1}$ m = [ ]

$J_{app} = [KI'(a_e)]^2/E'$

$T_{app} = (E/\sigma_f^2)*(dJ_{app}/da)$

Ductile Crack Growth Stability Criterion: $T_{app} < T_{mat}$

At instability: $T_{app} = T_{mat}$

Safety Factors		KI^*_p	KI^*_s	$KI^*(a)$	a_e	$KI'(a_e)$	J_{app}	T_{app}	Stable?
Primary	Secondary	(ksi√in)	(ksi√in)	(ksi√in)	(in.)	(ksi√in)	(kips/in)		
1.00	1.00	1.731	231.385	233.116	4.1923	273.795	2.337	5.314	Yes
1.50	1.00	2.596	231.385	233.982	4.2009	275.092	2.359	5.364	Yes
20.00	1.00	34.620	231.385	266.005	4.5407	325.143	3.295	7.494	Yes
50.00	1.00	86.549	231.385	317.934	5.1842	415.242	5.375	12.223	Yes
100.00	1.00	173.098	231.385	404.484	6.5110	592.037	10.926	24.847	No

Iterate on safety factor until $T_{app} = T_{mat}$ to determine $J_{instability}$:

							$J_{instability}$	T_{app}	T_{mat}
1.5764	1.5764	2.729	364.753	367.482	5.9048	512.230	8.179	18.599	18.599

at J_{mat} = 2.359 kips/in, T_{mat} = 82.380

Applied J-Integral Criterion: $J_{app} < J_{0.1}$

where, $J_{0.1} = J_{mat}$ at Δa = 0.1 in.

Safety Factors		KI^*_p	KI^*_s	$KI^*(a)$	a_e	$KI'(a_e)$	J_{app}	$J_{0.1}$	OK?
Primary	Secondary	(ksi√in)	(ksi√in)	(ksi√in)	(in.)	(ksi√in)	(kips/in)	(kips/in)	
1.50	1.00	2.596	231.385	233.982	4.2009	275.092	2.359	2.474	Yes

Figure A-3: J-T Diagram for Uphill Side – LLOCA

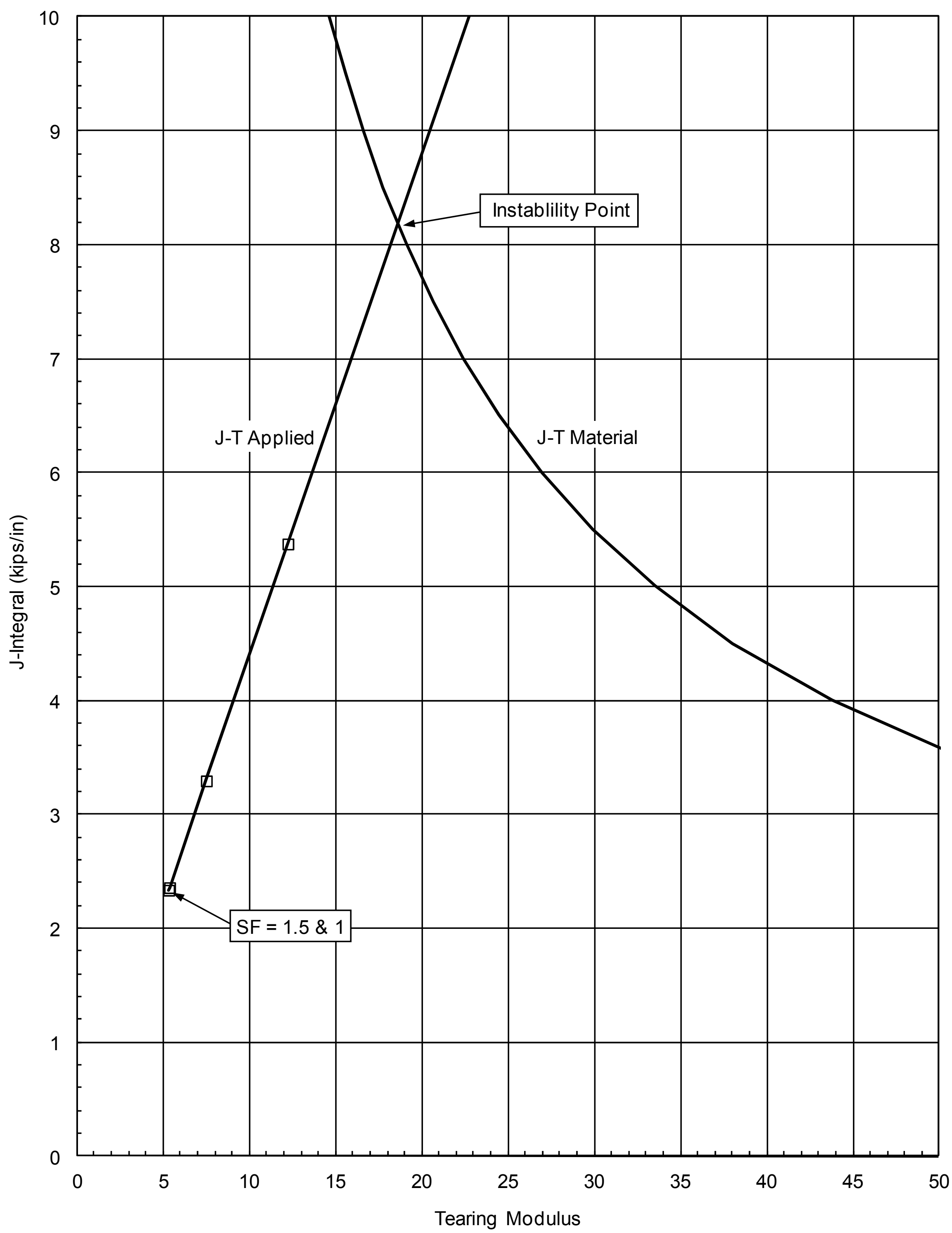

APPENDIX B: DETAILED FLAW EVALUATIONS FOR DOWNHILL SIDE

This appendix presents the fatigue crack growth tables and the elastic-plastic fracture mechanics flaw evaluations for the downhill side of the CRDM penetration.

Table B-1: Stress Intensification Factors for Downhill Side – Welding Residual Stress

Condition	WRS	
Temperature	70.0	F
Pressure	n/a	psig
Sy	50.0	ksi
KIc	98.0	ksi√in
KIa	55.2	ksi√in
Crack Front Position	KI (ksi√in)	
1	-1.701	
2	13.932	
3	15.717	
4	27.178	
5	33.890	
6	37.604	
7	40.501	
8	40.098	
9	37.638	
10	33.447	
11	24.673	
12	27.528	
13	26.926	
14	24.389	
15	21.701	
16	16.768	
17	5.776	

Table B-2: Fatigue Crack Growth for Downhill Side – Heatup/Cooldown

STRESS INTENSITY FACTORS

Condition*	HU1	HU2	CD	SD	
Temperature	557.0	349.0	120.0	70.0	F
Pressure	2317	467	467	0	psig
Sy	42.6	44.9	49.2	50.0	ksi
KIc	200.0	200.0	200.0	98.0	ksi√in
KIa	200.0	200.0	85.5	55.2	ksi√in
Crack Front	Stress Intensity Factor, KI				
Position	(ksi√in)	(ksi√in)	(ksi√in)	(ksi√in)	
1	0.943	1.525	-0.207	0.000	
2	2.680	-5.311	2.591	0.000	
3	3.692	-5.535	2.956	0.000	
4	7.332	-8.637	5.117	0.000	
5	10.761	-9.272	6.370	0.000	
6	12.898	-9.294	6.973	0.000	
7	14.706	-9.215	7.386	0.000	
8	15.467	-8.853	7.381	0.000	
9	15.906	-8.287	7.265	0.000	
10	15.601	-7.685	6.943	0.000	
11	12.347	-6.288	5.571	0.000	
12	14.585	-7.340	6.566	0.000	
13	15.201	-7.848	6.962	0.000	
14	14.925	-7.826	6.945	0.000	
15	14.388	-7.578	6.747	0.000	
16	11.322	-5.983	5.326	0.000	
17	2.718	-1.762	1.368	0.000	

* Condition	Description
HU1	Time step 6 at 7.67 hr. (Heatup) - Maximum KI
HU2	Time step 3 at 2.29 hr. (Heatup) - Minimum KI
CD	Time step 15 at 14.37 hr. - Maximum KI at Low Temperature
SD	Shutdown at Ambient Conditions

FATIGUE CRACK GROWTH

Transient Description: 200 cycles over 40 years

ΔN = 5.0 cycles/year

			Position 7					
Operating Time (end of yr.)	Cycle	a (in.)	HU1 KI(a) (ksi√in)	HU2 KI(a) (ksi√in)	ΔKI (ksi√in)	Δa (in.)	CD KI(a) (ksi√in)	SD KI(a) (ksi√in)
0	0.0		55.207	31.286	23.921		22.094	16.768
1	5.0		55.214	31.290	23.924		22.097	16.770
2	10.0		55.247	31.309	23.938		22.110	16.780
3	15.0		55.280	31.327	23.953		22.123	16.790
4	20.0		55.313	31.346	23.967		22.137	16.800
5	25.0		55.347	31.365	23.982		22.150	16.810
6	30.0		55.380	31.384	23.996		22.163	16.821
7	35.0		55.414	31.403	24.011		22.177	16.831
8	40.0		55.447	31.422	24.025		22.190	16.841
9	45.0		55.481	31.441	24.040		22.204	16.851
10	50.0		55.514	31.460	24.054		22.217	16.861
11	55.0		55.548	31.479	24.069		22.230	16.872
12	60.0		55.582	31.498	24.083		22.244	16.882
13	65.0		55.615	31.517	24.098		22.257	16.892
14	70.0		55.649	31.536	24.112		22.271	16.902
15	75.0		55.683	31.556	24.127		22.284	16.912
16	80.0		55.716	31.575	24.142		22.298	16.923
17	85.0		55.750	31.594	24.156		22.311	16.933
18	90.0		55.784	31.613	24.171		22.325	16.943
19	95.0		55.818	31.632	24.186		22.338	16.954
20	100.0		55.852	31.651	24.200		22.352	16.964
21	105.0		55.886	31.671	24.215		22.366	16.974
22	110.0		55.920	31.690	24.230		22.379	16.984
23	115.0		55.953	31.709	24.244		22.393	16.995
24	120.0		55.988	31.728	24.259		22.406	17.005
25	125.0		56.022	31.748	24.274		22.420	17.015
26	130.0		56.056	31.767	24.289		22.434	17.026
27	135.0		56.090	31.786	24.303		22.447	17.036
28	140.0		56.124	31.806	24.318		22.461	17.046
29	145.0		56.158	31.825	24.333		22.475	17.057
30	150.0		56.192	31.844	24.348		22.488	17.067

Table B-3: Fatigue Crack Growth for Downhill Side – Unit Loading/Unloading

STRESS INTENSITY FACTORS

Condition*	UL	UU	
Temperature	533.8	574.3	F
Pressure	2265	2209	psig
Sy	42.9	42.4	ksi
KIc	200.0	200.0	ksi√in
KIa	200.0	200.0	ksi√in
Crack Front	KI		
Position	(ksi√in)	(ksi√in)	
1	0.746	1.229	
2	3.671	0.911	
3	4.755	1.748	
4	9.072	4.086	
5	12.751	6.918	
6	14.950	8.813	
7	16.762	10.467	
8	17.430	11.286	
9	17.756	11.855	
10	17.317	11.772	
11	13.737	9.268	
12	16.213	10.975	
13	16.951	11.372	
14	16.691	11.113	
15	16.112	10.692	
16	12.687	8.404	
17	3.091	1.937	

* Condition	Description
UL	Time step 12 at 0.29 hr. - Maximum KI
UU	Time step 11 at 0.29 hr. - Minimum KI

FATIGUE CRACK GROWTH

Transient Description: 18300 cycles over 40 years

ΔN = 457.5 cycles/year

Operating Time (end of yr.)	Cycle	a (in.)	Position 7 UL KI(a) (ksi√in)	UU KI(a) (ksi√in)	ΔKI (ksi√in)	Δa (in.)
0	0.0		57.263	50.968	6.295	
1	457.5		57.277	50.980	6.297	
2	915.0		57.311	51.011	6.300	
3	1372.5		57.346	51.042	6.304	
4	1830.0		57.381	51.073	6.308	
5	2287.5		57.415	51.104	6.312	
6	2745.0		57.450	51.134	6.316	
7	3202.5		57.485	51.165	6.319	
8	3660.0		57.519	51.196	6.323	
9	4117.5		57.554	51.227	6.327	
10	4575.0		57.589	51.258	6.331	
11	5032.5		57.624	51.289	6.335	
12	5490.0		57.659	51.320	6.339	
13	5947.5		57.694	51.351	6.342	
14	6405.0		57.729	51.382	6.346	
15	6862.5		57.764	51.414	6.350	
16	7320.0		57.799	51.445	6.354	
17	7777.5		57.834	51.476	6.358	
18	8235.0		57.869	51.507	6.362	
19	8692.5		57.904	51.538	6.365	
20	9150.0		57.939	51.570	6.369	
21	9607.5		57.974	51.601	6.373	
22	10065.0		58.009	51.632	6.377	
23	10522.5		58.045	51.664	6.381	
24	10980.0		58.080	51.695	6.385	
25	11437.5		58.115	51.726	6.389	
26	11895.0		58.151	51.758	6.393	
27	12352.5		58.186	51.789	6.396	
28	12810.0		58.221	51.821	6.400	
29	13267.5		58.257	51.853	6.404	
30	13725.0		58.292	51.884	6.408	

Table B-4: Fatigue Crack Growth for Downhill Side – Step Load Increase/Decrease

STRESS INTENSITY FACTORS

Condition*	SLI	SLD	
Temperature	546.7	577.3	F
Pressure	2300	2290	psig
Sy	42.7	42.4	ksi
KIc	200.0	200.0	ksi√in
KIa	200.0	200.0	ksi√in
Crack Front	KI		
Position	(ksi√in)	(ksi√in)	
1	0.772	1.285	
2	3.722	0.748	
3	4.835	1.591	
4	9.238	3.871	
5	13.010	6.778	
6	15.276	8.792	
7	17.157	10.613	
8	17.864	11.582	
9	18.206	12.260	
10	17.751	12.215	
11	14.072	9.584	
12	16.598	11.333	
13	17.336	11.683	
14	17.050	11.350	
15	16.440	10.878	
16	12.943	8.536	
17	3.170	1.973	

* Condition	Description
SLI	Time step 9 at 0.041 hr. - Maximum KI
SLD	Time step 9 at 0.028 hr. - Minimum KI

FATIGUE CRACK GROWTH

Transient Description: 4000 cycles over 40 years

ΔN = 100.0 cycles/year

Operating Time (end of yr.)	Cycle	a (in.)	Position 7 SLI KI(a) (ksi√in)	SLD KI(a) (ksi√in)	ΔKI (ksi√in)	Δa (in.)
0	0.0		57.658	51.114	6.544	
1	100.0		57.676	51.130	6.546	
2	200.0		57.711	51.161	6.550	
3	300.0		57.746	51.192	6.554	
4	400.0		57.781	51.223	6.558	
5	500.0		57.816	51.254	6.562	
6	600.0		57.851	51.285	6.566	
7	700.0		57.885	51.316	6.570	
8	800.0		57.920	51.347	6.574	
9	900.0		57.955	51.378	6.578	
10	1000.0		57.991	51.409	6.582	
11	1100.0		58.026	51.440	6.586	
12	1200.0		58.061	51.471	6.590	
13	1300.0		58.096	51.502	6.594	
14	1400.0		58.131	51.533	6.598	
15	1500.0		58.166	51.565	6.602	
16	1600.0		58.202	51.596	6.606	
17	1700.0		58.237	51.627	6.610	
18	1800.0		58.272	51.659	6.614	
19	1900.0		58.308	51.690	6.618	
20	2000.0		58.343	51.721	6.622	
21	2100.0		58.378	51.753	6.626	
22	2200.0		58.414	51.784	6.630	
23	2300.0		58.449	51.816	6.634	
24	2400.0		58.485	51.847	6.638	
25	2500.0		58.521	51.879	6.642	
26	2600.0		58.556	51.910	6.646	
27	2700.0		58.592	51.942	6.650	
28	2800.0		58.627	51.973	6.654	
29	2900.0		58.663	52.005	6.658	
30	3000.0		58.699	52.037	6.662	

Table B-5: Fatigue Crack Growth for Downhill Side – Turbine Roll Test

STRESS INTENSITY FACTORS

Condition*	TRT1	TRT2	
Temperature	443.4	557.4	F
Pressure	1692	2317	psig
Sy	43.8	42.6	ksi
KIc	200.0	200.0	ksi√in
KIa	200.0	200.0	ksi√in
Crack Front	KI		
Position	(ksi√in)	(ksi√in)	
1	-0.097	1.296	
2	7.596	0.314	
3	8.926	1.073	
4	15.799	2.965	
5	20.199	5.609	
6	22.374	7.456	
7	23.858	9.127	
8	23.895	10.028	
9	23.591	10.686	
10	22.575	10.691	
11	18.078	8.372	
12	21.311	9.916	
13	22.588	10.205	
14	22.546	9.905	
15	21.928	9.491	
16	17.326	7.446	
17	4.367	1.684	

* Condition	Description
TRT1	Time step 5 at 0.278 hr. - Maximum KI
TRT2	Time step 8 at 1.418 hr. - Minimum KI

FATIGUE CRACK GROWTH

Transient Description: 80 cycles over 40 years

ΔN = 2.0 cycles/year

Operating Time (end of yr.)	Cycle	a (in.)	Position 7 TRT1 KI(a) (ksi√in)	Position 7 TRT2 KI(a) (ksi√in)	Position 7 ΔKI (ksi√in)	Position 7 Δa (in.)
0	0.0		64.359	49.628	14.731	
1	2.0		64.381	49.645	14.736	
2	4.0		64.419	49.675	14.745	
3	6.0		64.458	49.705	14.754	
4	8.0		64.497	49.735	14.763	
5	10.0		64.536	49.765	14.772	
6	12.0		64.575	49.795	14.780	
7	14.0		64.614	49.825	14.789	
8	16.0		64.653	49.855	14.798	
9	18.0		64.692	49.885	14.807	
10	20.0		64.732	49.915	14.816	
11	22.0		64.771	49.945	14.825	
12	24.0		64.810	49.976	14.834	
13	26.0		64.849	50.006	14.843	
14	28.0		64.888	50.036	14.852	
15	30.0		64.928	50.067	14.861	
16	32.0		64.967	50.097	14.870	
17	34.0		65.007	50.127	14.879	
18	36.0		65.046	50.158	14.888	
19	38.0		65.085	50.188	14.897	
20	40.0		65.125	50.219	14.906	
21	42.0		65.165	50.249	14.915	
22	44.0		65.204	50.280	14.924	
23	46.0		65.244	50.310	14.934	
24	48.0		65.283	50.341	14.943	
25	50.0		65.323	50.371	14.952	
26	52.0		65.363	50.402	14.961	
27	54.0		65.403	50.433	14.970	
28	56.0		65.443	50.464	14.979	
29	58.0		65.482	50.494	14.988	
30	60.0		65.522	50.525	14.997	

Table B-6: Fatigue Crack Growth for Downhill Side – Refueling

STRESS INTENSITY FACTORS

Condition*	RF1	RF2	
Temperature	32.0	140.0	F
Pressure	0	0	psig
Sy	50.0	48.5	ksi
KIc	63.5	200.0	ksi√in
KIa	43.2	105.3	ksi√in
Crack Front	KI		
Position	(ksi√in)	(ksi√in)	
1	-1.034	0.410	
2	6.136	-1.478	
3	6.728	-1.554	
4	11.118	-2.447	
5	12.933	-2.684	
6	13.508	-2.754	
7	13.636	-2.816	
8	13.111	-2.783	
9	12.453	-2.669	
10	11.656	-2.515	
11	9.511	-2.035	
12	11.218	-2.375	
13	12.125	-2.502	
14	12.312	-2.456	
15	12.086	-2.355	
16	9.579	-1.852	
17	2.556	-0.538	

* Condition	Description
RF1	Time step 7 at 0.171 hr. - Maximum KI
RF2	Time step 1 at 0.0001 hr. - Minimum KI

FATIGUE CRACK GROWTH

Transient Description: 80 cycles over 40 years

ΔN = 2.0 cycles/year

Operating Time (end of yr.)	Cycle	a (in.)	Position 7 RF1 KI(a) (ksi√in)	RF2 KI(a) (ksi√in)	ΔKI (ksi√in)	Δa (in.)
0	0.0		54.137	37.685	16.452	
1	2.0		54.156	37.698	16.458	
2	4.0		54.189	37.721	16.468	
3	6.0		54.222	37.744	16.478	
4	8.0		54.254	37.767	16.488	
5	10.0		54.287	37.790	16.498	
6	12.0		54.320	37.812	16.508	
7	14.0		54.353	37.835	16.518	
8	16.0		54.386	37.858	16.528	
9	18.0		54.419	37.881	16.538	
10	20.0		54.452	37.904	16.548	
11	22.0		54.485	37.927	16.558	
12	24.0		54.517	37.950	16.568	
13	26.0		54.551	37.973	16.578	
14	28.0		54.584	37.996	16.588	
15	30.0		54.617	38.019	16.598	
16	32.0		54.650	38.042	16.608	
17	34.0		54.683	38.065	16.618	
18	36.0		54.716	38.088	16.628	
19	38.0		54.749	38.111	16.638	
20	40.0		54.783	38.134	16.648	
21	42.0		54.816	38.158	16.658	
22	44.0		54.849	38.181	16.668	
23	46.0		54.882	38.204	16.679	
24	48.0		54.916	38.227	16.689	
25	50.0		54.949	38.250	16.699	
26	52.0		54.983	38.274	16.709	
27	54.0		55.016	38.297	16.719	
28	56.0		55.050	38.320	16.729	
29	58.0		55.083	38.344	16.740	
30	60.0		55.117	38.367	16.750	

Table B-7: Fatigue Crack Growth for Downhill Side – Loss of Load

STRESS INTENSITY FACTORS

Condition*	LL1	LL2	
Temperature	575.8	588.8	F
Pressure	2710	1844	psig
Sy	42.4	42.2	ksi
KIc	200.0	200.0	ksi√in
KIa	200.0	200.0	ksi√in
Crack Front Position	KI (ksi√in)	KI (ksi√in)	
1	0.950	1.766	
2	3.481	-2.663	
3	4.682	-2.204	
4	9.183	-2.532	
5	13.346	-0.958	
6	15.991	0.418	
7	18.333	1.738	
8	19.392	2.668	
9	19.973	3.496	
10	19.585	3.858	
11	15.468	2.902	
12	18.216	3.502	
13	18.870	3.448	
14	18.370	3.223	
15	17.573	3.041	
16	13.802	2.360	
17	3.440	0.326	

* Condition	Description
LL1	Time step 2 at 0.003 hr. - Maximum KI
LL2	Time step 12 at 0.033 hr. - Minimum KI

FATIGUE CRACK GROWTH

Transient Description: 210 cycles over 40 years

ΔN = 5.25 cycles/year

Operating Time (end of yr.)	Cycle	a (in.)	Position 7 LL1 KI(a) (ksi√in)	Position 7 LL2 KI(a) (ksi√in)	Position 7 ΔKI (ksi√in)	Position 7 Δa (in.)
0	0.0		58.834	42.239	16.595	
1	5.3		58.857	42.255	16.601	
2	10.5		58.892	42.281	16.611	
3	15.8		58.928	42.306	16.621	
4	21.0		58.963	42.332	16.631	
5	26.3		58.999	42.357	16.642	
6	31.5		59.035	42.383	16.652	
7	36.8		59.070	42.409	16.662	
8	42.0		59.106	42.434	16.672	
9	47.3		59.142	42.460	16.682	
10	52.5		59.177	42.486	16.692	
11	57.8		59.213	42.511	16.702	
12	63.0		59.249	42.537	16.712	
13	68.3		59.285	42.563	16.722	
14	73.5		59.321	42.589	16.732	
15	78.8		59.357	42.614	16.742	
16	84.0		59.393	42.640	16.753	
17	89.3		59.429	42.666	16.763	
18	94.5		59.465	42.692	16.773	
19	99.8		59.501	42.718	16.783	
20	105.0		59.537	42.744	16.793	
21	110.3		59.573	42.770	16.804	
22	115.5		59.610	42.796	16.814	
23	120.8		59.646	42.822	16.824	
24	126.0		59.682	42.848	16.834	
25	131.3		59.718	42.874	16.844	
26	136.5		59.755	42.900	16.855	
27	141.8		59.791	42.926	16.865	
28	147.0		59.828	42.952	16.875	
29	152.3		59.864	42.978	16.886	
30	157.5		59.900	43.005	16.896	

Table B-8: Fatigue Crack Growth for Downhill Side – Loss of Power

STRESS INTENSITY FACTORS

Condition*	LP1	LP2	
Temperature	553.8	600.5	F
Pressure	2295	2464	psig
Sy	42.7	42.1	ksi
KIc	200.0	200.0	ksi√in
KIa	200.0	200.0	ksi√in
Crack Front	KI		
Position	(ksi√in)	(ksi√in)	
1	0.946	1.583	
2	2.604	-0.933	
3	3.602	-0.235	
4	7.174	0.851	
5	10.560	3.271	
6	12.672	5.130	
7	14.460	6.893	
8	15.213	7.988	
9	15.652	8.849	
10	15.355	9.056	
11	12.150	7.048	
12	14.353	8.381	
13	14.958	8.536	
14	14.686	8.199	
15	14.157	7.823	
16	11.141	6.120	
17	2.671	1.294	

* Condition	Description
LP1	Time step 2 at 0.003 hr. - Maximum KI
LP2	Time step 11 at 0.053 hr. - Minimum KI

FATIGUE CRACK GROWTH

Transient Description: 100 cycles over 40 years

ΔN = 2.5 cycles/year

Operating Time (end of yr.)	Cycle	a (in.)	Position 7 LP1 KI(a) (ksi√in)	LP2 KI(a) (ksi√in)	ΔKI (ksi√in)	Δa (in.)
0	0.0		54.961	47.394	7.567	
1	2.5		54.986	47.416	7.570	
2	5.0		55.019	47.444	7.575	
3	7.5		55.053	47.473	7.580	
4	10.0		55.086	47.502	7.584	
5	12.5		55.119	47.530	7.589	
6	15.0		55.152	47.559	7.593	
7	17.5		55.186	47.588	7.598	
8	20.0		55.219	47.617	7.603	
9	22.5		55.253	47.645	7.607	
10	25.0		55.286	47.674	7.612	
11	27.5		55.319	47.703	7.616	
12	30.0		55.353	47.732	7.621	
13	32.5		55.386	47.761	7.626	
14	35.0		55.420	47.790	7.630	
15	37.5		55.454	47.819	7.635	
16	40.0		55.487	47.848	7.639	
17	42.5		55.521	47.877	7.644	
18	45.0		55.555	47.906	7.649	
19	47.5		55.588	47.935	7.653	
20	50.0		55.622	47.964	7.658	
21	52.5		55.656	47.993	7.663	
22	55.0		55.690	48.022	7.667	
23	57.5		55.723	48.052	7.672	
24	60.0		55.757	48.081	7.677	
25	62.5		55.791	48.110	7.681	
26	65.0		55.825	48.139	7.686	
27	67.5		55.859	48.169	7.691	
28	70.0		55.893	48.198	7.695	
29	72.5		55.927	48.227	7.700	
30	75.0		55.961	48.257	7.705	

Table B-9: Fatigue Crack Growth for Downhill Side – Reactor Trip

STRESS INTENSITY FACTORS

Condition*	RT1	RT2	
Temperature	457.4	537.4	F
Pressure	2205	1803	psig
Sy	43.6	42.8	ksi
KIc	200.0	200.0	ksi√in
KIa	200.0	200.0	ksi√in
Crack Front	KI		
Position	(ksi√in)	(ksi√in)	
1	-0.344	0.927	
2	9.813	2.017	
3	11.437	2.874	
4	20.106	5.810	
5	25.541	8.607	
6	28.273	10.252	
7	30.240	11.515	
8	30.411	11.924	
9	30.082	12.163	
10	28.819	11.886	
11	23.051	9.451	
12	27.143	11.204	
13	28.677	11.791	
14	28.509	11.714	
15	27.648	11.387	
16	21.824	8.989	
17	5.557	2.099	

* Condition	Description
RT1	Time step 13 at 0.171 hr. - Maximum KI
RT2	Time step 8 at 0.025 hr. - Minimum KI

FATIGUE CRACK GROWTH

Transient Description: 250 cycles over 40 years

ΔN = 6.25 cycles/year

Operating Time (end of yr.)	Cycle	a (in.)	Position 7 RT1 KI(a) (ksi√in)	RT2 KI(a) (ksi√in)	ΔKI (ksi√in)	Δa (in.)
0	0.0		70.741	52.016	18.725	
1	6.3		70.774	52.040	18.734	
2	12.5		70.816	52.071	18.745	
3	18.8		70.859	52.103	18.756	
4	25.0		70.902	52.134	18.768	
5	31.3		70.945	52.166	18.779	
6	37.5		70.987	52.197	18.790	
7	43.8		71.030	52.229	18.802	
8	50.0		71.073	52.260	18.813	
9	56.3		71.116	52.292	18.824	
10	62.5		71.159	52.324	18.836	
11	68.8		71.202	52.355	18.847	
12	75.0		71.246	52.387	18.859	
13	81.3		71.289	52.419	18.870	
14	87.5		71.332	52.450	18.881	
15	93.8		71.375	52.482	18.893	
16	100.0		71.418	52.514	18.904	
17	106.3		71.462	52.546	18.916	
18	112.5		71.505	52.578	18.927	
19	118.8		71.548	52.610	18.939	
20	125.0		71.592	52.642	18.950	
21	131.3		71.635	52.674	18.962	
22	137.5		71.679	52.706	18.973	
23	143.8		71.722	52.738	18.985	
24	150.0		71.766	52.770	18.996	
25	156.3		71.810	52.802	19.008	
26	162.5		71.853	52.834	19.019	
27	168.8		71.897	52.866	19.031	
28	175.0		71.941	52.898	19.043	
29	181.3		71.985	52.931	19.054	
30	187.5		72.029	52.963	19.066	

Table B-10: Fatigue Crack Growth for Downhill Side – Inadvertent Depressurization

STRESS INTENSITY FACTORS

Condition*	ID1	ID2	
Temperature	557.4	556.6	F
Pressure	2317	1161	psig
Sy	42.6	42.6	ksi
KIc	200.0	200.0	ksi√in
KIa	200.0	200.0	ksi√in
Crack Front	KI		
Position	(ksi√in)	(ksi√in)	
1	0.944	1.606	
2	2.677	-2.583	
3	3.690	-2.226	
4	7.328	-2.753	
5	10.757	-1.643	
6	12.894	-0.738	
7	14.702	0.007	
8	15.463	0.486	
9	15.902	1.001	
10	15.598	1.266	
11	12.345	0.914	
12	14.583	1.172	
13	15.199	1.177	
14	14.922	1.172	
15	14.385	1.175	
16	11.320	0.928	
17	2.717	-0.029	

* Condition	Description
ID1	Time step 1 at 0.0001 hr. - Maximum KI
ID2	Time step 9 at 0.022 hr. - Minimum KI

FATIGUE CRACK GROWTH

Transient Description: 100 cycles over 40 years

ΔN = 2.5 cycles/year

Operating Time (end of yr.)	Cycle	a (in.)	Position 7 ID1 KI(a) (ksi√in)	ID2 KI(a) (ksi√in)	ΔKI (ksi√in)	Δa (in.)
0	0.0		55.203	40.508	14.695	
1	2.5		55.235	40.531	14.703	
2	5.0		55.268	40.556	14.712	
3	7.5		55.301	40.580	14.721	
4	10.0		55.335	40.605	14.730	
5	12.5		55.368	40.629	14.739	
6	15.0		55.402	40.654	14.748	
7	17.5		55.435	40.678	14.757	
8	20.0		55.468	40.703	14.766	
9	22.5		55.502	40.727	14.775	
10	25.0		55.536	40.752	14.784	
11	27.5		55.569	40.777	14.792	
12	30.0		55.603	40.801	14.801	
13	32.5		55.637	40.826	14.810	
14	35.0		55.670	40.851	14.819	
15	37.5		55.704	40.876	14.828	
16	40.0		55.738	40.900	14.837	
17	42.5		55.772	40.925	14.846	
18	45.0		55.805	40.950	14.855	
19	47.5		55.839	40.975	14.864	
20	50.0		55.873	41.000	14.873	
21	52.5		55.907	41.025	14.882	
22	55.0		55.941	41.050	14.891	
23	57.5		55.975	41.075	14.901	
24	60.0		56.009	41.100	14.910	
25	62.5		56.043	41.125	14.919	
26	65.0		56.077	41.150	14.928	
27	67.5		56.111	41.175	14.937	
28	70.0		56.146	41.200	14.946	
29	72.5		56.180	41.225	14.955	
30	75.0		56.214	41.250	14.964	

Table B-11: Fatigue Crack Growth for Downhill Side – Excessive Feedwater Flow

STRESS INTENSITY FACTORS

Condition*	EFF1	EFF2	
Temperature	448.6	557.4	F
Pressure	1809	2317	psig
Sy	43.7	42.6	ksi
KIc	200.0	200.0	ksi√in
KIa	200.0	200.0	ksi√in
Crack Front	KI		
Position	(ksi√in)	(ksi√in)	
1	-0.519	0.944	
2	9.452	2.677	
3	10.871	3.690	
4	18.778	7.328	
5	23.040	10.757	
6	24.576	12.894	
7	25.052	14.702	
8	24.101	15.463	
9	23.123	15.902	
10	21.900	15.598	
11	17.871	12.345	
12	21.256	14.583	
13	23.048	15.199	
14	23.529	14.922	
15	23.259	14.385	
16	18.487	11.320	
17	4.524	2.717	

* Condition	Description
EFF1	Time step 4 at 0.013 hr. - Maximum KI
EFF2	Time step 1 at 0.0001 hr. - Minimum KI

FATIGUE CRACK GROWTH

Transient Description: 40 cycles over 40 years

ΔN = 1.0 cycles/year

Operating Time (end of yr.)	Cycle	a (in.)	Position 7 EFF1 KI(a) (ksi√in)	EFF2 KI(a) (ksi√in)	ΔKI (ksi√in)	Δa (in.)
0	0.0		65.553	55.203	10.350	
1	1.0		65.592	55.236	10.356	
2	2.0		65.632	55.269	10.362	
3	3.0		65.672	55.303	10.369	
4	4.0		65.711	55.336	10.375	
5	5.0		65.751	55.370	10.381	
6	6.0		65.791	55.403	10.388	
7	7.0		65.830	55.437	10.394	
8	8.0		65.870	55.470	10.400	
9	9.0		65.910	55.504	10.406	
10	10.0		65.950	55.537	10.413	
11	11.0		65.990	55.571	10.419	
12	12.0		66.030	55.604	10.425	
13	13.0		66.070	55.638	10.432	
14	14.0		66.110	55.672	10.438	
15	15.0		66.150	55.706	10.444	
16	16.0		66.190	55.739	10.451	
17	17.0		66.230	55.773	10.457	
18	18.0		66.270	55.807	10.463	
19	19.0		66.310	55.841	10.470	
20	20.0		66.351	55.875	10.476	
21	21.0		66.391	55.909	10.482	
22	22.0		66.431	55.943	10.489	
23	23.0		66.472	55.977	10.495	
24	24.0		66.512	56.011	10.501	
25	25.0		66.553	56.045	10.508	
26	26.0		66.593	56.079	10.514	
27	27.0		66.634	56.113	10.521	
28	28.0		66.674	56.147	10.527	
29	29.0		66.715	56.181	10.533	
30	30.0		66.756	56.216	10.540	

Table B-12: Fatigue Crack Growth for Downhill Side – Leak Test

STRESS INTENSITY FACTORS

Condition*	LT1	LT2	
Temperature	238.0	82.0	F
Pressure	2351	602	psig
Sy	46.4	50.0	ksi
KIc	200.0	115.6	ksi√in
KIa	200.0	60.6	ksi√in
Crack Front	KI		
Position	(ksi√in)	(ksi√in)	
1	-0.484	-0.180	
2	7.656	1.843	
3	8.820	2.100	
4	15.468	3.646	
5	19.687	4.609	
6	21.987	5.170	
7	23.902	5.696	
8	24.423	5.902	
9	24.437	5.952	
10	23.571	5.765	
11	18.741	4.566	
12	22.027	5.351	
13	23.041	5.545	
14	22.643	5.386	
15	21.785	5.139	
16	17.137	4.030	
17	4.398	1.055	

* Condition	Description
LT1	Time step 6 at 3.92 hr. - Maximum KI
LT2	Time step 2 at 0.12 hr. - Minimum KI

FATIGUE CRACK GROWTH

Transient Description: 280 cycles over 40 years

ΔN = 7.0 cycles/year

Operating Time (end of yr.)	Cycle	a (in.)	Position 7 LT1 KI(a) (ksi√in)	LT2 KI(a) (ksi√in)	ΔKI (ksi√in)	Δa (in.)
0	0.0		64.403	46.197	18.206	
1	7.0		64.442	46.225	18.217	
2	14.0		64.481	46.253	18.228	
3	21.0		64.520	46.281	18.239	
4	28.0		64.559	46.309	18.250	
5	35.0		64.598	46.337	18.261	
6	42.0		64.637	46.365	18.272	
7	49.0		64.676	46.393	18.283	
8	56.0		64.715	46.421	18.294	
9	63.0		64.754	46.449	18.305	
10	70.0		64.793	46.477	18.316	
11	77.0		64.832	46.505	18.327	
12	84.0		64.872	46.533	18.338	
13	91.0		64.911	46.561	18.350	
14	98.0		64.950	46.589	18.361	
15	105.0		64.990	46.618	18.372	
16	112.0		65.029	46.646	18.383	
17	119.0		65.068	46.674	18.394	
18	126.0		65.108	46.703	18.405	
19	133.0		65.147	46.731	18.416	
20	140.0		65.187	46.759	18.428	
21	147.0		65.227	46.788	18.439	
22	154.0		65.266	46.816	18.450	
23	161.0		65.306	46.845	18.461	
24	168.0		65.346	46.873	18.472	
25	175.0		65.385	46.902	18.484	
26	182.0		65.425	46.930	18.495	
27	189.0		65.465	46.959	18.506	
28	196.0		65.505	46.987	18.517	
29	203.0		65.545	47.016	18.529	
30	210.0		65.585	47.045	18.540	

Table B-13: Stress Intensification Factors for Downhill Side – Faulted Conditions

STRESS INTENSITY FACTORS FOR OPERATING CONDITIONS

Condition*	LLOCA	LSLB	
Temperature	32.0	207.8	F
Pressure	60	1316	psig
Sy	50.0	46.9	ksi
KIc	63.5	200.0	ksi√in
KIa	43.2	200.0	ksi√in
Crack Front	KI		
Position	(ksi√in)	(ksi√in)	
1	-6.103	-3.533	
2	38.630	26.671	
3	42.411	29.689	
4	70.343	50.026	
5	81.924	59.828	
6	85.195	63.651	
7	85.364	65.558	
8	81.305	64.020	
9	76.653	61.644	
10	71.333	58.060	
11	58.183	46.864	
12	68.598	55.118	
13	74.395	58.941	
14	75.853	59.256	
15	74.663	57.792	
16	59.246	45.712	
17	15.675	12.059	

TOTAL STRESS INTENSITY FACTORS WITH RESIDUAL STRESS

a_o = 2.1482 in.

Condition*	LLOCA	LSLB
Crack Front	KI	
Position	(ksi√in)	(ksi√in)
1	-7.804	-5.234
2	52.562	40.603
3	58.128	45.406
4	97.521	77.204
5	115.814	93.718
6	122.799	101.255
7	125.865	106.059
8	121.403	104.118
9	114.291	99.282
10	104.780	91.507
11	82.856	71.537
12	96.126	82.646
13	101.321	85.867
14	100.242	83.645
15	96.364	79.493
16	76.014	62.480
17	21.451	17.835

* Condition	Description
LLOCA	Time step 15 at 0.03889 hr. (140 sec.) - Maximum KI
LSLB	Time step 9 at 0.09222 hr. (332 sec.) - Maximum KI

Table B-14: EPFM Evaluations for Downhill Side – Reactor Trip

EPFM Equations:

$J_{mat} = C(\Delta a)^m$ C = [ ]

$T_{mat} = (E/\sigma_f^2)^*Cm(\Delta a)^{m-1}$ m = [ ]

$J_{app} = [KI'(a_e)]^2/E'$

$T_{app} = (E/\sigma_f^2)^*(dJ_{app}/da)$

Ductile Crack Growth Stability Criterion: $T_{app} < T_{mat}$

At instability: $T_{app} = T_{mat}$

Safety Factors		KI^*_p	KI^*_s	$KI^*(a)$	a_e	$KI'(a_e)$	J_{app}	T_{app}	Stable?
Primary	Secondary	(ksi√in)	(ksi√in)	(ksi√in)	(in.)	(ksi√in)	(kips/in)		
1.00	1.00	28.672	43.367	72.039	2.3726	74.344	0.185	0.591	Yes
2.00	1.00	57.345	43.367	100.711	2.5108	106.918	0.382	1.223	Yes
3.00	1.50	86.017	65.050	151.067	2.8646	171.305	0.982	3.139	Yes
8.00	1.00	229.378	43.367	272.745	4.3038	379.096	4.808	15.371	Yes
15.00	1.00	430.084	43.367	473.451	8.4835	923.906	28.558	91.296	No

Iterate on safety factor until $T_{app} = T_{mat}$ to determine $J_{instability}$:

							$J_{instability}$	T_{app}	T_{mat}
4.3064	4.3064	123.476	186.756	310.232	4.9137	460.742	7.102	22.705	22.705

at J_{mat} = 0.982 kips/in, T_{mat} = 242.047

Applied J-Integral Criterion: $J_{app} < J_{0.1}$

where, $J_{0.1} = J_{mat}$ at Δa = 0.1 in.

Safety Factors		KI^*_p	KI^*_s	$KI^*(a)$	a_e	$KI'(a_e)$	J_{app}	$J_{0.1}$	OK?
Primary	Secondary	(ksi√in)	(ksi√in)	(ksi√in)	(in.)	(ksi√in)	(kips/in)	(kips/in)	
1.50	1.00	43.008	43.367	86.375	2.4360	90.321	0.273	2.473	Yes

Figure B-1: J-T Diagram for Downhill Side – Reactor Trip

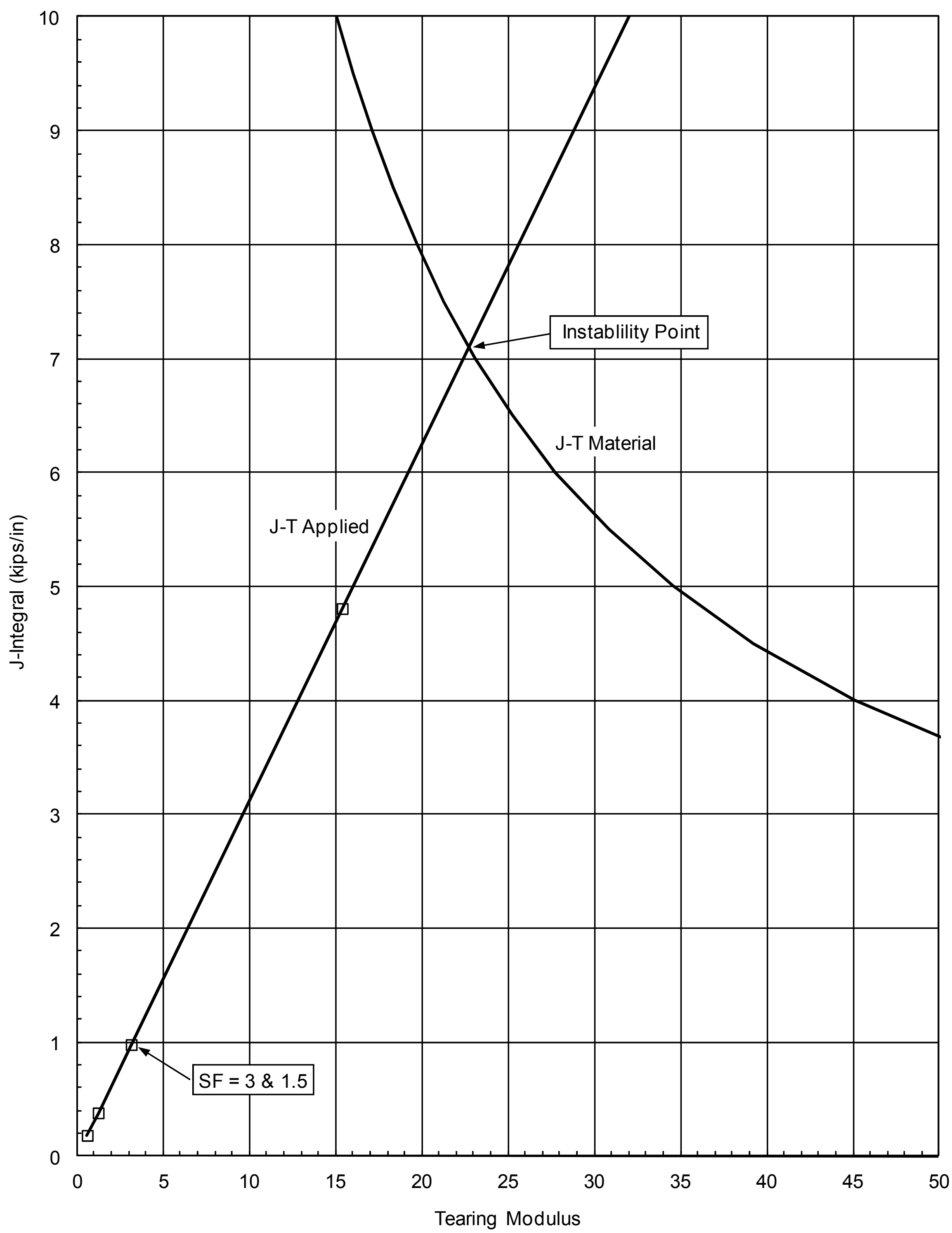

Table B-15: EPFM Evaluations for Downhill Side – Refueling

EPFM Equations:

$J_{mat} = C(\Delta a)^m$

$T_{mat} = (E/\sigma_f^2)*Cm(\Delta a)^{m-1}$

C = [ ]
m = [ ]

$J_{app} = [KI'(a_e)]^2/E'$

$T_{app} = (E/\sigma_f^2)*(dJ_{app}/da)$

Ductile Crack Growth Stability Criterion: $T_{app} < T_{mat}$

At instability: $T_{app} = T_{mat}$

Safety Factors		KI^*_p	KI^*_s	$KI^*(a)$	a_e	$KI'(a_e)$	J_{app}	T_{app}	Stable?
Primary	Secondary	(ksi√in)	(ksi√in)	(ksi√in)	(in.)	(ksi√in)	(kips/in)		
1.00	1.00	0.000	55.130	55.130	2.2923	55.923	0.097	0.302	Yes
3.00	1.50	0.000	82.695	82.695	2.3729	85.346	0.227	0.704	Yes
10.00	3.00	0.000	165.391	165.391	2.8082	185.692	1.075	3.335	Yes
10.00	4.00	0.000	220.521	220.521	3.2597	266.751	2.218	6.881	Yes
10.00	7.00	0.000	385.912	385.912	5.3881	600.168	11.228	34.834	No

Iterate on safety factor until $T_{app} = T_{mat}$ to determine $J_{instability}$:

							$J_{instability}$	T_{app}	T_{mat}
6.0382	6.0382	0.000	332.889	332.889	4.5793	477.273	7.101	22.029	22.029

at J_{mat} = 0.227 kips/in, T_{mat} = 1357.163

Applied J-Integral Criterion: $J_{app} < J_{0.1}$

where, $J_{0.1} = J_{mat}$ at Δa = 0.1 in.

Safety Factors		KI^*_p	KI^*_s	$KI^*(a)$	a_e	$KI'(a_e)$	J_{app}	$J_{0.1}$	OK?
Primary	Secondary	(ksi√in)	(ksi√in)	(ksi√in)	(in.)	(ksi√in)	(kips/in)	(kips/in)	
1.50	1.00	0.000	55.130	55.130	2.2923	55.923	0.097	2.474	Yes

Figure B-2: J-T Diagram for Downhill Side – Refueling

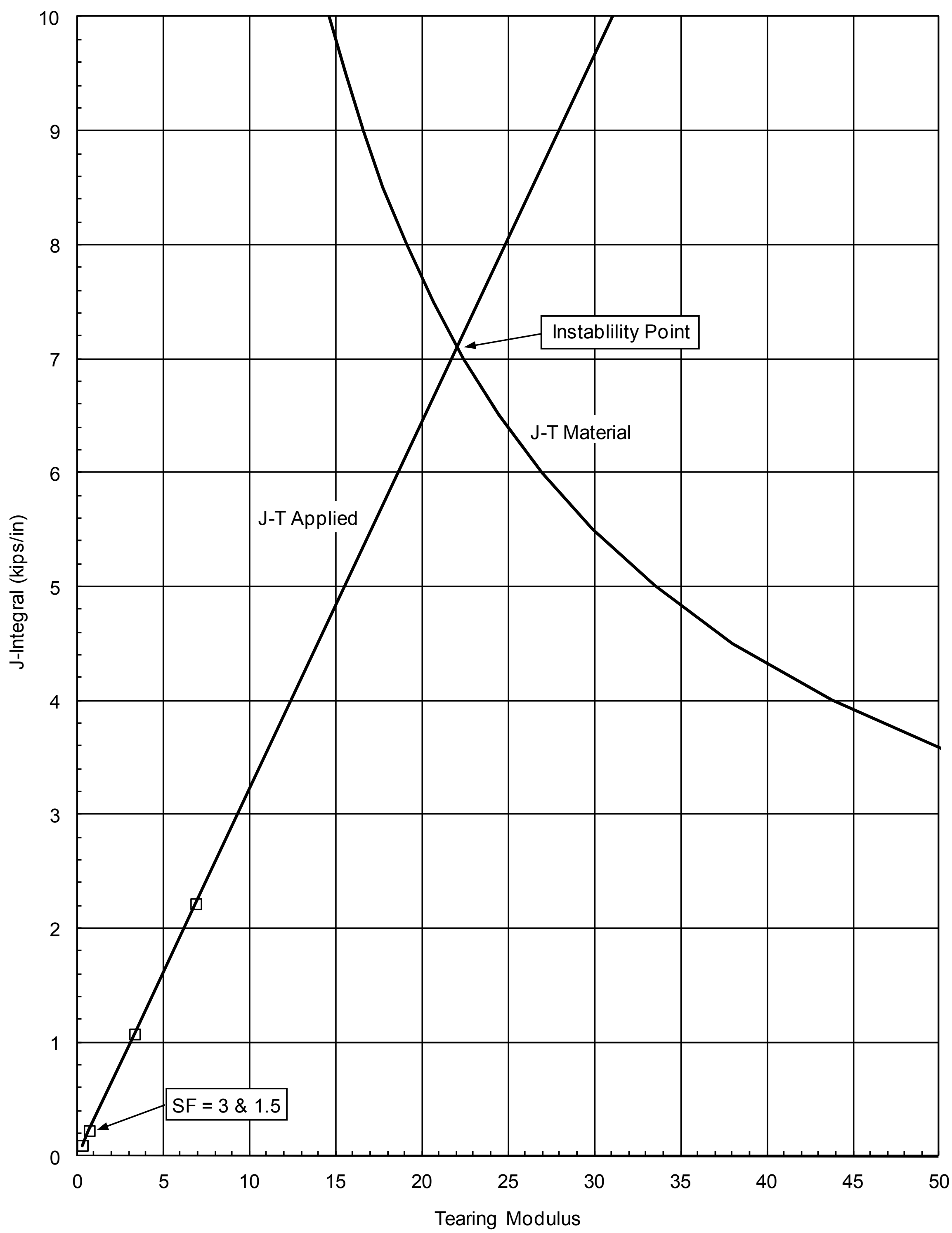

Table B-16: EPFM Evaluations for Downhill Side – LLOCA

EPFM Equations:

$J_{mat} = C(\Delta a)^m$ C = [ ]

$T_{mat} = (E/\sigma_f^2)*Cm(\Delta a)^{m-1}$ m = [ ]

$J_{app} = [KI'(a_e)]^2/E'$

$T_{app} = (E/\sigma_f^2)*(dJ_{app}/da)$

Ductile Crack Growth Stability Criterion: $T_{app} < T_{mat}$

At instability: $T_{app} = T_{mat}$

Safety Factors		KI^*_p	KI^*_s	KI*(a)	a_e	$KI'(a_e)$	J_{app}	T_{app}	Stable?
Primary	Secondary	(ksi√in)	(ksi√in)	(ksi√in)	(in.)	(ksi√in)	(kips/in)		
1.00	1.00	0.780	76.629	77.409	2.3549	79.587	0.197	0.613	Yes
1.50	1.00	1.170	76.629	77.799	2.3562	80.010	0.200	0.619	Yes
200.00	1.00	156.040	76.629	232.668	3.3765	286.443	2.558	7.935	Yes
300.00	1.00	234.059	76.629	310.688	4.2761	430.443	5.776	17.918	Yes
400.00	1.00	312.079	76.629	388.708	5.4341	607.088	11.489	35.642	No

Iterate on safety factor until $T_{app} = T_{mat}$ to determine $J_{instability}$:

							$J_{instability}$	T_{app}	T_{mat}
4.3004	4.3004	3.355	329.534	332.889	4.5793	477.273	7.101	22.029	22.029

at J_{mat} = 0.200 kips/in, T_{mat} = 1584.010

Applied J-Integral Criterion: $J_{app} < J_{0.1}$

where, $J_{0.1} = J_{mat}$ at Δa = 0.1 in.

Safety Factors		KI^*_p	KI^*_s	KI*(a)	a_e	$KI'(a_e)$	J_{app}	$J_{0.1}$	OK?
Primary	Secondary	(ksi√in)	(ksi√in)	(ksi√in)	(in.)	(ksi√in)	(kips/in)	(kips/in)	
1.50	1.00	1.170	76.629	77.799	2.3562	80.010	0.200	2.474	Yes

Figure B-3: J-T Diagram for Downhill Side – LLOCA

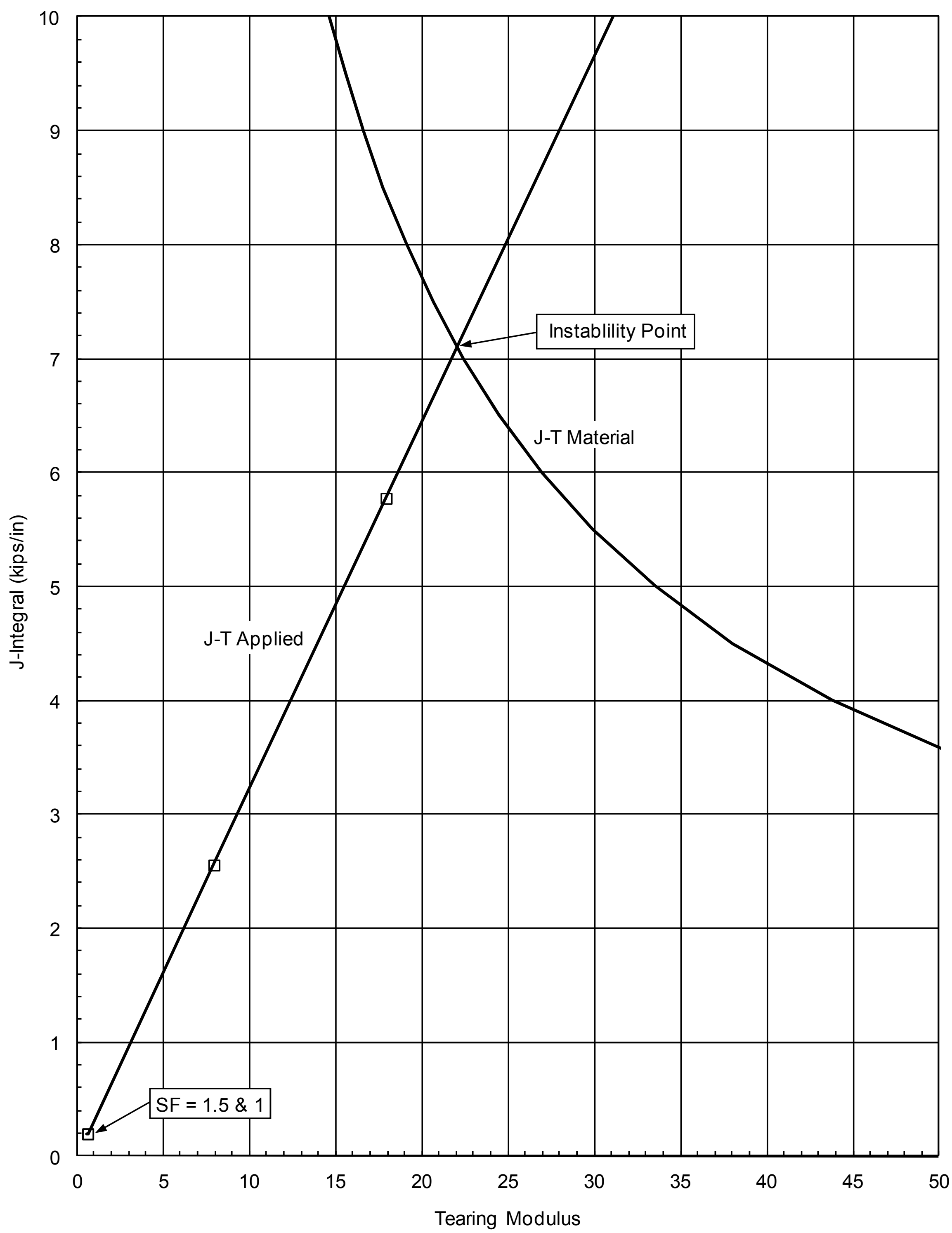

APPENDIX C: CALCULATION OF AVAILABLE YEARS OF SERVICE BASED ON AVAILABLE REINFORCEMENT AREA DUE TO CRACK GROWTH

C.1 Purpose

The purpose of this appendix is to demonstrate that the as-repaired RVCH continues to satisfy the primary stress limits of NB-3000, considering postulated flaws emanating from the original J-groove weld. This is accomplished by comparing the available reinforcement areas in the vicinity of the repaired nozzles with the areas removed from consideration of carrying primary load, in accordance with NB-3330. The acceptable life for crack growth is determined, and the limiting case is reported.

C.2 Analytical Methodology

The approach of calculating available years of service is based on determining the available area of reinforcement as required per NB-3330 Reference [C1]. The repair results in removal of the structural material. In addition for repaired nozzles, as left Alloy 600 region of the original J-groove weld is not considered as structural material as it contains flaws. Finally, additional area due to postulated crack growth into the carbon steel of the head is also discounted from the available structural area.

Analyzed nozzles are those already repaired and in operation as well as those being repaired. Nozzles previously repaired and in operation are: # 5, #14, #17, #18, #23, #37, #38, #49 and #63 (Reference [C11]). Nozzles being repaired in the 2016 outage are #30, #40 and #51 (References [C14] to [C16]). The dates for these repairs are listed as follows:

Nozzle	Repair Date
5	May 2012
14	May 2015
17	May 2012
18	May 2015
23	May 2015
30	Current Oct-2016 Outage
37	Nov 2013
38	May 2012
40	Current Oct-2016 Outage
49	May 2013
51	Current Oct-2016 Outage
63	May 2012

Note that for the previously repaired nozzles the detailed evaluations are contained in Sub-Sections C.3.6, C.4 to C.6, while for the current (2016) nozzle repairs the detailed evaluations are provided in Sub-Section C.7.

The calculation of the available years of service is performed in MS Excel spread sheet *Harris_Sizing_Tables.xlsx.*

There are two approaches which are used in this calculation. Both of them follow the guidelines of NB-3330 Reference [C1]. These approaches are described below:

Approach 1 is the more conservative approach and evaluates each repaired nozzle on an individual basis by imposing a limit of reinforcement equal to half the distance to the nearest nozzle. This is roughly equivalent to assuming that the repaired nozzle is surrounded by other nozzles that have been repaired. This approach is described below:

1) Calculation of structural area removed due to nozzle bore, repair and corrosion

2) Structural area of flawed J-groove weld is determined and considered as area removed

3) Calculation of limits of reinforcement for determination of area of reinforcement

4) Calculation of available head area of reinforcement

5) Calculation of reinforcement area of portion of the IDTB weld

6) Determination of structural area lost due to postulated crack growth in Alloy 600 and into the carbon steel of the head

7) Calculation of available area of reinforcement by adding all areas of reinforcement and subtracting areas lost due to bore and crack growth

8) Available years of service is determined as an iterative process by calculating loss of structural area due to corrosion and postulated crack growth until area of reinforcement is exhausted.

Approach 2 removes some of the conservatism of Approach 1 and was used to examine the bounding case as determined by Approach 1. This approach analyzes the ligament between adjacent nozzles, where one nozzle is in the repaired condition and one nozzle is unrepaired. This approach is appropriate for use as long as there are no repaired nozzles in neighboring penetrations. This approach is described below:

1) Calculation of structural area removed due to nozzle bore, repair and corrosion

2) Structural area of flawed J-groove weld (i.e. repaired nozzle) is determined and considered as area removed; the structural area of the unflawed J-groove weld (i.e. unrepaired nozzle) is determined and discounted based upon the material strength ratio

3) Calculation of limits of reinforcement for determination of area of reinforcement

4) Calculation of available head area of reinforcement

5) Calculation of reinforcement area of portion of the IDTB weld for the repaired nozzle only

6) Determination of structural area lost due to postulated crack growth in Alloy 600 and into the carbon steel of the head for the repaired nozzle location

7) Calculation of available area of reinforcement by adding all areas of reinforcement and subtracting areas lost due to bore, crack growth, and a portion of the unflawed J-groove area as determined by material strength ratio

8) Available years of service is determined as an iterative process by calculating loss of structural area due to corrosion and postulated crack growth until area of reinforcement is exhausted.

C.2.1 Conservatisms

- Crack growth is considered to be linear over the course of 30 years. This slightly overestimates flaw growth in the early years.
- The crack growth area at the IDTB weld anomaly was conservatively taken as [ ]. This crack is specified to have a maximum flaw radius of [ ], which would produce a smaller area when calculated (maximum flaw depth^2 x π / 4) [C6].
- For the IDTB Weld, the area is calculated assuming machining to remove IDTB overlap onto the original weld (Detail D, Ref. [C2], conservatively, doubled to account for the larger side of the weld in Approach 1.
- This method does not account for load distribution from weak ligament to stronger/larger structural area, compared to detailed limit load analysis.
- For Nozzle 23 Overbore, the diameter of the overbore is considered for the entire length of the opening. For all other repaired openings, the diameter is conservatively considered to be [ ]. This accounts for the counterbore from the outer surface of the head.
- In Section C.4, using Approach 2, the downhill J-groove weld for Nozzle 7 is conservatively considered to be 1.15 times larger than the value of the downhill J-groove weld for Nozzle 14 Minimum. This is conservative because J-groove weld areas should increase as the nozzle moves further from the head center and Nozzle 14 Minimum is further from center than Nozzle 7.
- Approach 2 uses the minimum design thickness for the head at the unrepaired nozzle.

C.3 Calculation of Available Reinforcement Areas using Approach 1

The following approach is used for calculation of the available reinforcement area.

C.3.1 Tentative Thickness Calculation

The tentative thickness of the Reactor Vessel Closure Head (RVCH) is determined by the approach specified in NB-3324 of the ASME Boiler and Pressure Vessel Code Reference [C1]. As stated in the article, except in local areas, the wall thickness of a vessel shall never be less than that obtained from the formula in NB-3324.2 for spherical shells.

Formula NB-3324.2 (Spherical Shells):

(Equation 1)

$$t = \frac{PR}{2S_m - P}$$

Where:

t = Tentative thickness of shell or head, in.

P = Design Pressure, psi

R = Inside radius of shell or head, in.

Sm = Design stress intensity values, psi

C.3.1.1 Closure Head (Spherical Head)

[ ] Reference [C3]

[ ] Reference [C2]

Temperature, design [ ] Reference [C3]

Sm = 26,700 psi at the design temperature for SA-533 Grade B Class 1, Reference [C1]

Substituting these values into Equation (1) yields the tentative thickness (t_t) of the RVCH to be:

[ ]

C.3.2 Calculation of Structural area removed due to nozzle bore

The following table shows the calculation of area lost due to nozzle bore used in MS Excel spread sheet *Harris_Sizing_Tables.xlsx*. Figure C1 shows used parameters.

Table C1: Area Removed from Selected Nozzles

Parameter		Reference
Nozzle Plane Coordinate x, in.	[ ]	[C10]
Nozzle Plane Coordinate y, in.	[ ]	[C10]
(1) Opening Diameter, d_o, in.	[ ]	[C5][C4][C13]
Plane Distance of center of nozzle, C, in.	$C = \sqrt{x^2 + y^2}$	[C10]
Inside radius of the head, R_i, in.	[ ]	[C2]
Tentative thickness of RVCH, t_t, in.	[ ]	Calculated
Tentative outside radius of head, R_t, in.	[ ]	Calculated
Vertical Distance to inside radius, H_i, in.	$H_i = \sqrt{R_i^2 - C^2}$	Calculated
Vertical Distance to outer tentative thickness, H_t, in.	$H_t = \sqrt{R_t^2 - C^2}$	Calculated
Depth of opening, t_o, in.	[ ]	Calculated
Opening area removed A_{rmv}, in^2	[ ]	Calculated

Note(s):

(1) The corrosion rate is considered to [ ] , reference [C4]. This is multiplied by 2 to account for corrosion on both sides of the diameter.

C.3.3 Minimum Reinforcement Area

The following calculations for the minimum required reinforcement are based on the approach listed in ASME Boiler and Pressure Code, Reference [C1].

Per NB-3334, the boundaries of the cross-sectional area in any plane normal to the vessel wall and passing through the center of the opening and within which metal shall be located in order to have value as reinforcement are designated as the limits of reinforcement for that plane.

First, metal will be identified that may be considered for reinforcement:

NB-3335 (b) and (e) of the ASME code require that the reinforcing metal be continuous with vessel wall metal or joined to it by full penetration weld. Since the nozzles are joined by partial penetration welds, the nozzle wall metal is not considered for reinforcement.

NB-3335 (c) states that “weld metal which is fully continuous with the vessel wall” may be considered for reinforcement. The IDTB weld satisfies this criterion and can contribute towards reinforcement; the j-groove weld and buttering do not satisfy this criterion under cracked conditions and therefore will not be considered as contributing towards reinforcement. NB-3335 (d) of the ASME Code requires that the mean coefficient of thermal expansion of the reinforcing metal (including weld metal) be within 15% of the value of the vessel wall material.

Second, the limits of reinforcement will be calculated:

NB-3334 establishes the limits of reinforcement area along and normal to the vessel surface. Since the nozzle wall metal is not considered for reinforcement, only the limit along the surface of the head mean radius (Lw) is relevant for this calculation. For the limit of reinforcement measured along the mid-surface of the nominal vessel wall thickness, NB-3334.1 requires:

a) One hundred percent of the required reinforcement shall be within a distance on each side of the axis of the opening equal to the greater of the following:

   1) The diameter of finished opening in the corroded condition, Lw1

   2) The sum of the radius of the finished opening in the corroded condition, the thickness of the nozzle wall, and the thickness of the vessel wall, Lw2

b) Two-thirds of the required reinforcement shall be within a distance on each side of the axis of the opening equal to the greater of the following:

1) $r + 0.5\sqrt{Rt}$, where R is the mean radius of the shell or head, t is the nominal vessel wall thickness, and r is the radius of the finished opening in the corroded condition

2) The radius of the finished opening in the corroded condition plus two-thirds the sum of the thicknesses of the vessel wall and the nozzle wall

Furthermore, the ASME Code prohibits the same reinforcing material from being applied to more than one opening and requires that one half of the reinforcing material lie on each side of the opening.

These conditions restrict Lw to one-half of the distance between similar adjacent penetrations less the radius of the opening. Axis-to-axis distances between adjacent nozzles are considered rather than distances along the curved surface of the RVCH mean radius.

The following table shows the calculation of limits of reinforcement used in MS Excel spread sheet *Harris_Sizing_Tables.xlsx*. Figure C1 shows used parameters.

Table C2: Limits of Reinforcement for Selected Openings

Parameter			References
Diameter d_o, in. (upper)		Specific for each nozzle	[C5][C13]
Radius, r, in. (upper)		$r = d_o/2$	*Calculated*
RVCH wall thickness, t, in.		Specific for each nozzle	[C5][C4]
Nozzle wall thickness, t_n, in.		No credit taken	-
Inside radius of RVCH, R_i, in.		[ ]	[C2]
Mean radius of RVCH, R_m, in.		$R_m = R_i + t/2$	Calculated
Distance to accommodate 100% reinforcement	NB-3334.1 (a)(1)	$Lw_1 = 2r$	Calculated
	NB-3334.1 (a)(2)	$Lw_2 = r+t+t_n$	Calculated
	> of Lw_1 & Lw_2		Calculated
Distance to accommodate 2/3 reinforcement	NB-3334.1 (b)(1)	$r + 0.5\sqrt{R_m t}$	Calculated
	NB-3334.1 (b)(2)	$r + 2(t + t_n)/3$	Calculated
	> of (b)(1) & (b)(2)		Calculated
Grid distance for nozzles, in.		[ ]	[C10]
Center line distance between this opening and the nearest CRDM opening, in.		[ ]	[C10]
Max. length available for reinforcement, L_r, in.		(see note below)	Calculated

The following considerations were taken in Table C2:

- Since the nozzle wall is not fully continuous with the head, the metal cannot be counted as contributing to the area of reinforcement per NB-3335. Therefore, the nozzle wall thickness is considered to be zero (t_n = 0 in.).

- The reinforcement limit (L_r) for the CRDM nozzle is calculated by one half of the centerline distance between the two nearest consecutive openings ([ ]).

C.3.4 Required Area of Reinforcement

NB-3332.2 indicates that reinforcement is required for the RVCH with the tentative thickness calculated in C.3.1 By NB-3332.2, the total cross-sectional area of reinforcement, A, shall not be less than:

$$A = dt_rF$$

Where d = finished diameter of a circular opening (or chord of an elliptical opening) in the corroded condition, F = a correction factor which compensates for the variation in pressure stresses on different planes with respect to the axis of a vessel (correlates to F = 1.00 with a 0.00° angle of the plane with the longitudinal axis), and tr (in this case) is the minimum required thickness in the absence of the opening. The body of this calculation will refer to d_o as the diameter of the circular opening and tr as the depth of reinforcement. Not less than half the required material shall be on each side of the center line. Figure C1 diagrams the reinforcement area above the tentative thickness.

Figure C1: Reinforcement Area Diagram

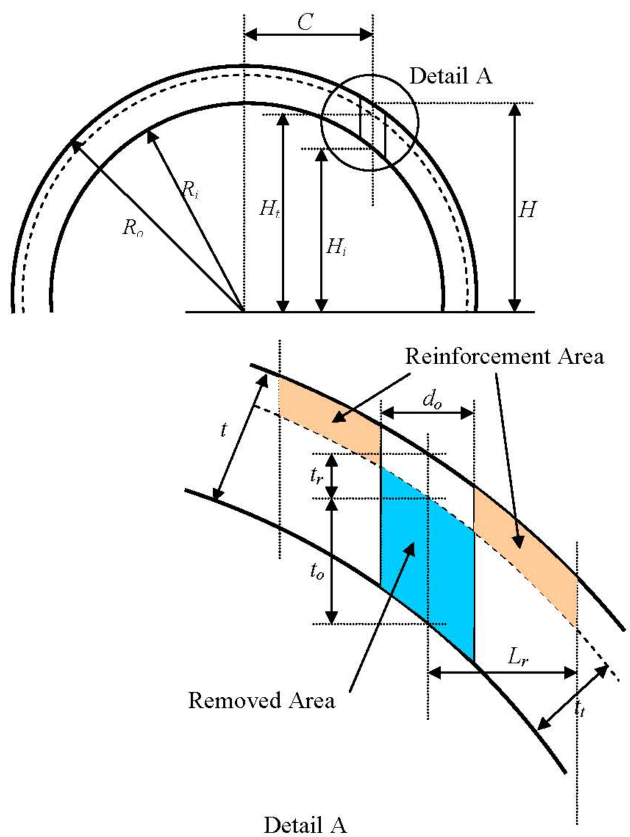

Figure C2: Overview of Approach 1

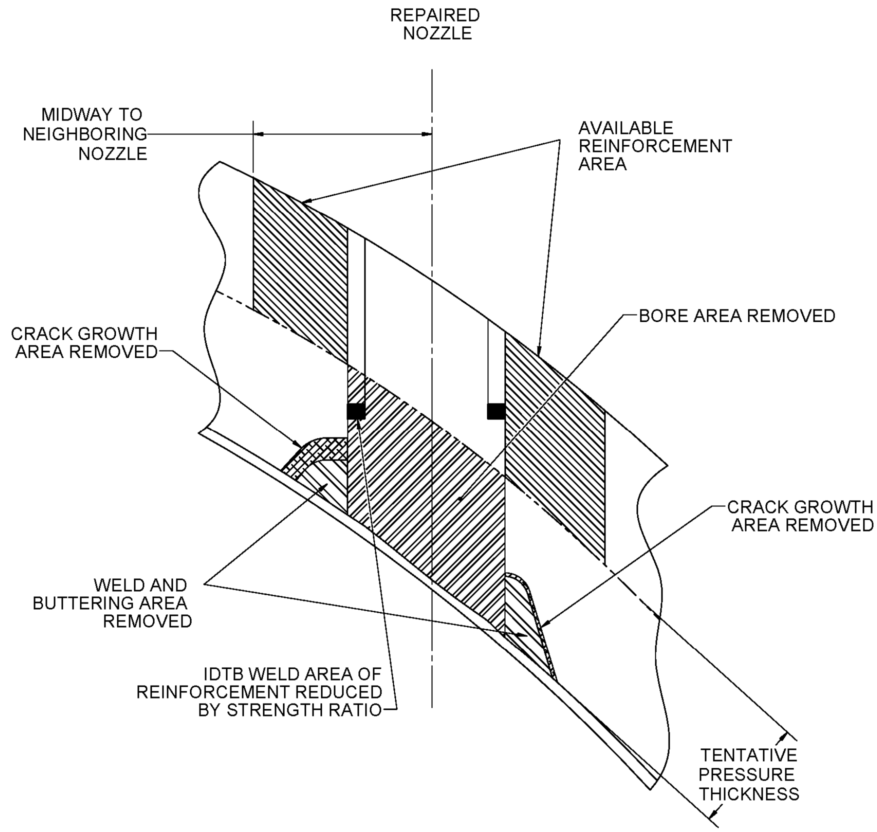

The following table shows calculation of IDTB weld reinforcement area used in MS Excel spread sheet *Harris_Sizing_Tables.xlsx*.

Table C3: IDTB Weld Reinforcement

Parameter		Reference
Outside Diameter at IDTB Weld, d_{wo} in.	[ ]	[C2]
Inside Diameter at IDTB Weld, d_{wi} in.	[ ]	[C2]
Width of IDTB Weld, w in.	[ ]	Calculated
Min. Ligament Thickness, t_{lig} in.	[ ]	[C2]
Area of IDTB Weld Anamoly, $A_{anamoly}$ in^2	[ ]	Section C.2.1
Area of IDTB Weld for Reinforcement, A_{IDTB} in^2	[ ]	Calculated

Note 1: [ ] The mean coefficient of thermal expansion at [ ] of the reinforcing metal of the IDTB weld ([ ] per Reference [C3]) is within of 15% of the mean coefficient of thermal expansion at 650 F of the head material. The ASME requirement is satisfied. Values are taken from the ASME code, Reference [C12].

Note 2: Reduction coefficient of [ ] for the IDTB weld area of reinforcement used in Table C3 is calculated as Sm_{IDTB} /Sm_{vessel} = [ ] . Values are taken from the ASME code, Reference [C1].

Note 3: Nozzle 23 Over Bore conservatively uses the smaller geometry for the standard IDTB welds.

The following table shows the calculation of head reinforcement area used in MS Excel spread sheet *Harris_Sizing_Tables.xlsx*. Figure C1 shows used parameters.

Table C4: Actual Reinforcement Margin

Parameter	
Opening Diameter, d_o, in.	[ ]
Reinforcement limit, L_r, in.	[ ]
Outer RVCH surface radius, R_o, in.	[ ]
Plane Distance of center of nozzle C, in.	$C = \sqrt{x^2 + y^2}$
Vertical Distance to outer tentative thickness, H_t, in.	$H_t = \sqrt{R_t^2 - C^2}$
Vertical Distance to outer RVCH surface, H, in.	$H = \sqrt{R_o^2 - C^2}$
Depth of reinforcement, t_r, in.	[ ]
Head reinforcement area, A_h, $in.^2$	[ ] $= 2t_r(L_r - {d_o}/{2})$

C.3.5 Calculation of area lost due to crack growth

The entire area of Alloy 600 is considered removed due to presence of flaws for repaired nozzles. In addition, area lost due to postulated crack growth into the carbon steel is considered. Area removed of the Alloy 600 is taken from Reference [C5]. These drawings give as-built areas of the uphill and downhill J-groove welds for each nozzle of interest. Those numbers are tabulated below in Table C5.

Table C5: Alloy 600 weld area lost

	J-Groove Weld Area			
	Uphill		Downhill	
Nozzle	Min Condition In^2	Max Condition In^2	Min Condition In^2	Max Condition In^2
5				
14				
17				
18				
23				
23 OB				
37				
38				
49				
63				

Area lost due to postulated crack growth is determined using a CAD feature of the Workbench program. The weld profiles of the uphill and downhill side taken from Reference [C5] are used and offset by the postulated crack growth. The area of the cracked carbon steel section is taken from the ANSYS Workbench program. The crack growth on the uphill side is [ ] for [ ] years of service and the downhill crack growth is [ ] inches for [ ] years of service taken from Section 6.3.1. Conservatively, crack growth per year is calculated as [ ] for the uphill side and [ ] for the downhill side. This growth is conservative for service that is less than 30 years since the crack propagates with slower rate at the beginning of the repair service.

In addition, the reinforcement area lost due to crack growth at the weld anomaly in the IDTB weld is also accounted for and reduced based upon a ratio of material strength.

Min and Max Conditions refer to minimum and maximum head thickness configurations.

QA Note: The crack growth areas have been checked with approximate hand calculations to verify the Workbench computer program results, based on the weld profiles give in Ref. [C5].

C.3.6 Calculation of available area of reinforcement

The total remaining reinforcement area is calculated by adding A_h (see Table C4), area of reinforcement available in the carbon steel head portion, to area of reinforcement due to portion of the IDTB weld (A_{IDTB} - see Table C3) and subtracting areas lost due to nozzle bore (A_{rmv} - see Table C1), Alloy 600 J-groove weld area (see Table C5), and crack growth at the weld anomaly point. This is calculated in MS Excel spread sheet _Harris_Sizing_Tables.xlsx_ without corrosion and without J-groove crack growth, initially to identify limiting nozzles (i.e. for screening purposes).

Table C6: Initial Calculation of Reinforcement Area Remaining

	Total Area of Reinforcement, in^2	Total Area Removed, in^2	Total Remaining Reinforcement, in^2
Nozzle 5 Minimum	(Special Case – See Section C.4)	(Special Case – See Section C.4)	(Special Case – See Section C.4)
Nozzle 14 Minimum			
Nozzle 14 Maximum			
Nozzle 17 Minimum			
Nozzle 18 Minimum			
Nozzle 18 Maximum			
Nozzle 23 Minimum OB			
Nozzle 23 Minimum			
Nozzle 37 Minimum			
Nozzle 37 Maximum			
Nozzle 38 Minimum			
Nozzle 38 Maximum			
Nozzle 49 Minimum			
Nozzle 49 Maximum			
Nozzle 63 Minimum			

Based on Table C6, Nozzle 14 Minimum and Nozzle 37 Minimum are identified as potential limiting cases. Since neither of these nozzles have an adjacent nozzle in the repaired configuration, they will be analyzed using Approach 2.

Since Nozzle 17 Minimum and 18 Minimum are adjacent and each nozzle is in the repaired configuration, these nozzles are analyzed using Approach 1 considering corrosion and crack growth for [ ] years. The J-groove weld crack growth areas are documented in Figures C3 – C6.

Figure C3: Nozzle 17 Minimum Uphill J-groove Weld Crack Growth Area for 30 Years

Figure C4: Nozzle 17 Minimum Downhill J-groove Weld Crack Growth Area for 30 Years

[ ]

Figure C5: Nozzle 18 Minimum Uphill J-groove Weld Crack Growth Area for 30 Years

Figure C6: Nozzle 18 Minimum Downhill J-groove Weld Crack Growth Area for 30 Years

The calculation for Nozzle 17 Minimum and 18 Minimum is documented in MS Excel spread sheet Harris_Sizing_Tables.xlsx and the results are represented below in Table C7 for [ ] years of operation.

Table C7: Nozzle 17 Minimum and 18 Minimum Results for 30 Years of Operation

	Total Area of Reinforcement, in^2	Total Area Removed, in^2	Total Remaining Reinforcement, in^2
Nozzle 17 Minimum	[		]
Nozzle 18 Minimum			

As shown above in Table C7, the area of reinforcement exceeds the area removed for the limiting case (Nozzle 17 Minimum) and therefore since Nozzle 17 was repaired in May 2012, this nozzle is acceptable for an additional [ ] years beyond this date to May [ ].

C.4 Calculation of Remaining Years of Service using Approach 2

The purpose of this section is to remove some of the conservatisms presented in Section C.3 for the reinforcement calculation when a repaired nozzle is *not* adjacent to another repaired nozzle. Section C.3 looked at each nozzle individually without considering additional reinforcement that could be gained from neighboring nozzles. This approach is overly conservative when no neighboring nozzles have been repaired.

To remove some conservatism, a second approach was taken to calculate the available reinforcement area and area removed for a repaired nozzle neighboring an unrepaired nozzle. This approach will utilize an iterative process to determine when reinforcement area is exhausted. The limiting condition will occur on the uphill side of the repaired nozzle as a result of the significantly greater crack growth rate on the uphill J-groove weld side. Nozzle 14 Minimum was chosen as the limiting case based upon information from Table C6, and by comparing the growth in the J-Groove uphill weld between Nozzle 14 Minimum and Nozzle 37 Minimum. Since Nozzle 14 Minimum has a greater growth in the area of the uphill weld ([ ] in^2 – see Figure C8) as opposed to Nozzle 37 Minimum ([ ] in^2 – see Figure C10), Nozzle 14 Minimum is still the bounding location. For this analysis, Nozzle 14 Minimum is paired with its uphill neighbor Nozzle 7. Nozzle 5 Minimum will also be evaluated since this nozzle has close proximity to the vent pipe.

The area removed was calculated by determining the area below the tentative thickness between each nozzle's respective axis and the outside of the nozzle wall in the corroded condition. The J-groove weld area with crack propagation area (shown in Figure C8) was removed for the uphill weld at Nozzle 14 Minimum. In addition, the J-groove weld area was discounted for Nozzle 7 downhill based upon the material strength in comparison with the RVCH, as specified in NB-3330 [C1]. The downhill J-groove weld for Nozzle 7 was conservatively considered to be [ ] times larger than the value of the downhill J-groove weld for Nozzle 14 Minimum (Figure C9). This is conservative

because J-groove weld areas should increase as the nozzle moves further from the center and Nozzle 14 Minimum is further from center than Nozzle 7.

Figure C7: Overview of Approach 2

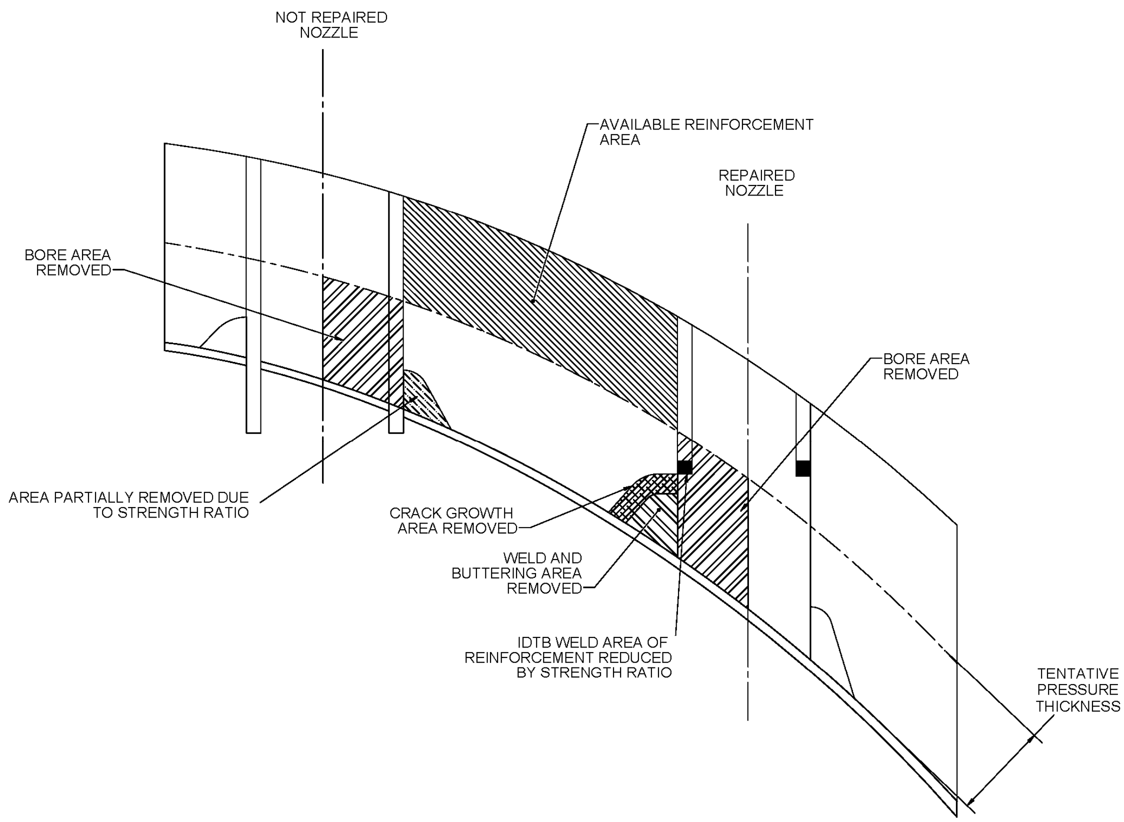

The length for the area of reinforcement was calculated by determining the distance between the two nozzles and subtracting the radius of each nozzle. This value was multiplied by the average thickness between the tentative thickness and the outer radius of the RVCH measured at each location. Since the as-built thickness was not available for Nozzle 7, the design minimum thickness was conservatively used ([ ] in [C2]). In addition to this reinforcement area, the IDTB weld on the uphill side was credited for reinforcement on Nozzle 14 Minimum. The IDTB weld was discounted for material strength and the weld anomaly, as described in Note 2 of Table C3.

Figure C8: Nozzle 14 Minimum Uphill J-groove Weld Crack Growth Area for 15 Years

Figure C9: Nozzle 14 Minimum Downhill J-groove Weld Crack Growth Area for 15 Years

Figure C10: Nozzle 37 Minimum Uphill J-groove Weld Crack Growth Area for 15 Years

The available years of service are calculated using an iterative process utilizing Approach 2. Area lost due to crack growth into the carbon steel is calculated for each year of service. The maximum number of years is determined at the point when the available reinforcement area is exhausted.

The calculation for Nozzle 14 Minimum and Nozzle 7 is documented in MS Excel spread sheet Harris_Sizing_Tables.xlsx and the results are represented below in Table C8 for 15 years of operation.

Table C8: Nozzle 14 Minimum and Nozzle 7 Results for 15 Years of Operation

	Ligament between Nozzle 14 Min / Nozzle 7
Total Area of Reinforcement, in^2	[
Total Area Removed, in^2	
Reinforcement Remaining, in^2	]

A special case exists for Nozzle 5, and therefore the lifetime of Nozzle 5 will be verified separately below. Nozzle 5 does not border any repaired nozzles, but it lies within a closer proximity to an opening than the other cases as a result of the placement of the vent line. The Nozzle 5 Minimum case was modeled using Approach 2 in which the ligament between Nozzle 5 Minimum and the vent line was examined. The Nozzle 5 Uphill weld was used for this analysis, because the crack growth on the uphill weld produces a larger area which requires reinforcement. For conservatism, the minimum design thickness was used for the vent line and a [ ] in^2 weld was conservatively used for the vent line J-groove weld. This J-groove weld area is conservative because it is larger than the J-groove weld areas on Nozzle 5 Minimum and the vent line does not require as large of a J-groove weld as the CRDM nozzles [C10]. In addition, corrosion was applied to the penetration diameter of the vent line to calculate area removed, despite the knowledge that this area would be protected by the vent line pipe. The calculation for Nozzle 5 Minimum and the vent line is documented in MS Excel spread sheet Harris_Sizing_Tables.xlsx and the results are represented below in Table C9 for 15 years of operation. This calculation uses the crack growth area for the uphill J-groove weld after 15 years for Nozzle 5 Minimum as shown in Figure C11.

Figure C11: Nozzle 5 Minimum Uphill J-groove Weld Crack Growth Area for 15 Years

[ ]

Table C9: Nozzle 5 Minimum and Vent Pipe Results for 15 Years of Operation

	Ligament between Nozzle 5 Min / Vent Pipe
Total Area of Reinforcement, in^2	[ ]
Total Area Removed, in^2	[ ]
Reinforcement Remaining, in^2	[ ]

Based upon the results represented in Table C9, it can still be concluded that Nozzle 14 Minimum is the bounding case for 15 years of operation.

C.5 Results/Conclusion

After analyzing all the critical nozzle locations, Nozzle 14 was identified as the limiting condition. Table C8 displays that Nozzle 14 is acceptable for 15 years of service from the date of the repair. Since this value is bounding for the other nozzles, this conclusion is applicable to all other cases. By this conclusion, and since the earliest repairs were performed in May 2012, the RVCH nozzles are acceptable for 12 years of additional operation, from April 2015.

C.6 Computer File(s)

Table C10: COLDStor - Official Computer Files

\cold\General-Access\32\32-9000000\32-9176350-002\

Date	Time	Size	File Name
4/29/15	14:47:22(EST)	36172 Bytes	Harris_Sizing_Tables.xlsx

This computer file inputs dimensions from References [C2], [C4], [C5], [C6], and [C10].

C.7 Additional Evaluation at Penetrations #30, #40 and #51 for 5 years operation

During the recent outage inspection according to References [C14], [C15] and [C16], additional nozzle repair is needed for nozzles 30, 40 and 51. However, no original J-groove weld dimensions nor RV head thickness at the three nozzle penetrations are available for a complete evaluation at the time this revision is prepared. The results presented in the Sections C.1 to C.6 for the nine repaired nozzles are then used as the basis to justify a 5-year operation for the three nozzle repairs.

RV head thickness at the nozzle:

As shown in previous sections, the head thickness is the most critical parameter in the evaluation. The following analysis is based on the assumption that the RV head wall thickness (*t* in Table C2) is no less than [ ] inches, i.e.,

$t \geq$ **[ ]** in.

J-groove weld size:

Table C6 indicates that the total remaining reinforcement area for a particular nozzle of the “minimum condition” is always less than that of the “maximum condition.” Therefore the J- groove weld size of the “minimum condition” is considered herein. Furthermore, the geometric symmetry of the nozzle penetrations indicates that the J- groove weld size of Nozzle 37 may be assumed for Nozzle 40, and that of Nozzle 49 for Nozzle 51; J-groove weld size of Nozzle 37 may be assumed for Nozzle 30.

Crack growth area:

Since no detailed J-groove weld dimensions are available, crack growth areas at the three nozzle penetrations are estimated by the crack growth areas at Nozzles 14 and 37 (Figures C8 to C10). A review of Figures C8 to C10 indicates that closer the nozzle to the head center higher the crack growth area results (in contrast to that away from the center the J-groove weld size is larger). Therefore the crack growth area of Nozzle 14 for 15 years operation is taken as the bounding case for the three nozzles. A linear crack grown is assumed in the 15 years which is conservative, as the crack growth area in earlier years is less than that in later years. The crack growth area of 5 years is estimated as follows in Table C11:

Table C11: Estimate of Crack Growth area at Penetrations 30, 40 and 51 for 5 Years of Operation

Crack growth area (in^2)	Area in in^2	Eq.
Crack growth area of Nozzle 14 (15 years), upper hill		
Crack growth area of Nozzle 14 (15 years), down hill		
Total crack growth area of 15 years		
Crack growth area of 5 years		

Nozzle 30 is adjacent to Nozzle 38, and Nozzle 51 is adjacent to Nozzle 63. Approach 1 mentioned in Section C.2 is used. The calculation procedure is the same as in Section C.3.6 for Nozzles 17 and 18.

MS Excel spread sheet “Harris_Sizing_Tables.xlsx” from Rev. 002 is used in the calculation, and the results are presented in Table C12.

Table C12: Results of Nozzle Repair at Penetrations 30, 40 and 51 for 5 Years of Operation

Penetration area (in^2)	30	40	51	Eq.
Head reinforcement area				
IDTB weld reinforcement area				
Total area of reinforcement				
J-groove weld area before crack growth				
J-groove weld area after crack growth				
Area removed due to opening and corrosion				
Total area removed				
Total area remaining				

Computer File:

Updated MS Excel spread sheet of the same file name is uploaded to the COLDStor at \cold\General-Access\32\32-9000000\32-9176350-003\:

Table C13: COLDStor - Official Computer File of Rev. 003

Date	Time	Size	File Name
10/17/2016	1:35 PM (CT)	43026 Bytes	Harris_Sizing_Tables.xlsx

C.8 Appendix References

References identified with an (*) are maintained within Duke Energy Records System and are not retrievable from AREVA Records Management. These are acceptable references per AREVA Administrative Procedure 0402-01, Attachment 8. See page 2 for Project Manager Approval of customer references

C1 ASME Boiler and Pressure Vessel Code, Section III, Rules for Construction of Nuclear Facility Components, 2001 Edition with Addenda through 2003.

C2 AREVA Drawing 02-9175500E-007, "Shearon Harris CRDM ID Temper Bead Weld Repair"

C3 AREVA Document 08-9172870-003, "Design Specification for Shearon Harris RVCH CRDM and CET Nozzle Penetration Modification"

C4 AREVA Document 51-9176114-002, "Corrosion Evaluation of Shearon Harris RV Head Penetration IDTB Weld Repair."

C5 AREVA Drawing 02-9239552B-001, "Shearon Harris RVCH Repaired Penetration J-Groove Details"

C6 AREVA Document 32-9176345-002, "Shearon Harris Unit 1 RVCH CRDM/CET Nozzle IDTB Repair Weld Anomaly"

C7 Reference Removed

C8 Reference Removed

C9 ANSYS/Workbench Finite Element Computer Code, Version 15.0, ANSYS Inc. Canonsburg, P.A.

C10 AREVA Document 38-2200979-000, "Shearon Harris - Proprietary Document LTR-MRCDA-12-8

C11 AREVA Document 50-9176411-005, "Shearon Harris CRDM Nozzle IDTB Weld Repair Traveler"

C12 ASME Boiler and Pressure Vessel Code, Section II, Rules for Construction of Nuclear Facility Components, 2001 Edition with Addenda through 2003.

C13 CR 2015-3494

C14 *Duke Energy NCR #02070424

C15 *Duke Energy NCR #02070179

C16 *Duke Energy NCR #02070259